Efficient Design of Precision Medical Robotics

by

NEVAN CLANCY HANUMARA

S.M. Mechanical Engineering
Massachusetts Institute of Technology, 2006
B.S. Mechanical Engineering, B.A. French
University of Rhode Island, 2004

Submitted to the Department of Mechanical Engineering in
Partial Fulfillment of the Requirements for the Degree of

Doctorate of Philosophy in Mechanical Engineering
at the
Massachusetts Institute of Technology
September 2012

Author:

Department of Mechanical Engineering
30 August 2012

Certified by:

Alexander H. Slocum
Pappalardo Professor of Mechanical Engineering
Thesis Supervisor

Accepted by:

David E. Hardt
Professor of Mechanical Engineering
Graduate Officer

Efficient Design of Precision Medical Robotics

by

NEVAN CLANCY HANUMARA

Submitted to the M.I.T. Department of Mechanical Engineering on
30 August 2012 in Partial Fulfillment of the Requirements of the
Degree of Doctorate of Philosophy in Mechanical Engineering

Abstract

Medical robotics is increasingly demonstrating the potential to improve patient care through more precise interventions. However, taking inspiration from industrial robotics has often resulted in large, sometimes cumbersome designs, which represent high capital and per procedure expenditures, as well as increased procedure times. This thesis proposes and demonstrates an alternative model and method for developing economical, appropriately scaled medical robots that improve care and efficiency, while moderating costs. Key to this approach is a structured design process that actively reduces complexity. A selected medical procedure is decomposed into discrete tasks which are then separated into those that are conducted satisfactorily and those where the clinician encounters limitations, often where robots' strengths would be complimentary. Then by following deterministic principles and with continual user participation, prototyping and testing, a system can be designed that integrates into and assists with current procedures, rather than requiring a completely new protocol. This model is expected to lay the groundwork for increasing the use of hands-on technology in interventional medicine.

Thesis Supervisor: Alexander H. Slocum
Title: Pappalardo Professor of Mechanical Engineering

Table of Contents

1. Introduction

The practice of interventional medicine is currently being improved by the introduction of robotics into the clinic. In the media, this often gives rise to fanciful visions, ranging from nanobots coursing through the bloodstream and attacking pathogens to autonomous surgical interventions. However, in the quest to provide patients with better, faster and cheaper care, these visions are still well in the future. In reality, interventional medical practice is still predominantly manual, relying heavily on operator skill and dexterity, but where the clinician encounters limitations, opportunities for robotic assistance can be identified.

Early medical robotic research drew inspiration from articulated industrial robots, often fitting them with end effectors customized for medical procedures. While significant progress has been made in developing robots to augment clinicians' capabilities, most current robots still evidence high capital and operational costs, large size scales and complex mechanisms that are reminiscent of industrial robots, as well as necessitate significant operator training. However, as the state-of-the-art advances, it is becoming apparent that a structural loop anchored to the floor and typically able to achieve sub millimeter endpoint precision, is mismatched to a human "workpiece" having a density on the order of water and comprised of soft, moveable tissues. Moreover, with the costs of medical care in the US reaching unsustainable levels, as well as the demand for improved care in secondary and developing markets, it is imperative to consider the economics of technology in medicine.

In the *Innovator's Dilemma* [1], Christensen explains how the trajectory of steadily increasing technological sophistication, which chases the "high end" of the market, creates room for *disruptive innovation*, which seeks to serve the bottom of the market with simpler, reasonably satisfactory products at a much lower price point. Accordingly, this thesis proposes and demonstrates an alternate and model for medical robot development. The underlying philosophy is that of *appropriate scale medical robotics.* This asserts that the robots and tools used to conduct a procedure ought not to greatly exceed the physical size or characteristic dimensions of the procedures. Rather than revolutionizing clinicians' practice with a multifunction robot, the aim is to target specific procedures and sub tasks that are identified as inefficient, i.e. repetitious or precision limiting, with tightly constrained solutions that work in partnership with clinicians and integrate into existing procedures' workflows. The methodology presented in this thesis is proposed as a means to prototyping robotic "smart tools" that are appropriate in scale, cost and complexity and, potentially, represent disruptive technology.

This thesis first provides an overview of the history of medical robotics, including those where their industrial heritage is evident to more recent developments of patient-mounted robotics. Special consideration is given to the da Vinci Surgical System, the most successful and advanced robot, particularly its cost and the challenge of demonstrating efficacy. With this background, the core design process is presented, the goal of which is to rapidly and efficiently place prototypes into clinicians' hands. This method follows deterministic principles and was developed and demonstrated during two prototype projects: Robopsy, a system to assist in the performance of image-guided percutaneous biopsies, and the Minimally Invasive Tissue Extractor (MITE), a hand tool that morcellates, extracts and contains excised tissue during minimally invasive surgery. The method was further optimized and formalized during four years teaching experience with the MIT *Precision Machine Design* course that

pairs student teams with local clinicians to conceive, prototype and test new devices in just 14 weeks. The best practices from the course, three case studies that epitomize this method and student and project outcomes are reported.

1.1. Definitions

Three terms require definition: e*fficient*, *precision* and *robot*. Firstly, the Oxford English Dictionary provides a broad definition of *efficient* as "Productive of effects; effective; adequately operative" [2]. Colloquially, it refers to a maximization of results for a given, limited set of inputs. In the context of designing medical devices, a device is efficient if it improves patient care, reduces physician strain and/or decreases procedure time, without substantially increasing overall per-procedure costs. The importance of this is highlighted by quoting an editorial comment in a urological article on the costs of robot assisted prostatectomies: "We must be aware of our responsibility to society and to our patients to deliver the best possible care at justifiable cost" [3].

Secondly, the engineering definition of *precision* comprises accuracy, repeatability and resolution [4]. Of primary concern in interventional procedures is the ability to address a target within the body while minimizing damage to surrounding tissues. In current practice, accuracy is often limited by the manual dexterity of the operator, who must manipulate tools within patients' bodies, often through small openings ranging from a 19 gauge needle (0.912 mm) to a 12 mm trocar port, while closing the control loop visually.

Thirdly, according to ISO 8373 [5] *robots* are "automatically controlled, reprogrammable, multipurpose manipulators that are programmable in three or more axes and may either be fixed in place or mobile for use in industrial automation applications." Furthermore, robots used in welding, assembling, painting, and general handling tasks comprise more than 75% of the world's stock of robots [6]. Broadening and adjusting this to the context of medical tools, the proposed definition is: *An electromechanical tool having one or more axes which are actuated semi-autonomously under the guidance of a physician to perform a task upon a patient.* This rules out devices which are operated by a clinician but have no autonomy, such as a drill, as well as those with only monitoring capabilities, such as an EKG machine. The goal is to develop devices that incorporate decision making aids and/or mechanize multiple procedural steps. This encourages the division of tasks between the operator and the tool, rather than focusing on maximizing procedural automation. Physicians and patients already respond positively to robotic technology and as comfort levels rise, increased autonomy can be incorporated into medical robotics. Additionally, increasing the use of technology in medicine has the potential to serve as a "skills leveler" by enabling clinicians with variable levels of training to conduct procedures in a repeatable manner that follows "best practices."

A useful distinction is suggested in [7] between robots that serve as "CAD/CAM" systems and "Surgical Assistants." The former utilize medical imaging for pre-procedural planning and modeling purposes and then guide the clinician in procedure, with the aid of a registration step. The latter are tools that provide clinicians with "superhuman" capabilities, by increasing dexterity and assisting in positioning tools. Such robots can reduce cognitive load and reduce staffing needs. Thirty-six medical robotics projects in development up until 2003 were reviewed, with 21 categorized as CAD/CAM and 15 as Surgical Assistants. The paper identified "small, reduced power robots" as offering ergonomic and

safety advantages, thus reinforcing the concept of appropriate scale medical robotics, as well as providing a good summary of typical challenges encountered during medical robot design, all of which are touched upon in this thesis and re reproduced here:

- Placement and mounting of the robot in the confines of the operating environment while not hindering patient access.
- Ensuring sterility through sheathing and disposable components.
- Compatibility with imaging modalities, with magnetic resonance imaging (MRI) identified as particularly challenging.
- Designing for safe operation.
- Trading off between multi-purpose robots, which represent a high capital expense, and simpler more focused systems with modular elements.

1.2. Economics in Medical Robotics Design

Focusing on efficient design is important, particularly in the United States where healthcare is one of the largest industries. In 2009 total healthcare expenditures totaled $2.65 trillion, comprising 17.6% of the Gross Domestic Product, as reported by the Centers for Medicare & Medicaid Services (CMS). Annual spending growth is projected at 6.1% with a predicted rise to 19.3% by 2019 [8]. Additionally, the Agency for Healthcare Research and Quality (AHRQ) began a large-scale, ongoing *Medical Expenditure Panel Survey* in 1996 which tracks households, medical providers and employers with the primary goal of tracking health care use expenditures [9].

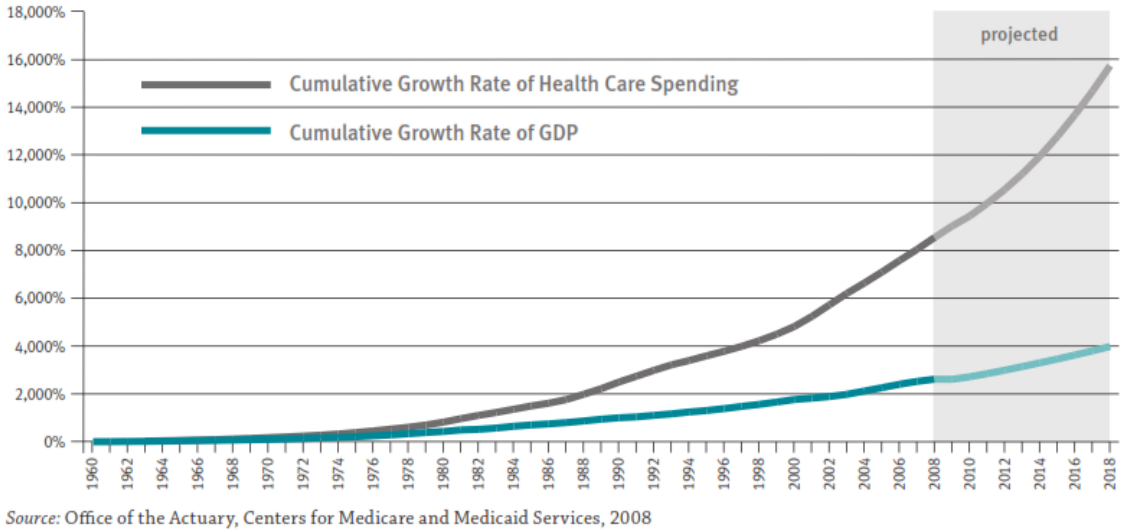

Figure 1 – Cumulative growth rates of GDP and health care spending: United States, 1960-2007 and projected for 2008-2018 [10].

The key issue, pinpointed in a 2009 Social Security Advisory Board report entitled "The Unsustainable Cost of Health Care," is that since 1960 healthcare expenditures have grown at a rate 2.1% faster than the GDP, as shown in Figure 1 [10]. Additionally, out-of-pocket expenses are growing faster than the incomes of Medicare beneficiaries and 60% of those workers who receive employer health coverage. New technologies, including procedures, drugs and devices, are estimated to account

for 38% – 65% of that growth and the Board states: “Some technology may provide tremendous value while other forms are simply more expensive ways of producing similar outcomes.” Frequently cited are “high-tech” imaging procedures, such as computed tomography (CT) and MRI. Comparisons with other industrialized nations indicate that the US spends more for similar levels of care, attributable to higher prices and, possibly, technology and obesity [11]. In sum, continually increasing medical costs are becoming politically and financially untenable.

Device companies are also recognizing that designing for production and operational cost efficiency will enable them to access secondary and developing markets, i.e. those outside Canada, the US, Western Europe and Japan. Many of the National Institutes of Health’s calls for proposals identify improving care *and* reducing costs as mutual goals. Cost minimization is of great concern in developing regions where improving overall patient care is more important than revolutionizing a single procedural subset, as a recent editorial in Pakistan exemplifies: “Robotic Surgery in Public Sector Hospitals: Irrational Use of Healthcare Resources” [12]. To date robotic surgery has not demonstrated cost competitiveness, so defining cost reduction as a design goal is a key feature of this method.

While there is no strict definition of “low cost,” hospital and government purchasers typically categorize equipment as capital or non-capital. The former is comprised of durable items costing on the order of $5K or more, an estimate used by local hospitals, that require independent line items on the budget. The latter typically includes items consumed during procedures, such as ablation probes, endoscopic grippers, needles, syringes and dressings. Medical robots, such as the daVinci Surgical System, represent a (large) capital expense to a healthcare institution while each procedure also requires a set of consumables, such as sterile protective sheaths. Unlike disposables, capital expenditures can be planned, budgeted and amortized with general operations; therefore, in some hospitals they are not accounted for in per-procedure costs.

Unfortunately, monetizing the benefits of robot aided surgery proves consistently challenging. The US healthcare system is based on a complex public and private reimbursement model and a description of it is beyond this document’s scope. Baseline rates which will be reimbursed to a hospital (or other care facility) and a physician (or his/her organization) for a specific procedure are set by the CMS [13] and are adjusted geographically. Private insurers or payees often reimburse at higher rates, which are negotiated with each healthcare chain, though these rates are not public. Unfortunately, a hospital’s billed rates and actual fees collected rarely agree. It is not possible to reliably determine the exact costs or revenues associated with a particular procedure. In most cases where a device (or consumable) is employed in a procedure, the cost of its use is borne by the facility. For example, during a biopsy procedure the drapes, needles, anesthetic, etc., consumed by the procedure are not billed separately. It is only after a device’s efficacy is well proven that it receive a Common Procedure Terminology (CPT) code and payees will reimburse its use directly; only at this point does it cease to be a cost for the healthcare provider. Therefore, any new device introduced into a procedure should either improve patient care and outcomes so substantially that it becomes the “gold standard,” irrespective of cost, or indirectly reduce hospital expenses, through the reduction of procedure time, hospital stays or complication rates.

2. Background on Medical Robotics

Medical robotics has been an area of active research since the 1980's. A 1991 IEEE paper [14] provides an overview of the early art as well as the varied fields in medicine where robots are applicable, including automation of repetitive laboratory work, rehabilitative and assistive technology, prosthetics and surgery in an assistive capability, i.e. tool positioning, and an active capability, i.e. for conducting transurethral resection of the prostate (TURP) and arthroplasty (joint repair). The foreword of the 2006 IEEE *Special Issue on Medical Robotics* [15] broadly defined the field to encompass surgical planning and execution tools, rehabilitation devices and assistive technology, targeted for the elderly and disabled. In the lead article [16], Taylor provides an overview of the state of the art based upon his 17 years of research experience in the field. He states that "surgical robots and robotic systems may be thought of as "smart" surgical tools that enable human surgeons to treat individual patients with improved efficacy, greater safety, and less morbidity than would otherwise be possible."

This paper provides a chart, reproduced in Table 1, which summarizes the strengths and limitations of robots and humans. When designing a new tool to be integrated into a procedure, this is an aid in apportioning tasks between the clinician and the tool. As detailed in the chart, humans are able to process complex information, develop creative solutions and operate with dexterity within a human range of motion (ROM) while robots respond well to numerical data, provide operations requiring great strength or fine dexterity and operate within hostile environments.

Table 1 – Strengths and limitations of robots and humans, adapted from [16], originally presented in [17].

	Strengths	**Limitations**
Humans	Judgment Hand-eye coordination Dexterity & haptics (human-scale) Complex information integration Easily trained Able to improvise	Fatigue & inattention Fine motion tremor Dexterity (non-human scale) Human vision Physical finger size Difficult to maintain sterility Radiation sensitivity
Robots	Geometric accuracy No fatigue or inattention Stable Radiation insensitive Fine/coarse capability Integration of numerical & sensor data	Non-autonomous judgment Low adaptability Dexterity Hand-eye (or imaging) coordination Haptics (not yet perfected) Complex information synthesis

2.1. Early Robots

The first commonly accepted use of a robot in medicine took place in 1985 when a 6 degree of freedom (DOF) Unimation PUMA 200 (Programmable Universal Machine for Assembly), an off-the-shelf industrial robot, was used with CT guidance to position a needle guide through which a brain biopsy was

conducted. Proposed as a replacement for stereotactic frames, the robot's relative accuracy was specified as 0.05 mm [18]. As further literature review indicates, the lowest barrier to entry from a safety (and liability) perspective exist for robots which position a tool guide, but do not actively manipulate it within the body.

A PUMA-based solution was also tested for applicability to TURP procedures. These involve inserting a resectoscope (endoscope with an electrocautary ring) through the penis into the prostate and moving it so as to remove a conical section of tissue. Executing this motion is challenging and can lead to back and neck strain in surgeons. A PUMA was fitted with an endoscope and rotary cutting apparatus and inserted through an artificial penis into a prostate, simulated with a potato[1]. The surgeon then specified the desired conical trajectory which was semi-autonomously executed. Robot execution reduced the cutting task time from 1 hr to approximately 5 min. However, the unconstrained industrial robot was deemed too unsafe; therefore a "safety frame" was developed, shown in Figure 3. This comprised a clamp for the resectoscope attached to an arc that, in turn, was attached to a ring; together the arc and ring confined the scope to adjustable, conical volumes. In a 30 patient clinical study outcomes were similar to that of the traditional procedure. [19]

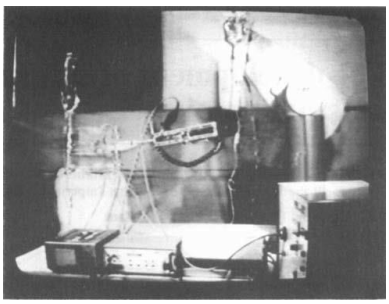

Figure 2 – Safety frame used with PUMA robot setup [19].

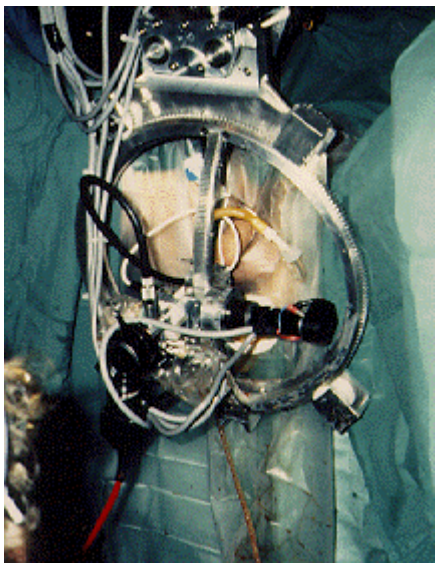

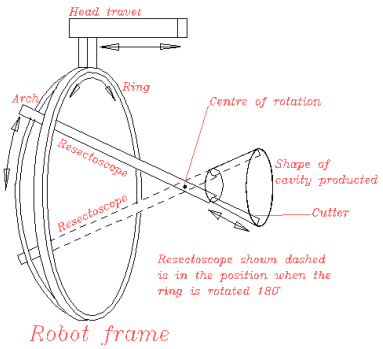

Figure 3 – PROBOT testing and operation [20].

Shortcomings of the PUMA-based system inspired the addition of motors to the frame and the resulting limited DOF and ROM robot was called the PROBOT, shown in Figure 3. Driving the resectoscope holder along the arc, rotating the ring and extending the cutter enables a cone shaped tissue profile to be removed. To operate: first the prostate's position was measured with the scope, than an ultrasound probe was inserted to scan and create a 3D model which was used to design the "cutting cones" and, finally, the surgery was executed. The PROBOT was tested at Guy's Hospital, London, first only to position a transurethral ultrasound probe, then in a successful 10 patient validation trials where only a small amount of manual "tidy up" was needed. [20-22]

[1] Long term potato outcomes are not reported, though salt and vinegar may have been involved.

2.2. Orthopedic Robots

Robots have successfully brought computer numeric control (CNC) machining to total joint replacement surgery, where an accurate fit and alignment of the joint is crucial to ensure its stability and reduce the incidence of revision surgery. The history of both the Robodoc and the Acrobot highlight the challenges in bringing a medical device concept from early prototype through to Food and Drug Administration (FDA) approval and clinical use. Time frames often exceed 10 years, with projects passing through multiple financings and corporate hands. However, both systems are currently enabling significantly more precise implantations.

2.2.1. Robodoc

The Robodoc is reputedly the first surgical robot to complete a task autonomously. Development was begun in the late 1980's in Sacramento, CA by an orthopedic surgeon and a veterinarian, with the goal of precisely milling cavities for femoral stems during total hip arthroplasty, as an alternative to manual broaches. Bone cement breakdown was proving to be a long-term implant failure mode and the newer cement-less porous implants required a close press fit to promote bone ingrowth. The system is comprised of two parts: the Orthodoc orthopedic presurgical planner console and the Robodoc, which consists of a mobile base, a 5-axis SCARA (Selective Compliance Assembly Robot Arm), a 6-axis load cell (for monitoring cutting force) and a rotary cutting head. To use the system, three bone screws are placed as fiducials into the femur, which is then CT imaged. A 3D model of the femur is generated on which the implant insertion is planned. The patient's leg is secured in a frame, connected to the robot, and a ball probe touched to each screw to register the head. The probe is then replaced with a ball grinder and the pocket milled in the femur under CNC control.

Figure 4 – Robodoc [23].

In a laboratory cadaveric bone study the desired geometry was achieved to within 0.5 mm, with minimal gaps when using the robot. Milled cavities were only 0.54% oversized as compared to 31.33% when hand broached. Hand broaching was found to be limited by manual dexterity and the tools tended to tear out chunks of bone as well as misalign during insertion. In contrast, burr grinders provide smooth cuts, but manually they can only be used for clearing tissue, rather than precise countering. This demonstrates how robotics can enable the use of new tools and techniques. [24]

The first in vivo Robodoc trials were conducted on 26 pet canines with hip injuries. In 1992 a 10 person, FDA approved IDE (Investigational Device Exemption) trial was conducted at Sutter General Hospital, Sacramento, CA. In 1994, a multi-center, 300 patient PMA (Pre-Market Approval) study began, and a system was also installed at the Berufsgenossenschaftliche Unfallklinik, Frankfurt, Germany. Results from both trials (partial from the US study) are reported in [25]. The US study of 65 Robodoc and 62 control patients showed improved fit. However, using the robot significantly increased surgical time; with 1 hour attributable to fixation, registration and milling. Blood loss also increased due to longer

surgical time. The German study comprised 900 patients and focused on the human factors of implementing the robot and patient safety. In 30 revision surgeries the robot successfully removed cement and fibrous tissue. While the robot hardware performed adequately, in 32 cases CT, user and software errors required that the procedure be aborted and continued manually. Overall, the authors assert: “Robot assisted surgery can be performed without exposing the patient to uncertain risks. The fear of engineers that a rather powerful robot with a large workspace can endanger patients or personnel seems to be unfounded.” However, the authors also state that, while aiding in implant sizing and selection, “placing a dollar figure on effectiveness is very difficult, if not impossible.” The efficacy of the system was questioned by a study [26] of 143 hip replacements at the BG Trauma Hospital, Germany, which failed to show any clear advantages and also demonstrated technical issues.

Commercialization of the Robodoc also followed a long path, summarized in [27-29]. Initially, in 1986, the inventors partnered with IBM Research, U.C. Davis and the US division of Sankyo Seiki Mfg. Co. Ltd., Boca Raton, FL, which manufactures industrial robots. In 1990 Integrated Surgical Systems Inc., Fremont, CA was founded with IBM seed funding. CE (Conformité Européenne) approval was received in 1996; sales began and in 1997 the company was floated on the NASDAQ. In the same year the Orthodoc received FDA 510(k) clearance, but not the Robodoc, for which the PMA required study was ongoing. In 2002 this was converted to a lower threshold 510(k) filing, citing the da Vinci Surgical System as a predicate device. ISS ran out of capital in 2004 and suspended operations until 2006 when it was bought entirely by Curexo Inc., Seongnam, South Korea [30]. Clearance was received in 2008 [31] and the system is currently marketed by the Robodoc subsidiary of Curexo, Freemont, CA.

2.2.2. Acrobot

While the Robodoc operates autonomously, the Acrobot (Active Constraint Robot) is directly guided, hands-on by a surgeon. Designed at Imperial College, London as a replacement for the complex set of jigs and fixtures used to shape a patient’s femur, tibia and patella to receive total knee replacement implants, the system consists of a planning station and cutting head mounted to a micro-macro mechanism. The system uses 3D CT scan data to model the knee, size the prosthesis and plan its placement. Registration was initially accomplished by implanted fiducials, as was done with the Robodoc, but was later accomplished by probing the exposed bone at the beginning of the surgery to generate a point cloud. The orthopedic cutter is mounted to a 3DOF (yaw, pitch, extension) head that has a limited ROM and low force. Gross position of the head is accomplished by a robot arm, which locks in place for the cutting of each plane. The Acrobot is guided by the surgeon via a handle attached to the head through a 6-axis load cell. “Active constraint control” is applied whereby the robot is permitted to move freely within the defined cutting region, but as the cutting head approaches the boundaries resistance is applied. This guidance approach keeps the surgeon “in the control loop” and utilizes his “superior human senses and overall understanding of the situation to perform the surgery.” [32, 33]

Initial trials were conducted in 2002 and in 2004 the system was validated in a randomized clinical study [34], published in the J. of Bone and Joint Surgery, where 13 of 28 unicompartmental knee arthroplasties (partial replacement) were performed with the Acrobot. The results showed that angular alignment, measured with post procedure CT scanning, of the femoral and tibial components was achieved within 2° (the minimum reasonable measurable amount) for all Acrobot cases, as compared to only 40% of the traditional cases. The Acrobot Co. Ltd., London was spun off from Imperial by the

project's lead investigators and the London Technology Fund co-lead B round funding in 2007 [35]. In 2010, with a 4 hospital installed base, the Acrobot Co. was sold to Stanmore Implants Worldwide Ltd., which manufactures patient specific implants. Ten years after the initial trials, this technology underlies the innovative, personalized "Savile Row" knee replacement system, which epitomizes the precision improvements which can be enabled by robotics. Pre-procedure CT scans are uploaded to Stanmore whereupon the implant is designed and approved using an online conference. Then during surgery the same model used to design the implant guides the Stanmore Sculptor (Robotic Guidance Arm) RGA and the surgeon. As of 2012, 20 cases had been successfully completed using this system.

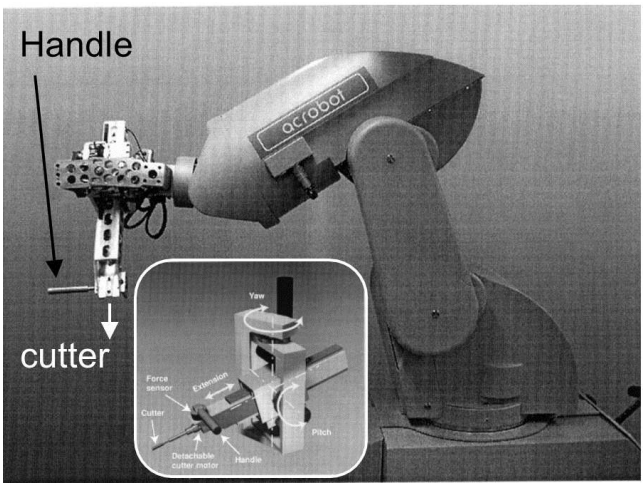

Figure 5 – Acrobot showing cutting head and robot arm [32, 33].

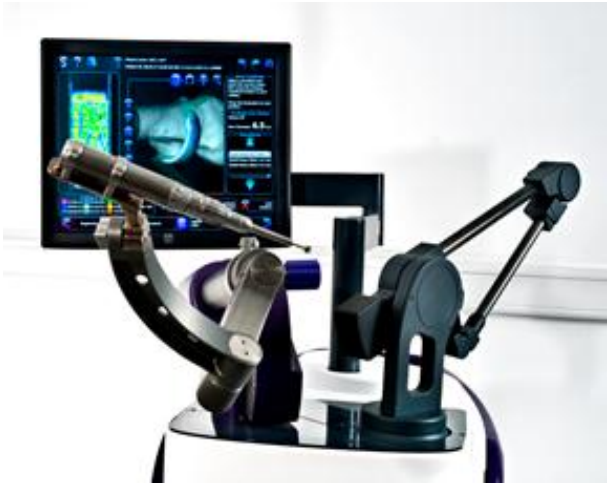

Figure 6 – Stanmore Sculptor RGA [36].

2.2.3. Zeus

A group of interventional surgical systems were created in the 1990s by Computer Motion, Inc., Santa Barbara, CA. The first system, the AESOP 1000 (Automated Endoscopic System for Optimal Positioning), was a foot pedal operated arm which held and positioned an endoscope. This received FDA clearance in 1993 and later models added voice activation and greater DOF. The master-slave, joystick driven Zeus Robotic Surgical System attached to an operating table, filtered the surgeon's hand tremors and manipulated surgical instruments. Eventually, 28 laparoscopic surgical instruments were manipulated. The first human procedures were conducted in 1998: a tubal re-anastomosis and a coronary artery bypass graft. The Hermes system networked various elements of the operating room, including the surgical table, lighting and instruments, to place them all under voice control and link them to the robotic system. The Socrates system sought to extend these capabilities to enable tele-surgery. No evidence was found that these two systems were widely accepted. Computer motion was acquired by Intuitive Surgical in 2003 after a lengthy and costly patent infringement battle. [37-39]

2.2.4. Steady Hand

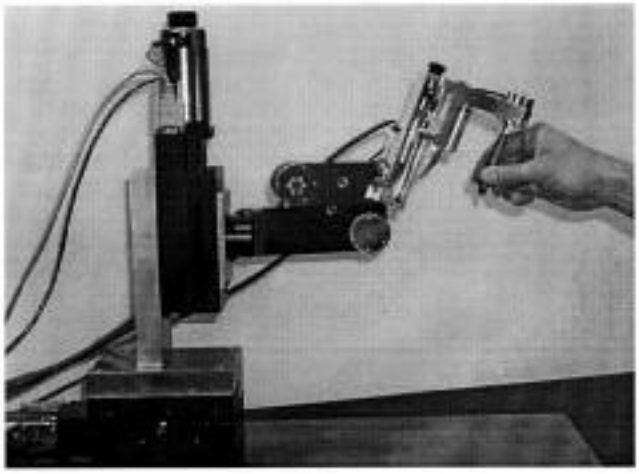

Figure 7 – JHU Steady Hand, [40].

The Steady Hand, developed in the late 1990's at John Hopkins University, Baltimore, MD, is another example of the surgeon-robot partnership, illustrated previously with the Acrobot. Its development spanned departments and made significant progress away from the industrial model of medical robotics. The Steady Hand increases the precision of ophthalmic surgery via "interactive cooperation" which enables micromanipulation. The system consists of a traditional XYZ Cartesian frame, a 2-angle DOF remote center of motion module (RCM) developed for percutaneous biopsies and discussed in Section 2.3.1, and an end piece/tool holder with axial rotation and insertion. The tool is connected to the arm via a load cell and grasped by the operator, this way the operator's commanded forces are detected. Microsugical tools, such as picks and forceps are instrumented with strain gauges to monitor the forces delivered to the tissue. A control algorithm filters out tremors, translates the operator's forces into motions and applies safety limits. As with the Arcobot, this system has the advantages over a master-slave system of transparent tool manipulation; continuing development of such systems may facilitate the introduction of more robots into clinical practice. [40, 41]

2.3. Probe Insertion Robots

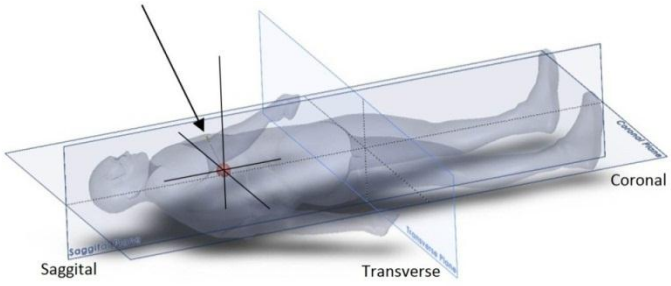

Figure 8 – Insertion of probe into a target location in patient's chest also showing anatomical planes.

A special subset of robots is devoted to the percutaneous probe insertion challenge. Typical percutaneous procedures include: needle biopsies for pathological analysis, fluid drainages, catheter placement, deep medication injection and thermal or cryo ablation of tumors. In all these cases, the practitioner must first locate a desired insertion point on the patient's skin, orient a tool about a compound angle in Cartesian space and insert it at this point, as shown in Figure 8. While some procedures can be conducted by feel, such as spinal taps, many require the assistance of X-ray, C-arm fluoroscopy or CT image guidance, which can provide coordinate positional data. When using fluoroscopy, the clinician wears a lead vest and uses graspers to reach into the beam and manipulate the probe under real-time guidance. With X-ray and CT guidance, the clinician takes limited measurements from the imaging display and uses these to manually place the probe. This often results in a procedure that is iterative and time consuming. The probe is gradually introduced to the target angular and depth adjustment alternating with imaging. This differs from laparoscopic procedures

where probes are inserted then moved relatively freely under direct visual guidance with a laparoscope. There are clear opportunities to improve percutaneous probe insertion procedures by developing robots that harness coordinate image data in guiding the instrument more directly to its target location.

2.3.1. PAKY-RCM

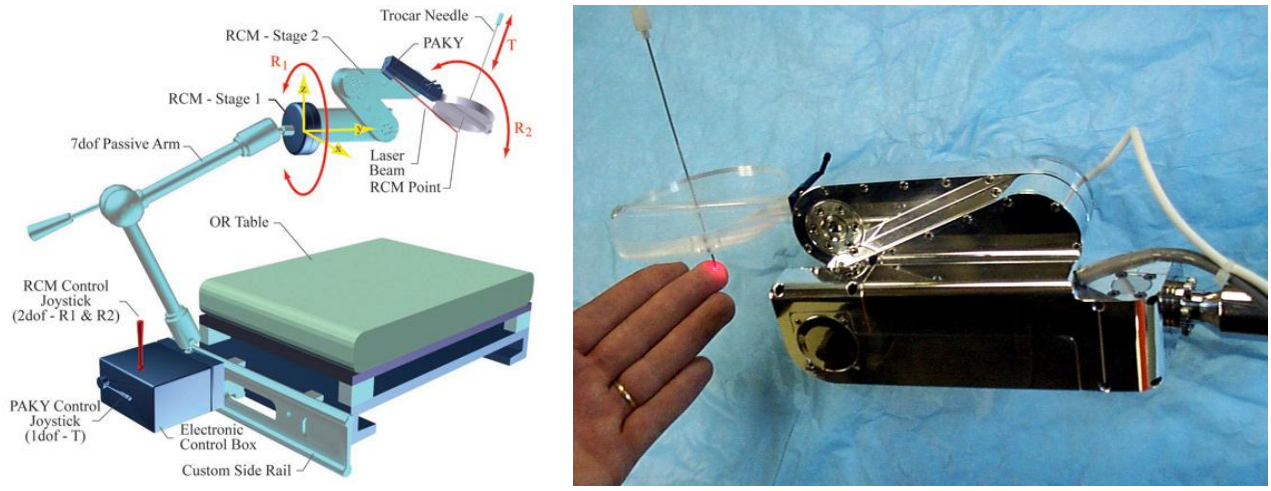

Figure 9 – Left: PAKY-RCM schematic. Right: Detail of PAKY and RCM with laser indicating the needle tip and insertion point [42].

The URobotics (Urology Robotics) program at Johns Hopkins University, Baltimore, MD, has worked on the minimally invasive percutaneous needle insertion challenge and one notable system, summarized in a 1998 paper [42], consists of the percutaneous access of the kidney (PAKY) needle driver coupled with a remote center of motion mechanism (RCM). The PAKY comprises a pair of radiolucent acrylic rollers that grip and drive a needle. The motor, with its x-ray-distorting metallic elements, is offset so as to lie outside the imaging range of interest. The driver is coupled to the compact RCM module, which tilts it in two directions about the center of rotation. A laser shines from the device and a needle is inserted until its tip just contacts the beam; this is the remote center of rotation. Subsequently, this is positioned in contact with the desired insertion point via a 7 DOF, multi-joint, passive arm attached to the imaging table. Then the clinician uses a joystick to orient and advance the needle about 3 DOF under C-arm fluoroscopic guidance. The clinician remains completely separated from the radiation field. More automated control under CT guidance is proposed as a further advancement. Recently, Johns Hopkins has developed and patented a fully non-ferromagnetic pneumatic stepper motor, capable of operating inside the MRI bore, described in [43].

Between 1997 and 2001 a 48 patient clinical study [44] was conducted at the Johns Hopkins Hospital whereby half the patients received completely manual percutaneous nephrolithotomy (kidney stone removal) and half with assistance from the PAKY. The procedure entails inserting a needle into the kidney towards the target calix(s) (stone) then passing a guide wire down its length. The needle is then removed and a series of dilators inserted until a sheath can be placed through which a nephroscope and various tools are used to remove the stones. The PAKY-RCM was used for placement of the 18 gauge needle and the primary result was partial validation of the system's functionality with 20 of the 23

procedures completed with its assistance. Mean access attempts were reduced from 3.2 to 2.2, albeit not significantly, and procedure time from 15.1 to 10.1 min with marginal significance.

A further development of the PAKY-RCM system is the AcuBot [45] which mounts it onto a bridge that straddles a patient on a CT scanner, shown in Figure 21. Added to this system is an X-Y-Z stage at the base of the passive arm; the passive arm effects gross alignment and the stage is used to place the needle tip at the desired insertion point under CT guidance and align it to the scanner's laser indicators. At all times the clinician remains in direct control of the robot's motion. Despite the AcuBot's large structure, the combined system is specialized and represents significant advancement over repurposed industrial robots.

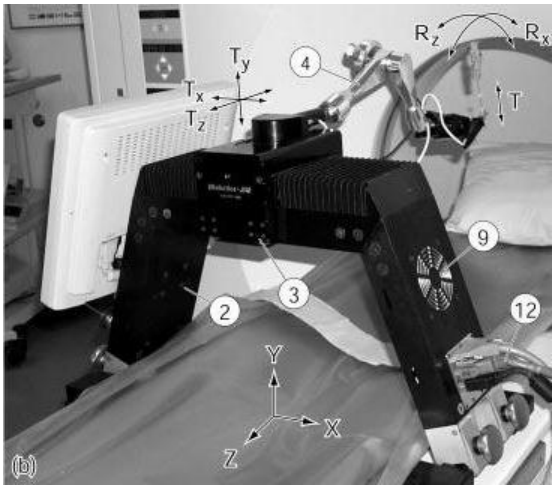

Figure 10 – AcuBOt mounted to CT table [45].

2.3.2. Piga CT

More recently, there have been commercially successful probe insertion robots. One such is the Piga CT, manufactured by Perfint Healthcare Pvt. Ltd., Madras, India [46]. The system was observed in operation during a visit to Madras in July 2011. This Cartesian robot docks to a plate in the floor of a computer tomography (CT) room and moves a biopsy needle about X-Y-Z and two inclinations. A software interface allows 3D needle path planning, from insertion point to target, directly on the CT images. [47, 48] Considering that a much smaller scale solution to the biopsy challenge is developed in Section 5, it is pertinent to review the Piga's operating procedure in Table 2.

Table 2 – Piga CT-guided Biopsy Protocol

1. Robot maneuvered and docked to fixed floor plate and system initialized.
2. Patient is placed on the bed, inserted into the scanner bore and a planning scan acquired.
3. Data is transmitted to the Piga console where the needle placement is planned from insertion point on the skin to the target.
4. Patient is withdrawn from the bore up to a set axial stop position.
5. The robot is activated and positions its end piece in 3D space, just above the selected insertion point, and angled appropriately.
6. A sterile, plastic guide bushing is placed into the robot's gripper and clamped.
7. The needle is inserted manually through the busing to the target's depth in a single pass.

From observation, the initial docking procedure involving wheeling the robot into position and engaging the plate with a foot pedal was identified as cumbersome. During positioning, the robot moved smoothly and successfully used the CT image to locate and orient the guide bushing at the desired position and angle. The disposable bushing successfully addressed the need for sterility. Placing the actual needle insertion step in the clinicians' hands reduced risk and was expected to ease the path to adoption and regulatory approval.

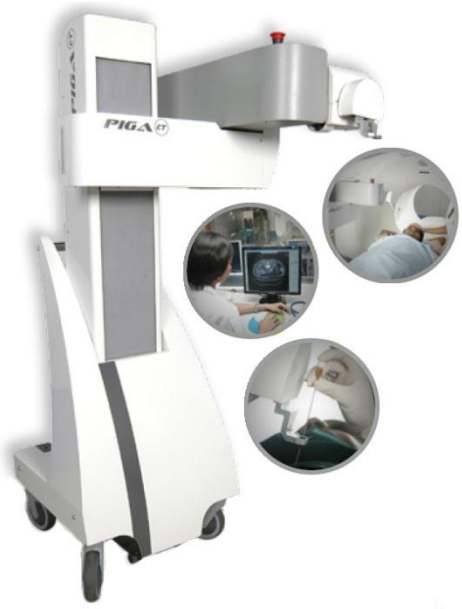

Figure 11 – PIGA CT system [47].

A significant challenge with this product, however, is the requirement that the patient remains stationary between the scan and the probe placement. Should he or she move, scanning and robot orientation will need to be repeated. Moreover, the needle must be inserted with a single pass; the system does not facilitate an incremental needle insertion and adjustment. Nevertheless, the PIGA CT shows promise, has received the European CE mark and is being tested worldwide. (Currently there is no clear regulatory procedure in India.)

2.3.3. CT Bot

The CTBot, developed at the Institut National des Sciences Appliquées and the Laboartoire des Sciences de l'Image, de l'Informatique et de la Télédétection in Strasbourg, France, targets abdominal tumor biopsies and ablation. It is ostensibly the first example of a patient-mounted robot. Described in 2004-8 [49-51], the robot consists of a 5 DOF actuator weighing 3 kg that straps directly onto the patient. Together they fit into a 700 mm diameter CT bore. The investigators identified patient motion and respiration, which causes both external and internal organ motion, as posing challenges in robotic interventions and thus, the robot is intended to rise and fall with respiration, while internal organ motion is addressed by assuming that the needle will only be inserted during the low point in a respiratory cycle.

The frame consists of a combined 6 and 4 bar mechanism that can describe an approximately spherical workspace and is capable of withstanding 20 N of force. Five ultrasonic motors with 50:1 backlash-free harmonic drives and encoders actuate the robot to translate in Cartesian space to locate the insertion point and then angulate the needle about 2 DOF. Surmounting the top platform is a separate module that inserts and simultaneously rotates the needle and incorporates 3 load cells that measure the insertion force and send it to a commercially available haptic interface. As with the PAKY, the frame is designed so as to leave a central region unobstructed with metallic elements for imaging the needle. The base also comprises integrated fiducials, in the form of a plastic block with embedded metallic rods that enable automated registration. Position guidance is provided via a point-and-click interface that uses the CT's Digital Imaging and Communications in Medicine (DICOM) data standard.

As the device improved over the years, the base was separated into two parts so that the robot could be placed in varied angular orientations as well as rapidly removed independently of the straps. Attached to the underside of the base is a bag filled with small polystyrene balls that conforms to the geometry of the patient and is then locked into position by drawing a vacuum on the bag. Testing of the device with a passive needle guide and manual insertion into a phantom yielded an accuracy of 5 mm at 10 cm depth, appropriate for the target procedure.

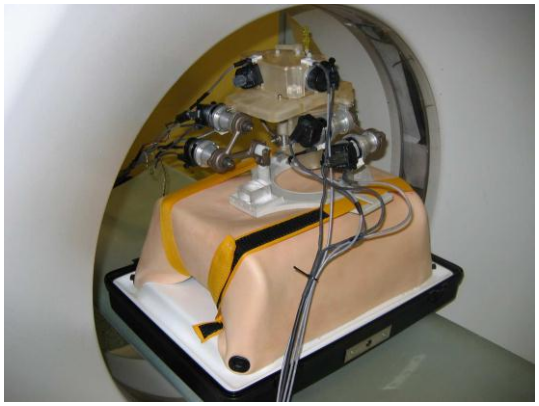

Figure 12 – CTBot on phantom in CT [50].

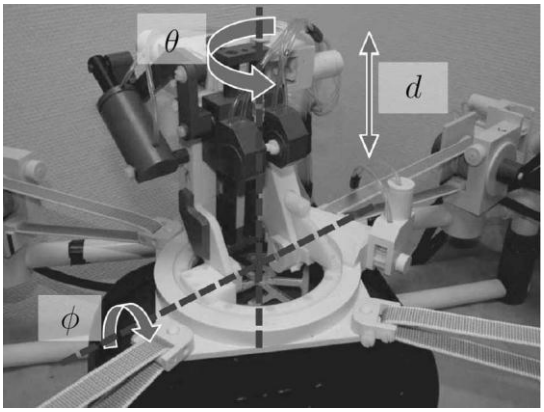

Figure 13 – Light Puncture Robot [52].

2.3.4. Light Puncture Robot

Another, similar French project, the Light Puncture Robot (LPR), was executed at the Université de Grenoble's Techniques de l'Ingénierie Médical et de Complexité Laboratoire and described in 2008 [52]. Like the CTBot, the LPR sits directly upon the patient's abdomen or thorax to account for patient motion. The entire device is fabricated from polymers and non-ferromagnetic metals which are MRI safe. The needle-holding module rotates and inclines (2 DOF), so as to access a conical needle workspace. Perpendicular straps connect the needle-holding module to a frame that mounts to the CT bed and straddles the patient. Once the robot is placed approximately in the desired location the straps are tensioned to keep it in contact with the patient and then actuated to slide the robot about in the X-Y plane. Various pneumatic actuators, including a dual ratchet and pawl that converts linear to bidirectional rotary motion, are employed and connected by 7 m tubes to a controller and compressor outside the MRI room.

The needle is held with pneumatically actuated clamps and passes through a guide in the base, which keeps it centered. Needle insertion is accomplished in a multistep procedure. First the rotary actuator positions a stop. Then a piston rapidly actuates a linkage that moves the needle clamp downwards at 9 cm/s until it reaches the stop. This rapid plunging motion closely replicates clinical practice for many biopsy procedures, particularly a percutaneous lung biopsy where a slow insertion can cause a localized depression in the lung's pleura (covering membrane). This clamp and variable-stop mechanism allows the needle to be inserted incrementally, with the clamp releasing the needle and regripping it further up to continue the insertion. Reference is made to ungripping of the needle allowing for organ motion. Both the quick plunge and needle releasing abilities were independently verified to be essential features that set this robot apart from other research efforts.

The robot's initial position is determined via a fiducial frame incorporated into the base of the needle holder, consisting of glass tubes containing a solution visible under MRI. An algorithm is used to identify and localise the needle holder's position and rotation in the image. However, inclination is not directly sensed and relies upon a known start position. Reimaging for position confirmation is possible after each step of the insertion. The physician executes control via a point-and-click graphical user interface (GUI). Phantom experiments achieved millimetre accuracy. Four in-vivo porcine experiments confirmed functionality and achieved 1 cm accuracy, which was deemed clinically acceptable, especially considering that the porcines could not hold their breath on command. One of the challenges identified was the fitting of a bariatric patient and robot with needle into a MRI bore.

2.3.5. Innomedic

At the time of the LPR project, only one other MRI compatible robot had been developed, the Innomedic [53] by Innomotion GmbH, Herxheim, Germany based on work begun in 1998 at the Forschungszentrum Karlschule, Baden-Württemberg, Germany. This robot was a large 6 DOF arm, mounted to a semicircular bridge that spanned the MRI bed and reached into the bore. This system reached a product-level of development, received the CE mark in 2005 for MRI-guided sciatic pain treatment, biopsies, drainages, etc. and a trial unit was even shipped to the US for testing in a clinical setting. In personal conversation with Innomotion's founders at the 2006 Radiological Society of North America (RSNA) conference in Chicago the technology to develop feedback-based position control with pneumatic actuators, as opposed to stepper control, took years to develop and was not publically disclosable. Additionally, while the system originally included a system for needle insertion, it was later removed to reduce complexity and address safety concerns, leaving a passive needle guide with insertion accomplished by the clinician. The system showed promise; however Innomedic was purchased by Synthes, Zuchwil, Switzerland, and no longer appears active.

Figure 14 – Innomotion system, photo origin unknown.

2.3.6. Spine Assist

The SpineAssist, and updated Renaissance system, from Mazor Robotics, Caesarea, Israel [54], brings increased precision to spinal interventions and is marketed as a way for hospitals to set themselves apart from the competition. The company's product assists with a wide range of spinal interventions including biopsies, fusions, scoliosis treatment, osteotomies and pedicel screw implant placement. The technology is based on a patent [55] filed in 2001, the same year that the company was founded, and issued in 2004. The system consists of a frame that mounts to and stabilizes the vertebrae and a soda can-sized robotic hexapod that mounts to the frame, is encased in a rubber sheath and positions an arm and guide [56]. The procedure begins with a 3D CT scan that is used to plan the intervention. During surgery the frame is attached to the patient's spine with a clamp or a supporting mount and K-wires. A plastic grid containing fiducial markers is mounted to the frame and two perpendicular fluoroscopic scans are taken, whereupon the software matches the frame to the surgical plan. The robot is placed upon the control station's base and zeroed. Then the clinician selects each vertebra where he intends to intervene and the software indicates the appropriate robot placement on the frame, as well as the correct arm and drill guide that should be fitted to the robot. As with the PIGA,

and Innomedic the ultimate responsibility for the tool insertion or implant placement relies upon the doctor. Mazor indicates that with their system 1 mm placement accuracy is obtainable, radiation dose is lowered because only a single pair of fluoroscopic images is needed and complications and revisions are reduced.

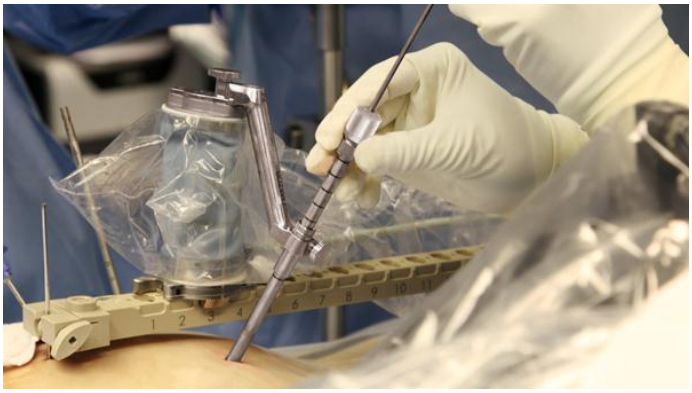

Figure 15 – Mazor Robotics Renaissance system showing frame, robot and arm with guide, through which clinicain is inserting a tool [51].

Multiple studies have demonstrated Mazor's robots' efficacy. An early 10-cadaver study [56] examined 54 implant placements, using a variety of procedures. After eliminating failures where the implant broke or bent, 47 placements were within 1.5 mm of target, with all procedure types exhibiting an average accuracy of 1 mm. In 2006, 65 clinical cases were performed in the US, Germany and Israel, with the SpineAssist aiding in the insertion of 316 screws, of which 235 (93%) were implanted as planned. More extensive studies have continued to demonstrate efficacy. In 2011 the results of a 112-case study [57] comparing traditional open (midline incision) and robot guided open and percutaneous (2-3 cm incision for clamp and 2 cm for screw placement) surgery between 2006 and 2009 were published. Out of 536 screws, 286 were placed conventionally and 250 with robotic guidance, with respective accuracy rates of 94.5% and 91.5%. Average X-ray exposure time was significantly reduced from 77 to 34 seconds, though dose was not recorded, and a non-statistical significant increase in per-screw procedure time was observed. Significant reductions in postoperative hospitalization, pain, infections and revision surgeries were evidenced with the robotically assisted procedures conducted via percutaneous approach.

Mazor has been listed on the Tel Aviv exchange since 2007 and in 2009 closed a $13 million public offering [58]. Mazor's revenue model consists of capital, disposable and service sales. These include: Capital sale of the entire system for approximately $759K, implantables valued at $6-8K per procedure, disposable clamps and fiducial grid costing $1.2K per procedure and a $76K service agreement per year. Surprisingly, despite being a much smaller robot with a more limited application, the sale price is only about half of that of a da Vinci Surgical System, described in Section 2.5. In 2010 Mazor reported $4.18 million in revenues, minus $1.01 million in cost of goods sold (COGS) for a gross profit of $3.17 million. The next product under development and approval is an adaptation of the current system for cranial applications including brain biopsies, deep brain stimulation (DBS) implant and shunt placement. [59]

In its introduction, Mazor's seminal patent [55] highlights some of the challenges associated with surgical navigation systems. Although a detailed discussion of these is beyond the scope of this work, all rely on a preoperative (or intraoperative) image and overlay images of the tracked tools, thus enabling blind access while reducing the need for x-ray imaging. Optical tracking fits tools' handles with multiple fiducials, typically reflective spheres, and requires a clear line of sight between an emitter/detector and the tool. Magnetic tracking employs a magnetic field generator and small detector coils wired to the tools, which must be nonferrous. Both methods are still limited by the clinician's hand–eye coordination

and, unless a coil can be embedded in the tool, working tip position is extrapolated and not directly sensed. An informative comparison between navigation systems, floor mounted robots and patient-mounted surgical tools is provided in [60] describing the SpineAssist's first iteration and reproduced in Table 3. This shows clear benefits resulting from smaller scale robots which reference directly to the patient.

Table 3 – Characteristics of three types of computer-aided surgery (CAS) systems: Navigation systems, fixed floor or bed mounted and patient-mounted, [60].

CAS system type	Accuracy	Operating Room space	Simplicity	Safety
Navigation systems	Accuracy is limited by the surgeon free hand motion	Requires a tracking system with either direct line of sight or non-ferrous instruments.	Requires manual spatial tool alignment based on screen image and a setup for direct line of sight	All tools are marked. No mechanical arm. Relies on a real-time tracking system.
Floor/bed mounted surgical robot	Medium relative accuracy due to the robot remote location and require to either immobilize or to track anatomy motion in real-time	Requires large space around the operating room table	Requires patient immobilization or real-time tracking	Large robot motion and high inertia potentially unsafe to the patient and staff.
Patient mounted surgical robot	High accuracy due to the robot structure and the close proximity to the surgical site	Requires minimal operating room space	No need for patient immobilization or patient attached dynamic referencing.	Small workspace in the vicinity of the surgical site. Low inertia and small motors that cannot harm the patient or the operating room staff.

2.4. Steerable Robots

2.4.1. Hansen Medical

Significant work has focused on manipulating endoscopic tools from outside the body, another class of robots is able to semi-autonomously navigate within the body. The most prominent of these is the Sensei X Robotic Catheter System produced by Hansen Medical, Mountain View, CA. The system is designed for electrophysiology procedures under X-ray guidance. Traditionally, the clinician wears a lead vest, for protection from x-rays, and stands bedside while manually threading a catheter from a patient's groin through the femoral vein to the heart. Once in the heart the catheter is curved into the ventricles and into contact with their walls. Various probes are inserted through its annulus to monitor signals, stimulate the heart so as to induce irregularities and ablate faulty tissue "wiring."

The Sensei X consists of multiple modules that, together, enable remote operation and eliminate the clinician's radiation dose. The Artisan Extend Control Catheter has a flexible, cable driven tip that extends and can execute c-shaped curves. The IntelliSense Fine Force Technology Interface provides the operator with a handle that is manipulated about 5 DOF in space (axial rotation of the catheter is not necessary) to specify the catheter insertion, curvature and direction. This is used in conjunction with the CoHesion 3D Visualization Module, which integrates C-arm fluoroscopy images and a model of the catheter position within the heart. Once in place, the sensing and ablation occurs normally.

Figure 16 – Hansen medical system showing (left to right) the catheter, the patient side base unit and the operator interface with detail of the hand piece, [61].

Hansen medical was co-founded in 2002 by Dr. Moll after leaving Intuitive Surgical and in 2005 the two firms executed a cross-licensing agreement [62]. Industry, experience clearly shortened the development and commercialization process and in the following year Hansen went public. In 2007 the early Sensei Robotic Catheter System and the Artisan Control Catheter received FDA 510(k) approval and a CE mark, Hansen made its first sale and a European subsidiary was opened. Approval of the newer Sensi X and Artisan Extend was received in 2009 and Hansen is actively partnering with Siemens and Phillips.

A recent study at the Texas Cardiac Arrhythmia Institute, Austin, was conducted with 197 patients receiving radio frequency ablation treatment for atrial fibrillation via manual catheter manipulation and 193 via robotic navigation [63]. An increased success rate from 81 to 84% (with medication previously ineffective) was observed and mean fluoroscopy time dropped from an average of 58.4 to 48.9 min. A significant learning curve was observed, with robotic procedure times longer for the first 50 procedures and overall no faster than the manual procedure. This demonstrates the observed trend toward increased procedure times with the use of robotic surgery.

2.4.2. TU Delft

Extensive and promising work has also been conducted into miniature, steerable robots at TU Delft, Netherlands, by Prof. Paul Breedveld. A summary of recent work is provided in [64] which has focused on the mechanics of small, highly flexible scopes and graspers; the smallest 0.5 mm in diameter for retinal surgery is pushing the boundaries of manufacturing technology. One of his key innovations is to eliminate the jointed segments, seen in Figure 16, and use instead a tight ring of cables that operate in both tension and compression, which were inspired by squid tentacles. Currently, manual tools are being developed by the spinoff Deem Corp., Amsterdam, but there are clear robotic applications.

2.5. daVinci Surgical System

The most recognized medical robot and the only one to have gained significant market traction, is the pioneering da Vinici Surgical System, from Intuitive Surgical, Inc., Sunnyvale, CA [65]. The da Vinci's technology originated during the late 1980's at SRI International, an independent, non-profit research institute (formerly Stanford Research Institute), under contract with the US army to develop a system for conducting battlefield surgery. Intuitive Surgical was founded in 1995 with Dr. Frederic Moll, a surgeon with previous medical device experience, with Mayfield Capital venture funding; later funding came from Sierra Ventures and Morgan Stanley Ventures. The system operates in a master-slave configuration and consists of two main parts: the patient side cart, shown in Figure 18, with four robotic arms that manipulate minimally invasive tools within the patient, and the surgeon console from which the robot is controlled. The system launched in 1999 and in the following year the system received FDA approval for general laparoscopic procedures and the company went public. The da Vinci has been approved for thorascopic, cardiac, urological and gynecological applications and was initially targeted for cholecystectomies (gall bladder removal), though it is currently predominantly used for minimally invasive prostatectomies. [66] Effectively, the daVinci is the de facto benchmark against which all other medical robots are currently compared. Intuitive's technology is protected by 160 US and 60 foreign wholly owned patents and 260 US and 165 foreign licenses.

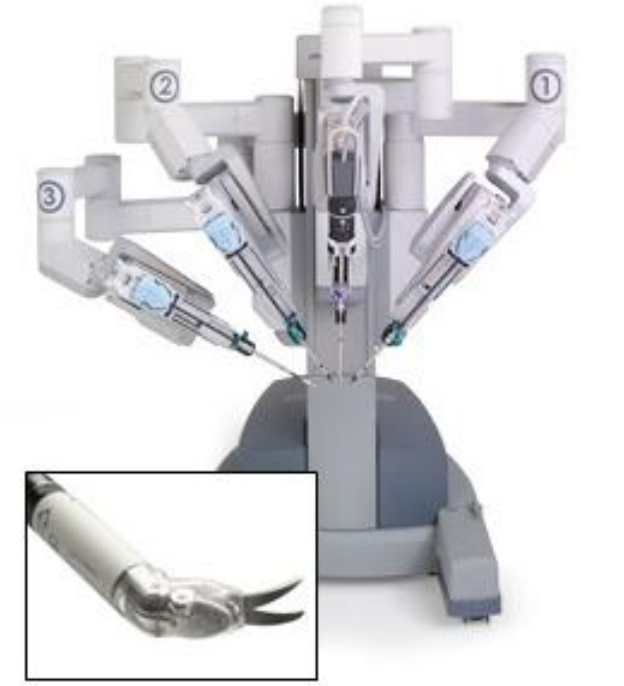

Figure 17 – da Vinci patient-side cart and sample EndoWrist attachment [65].

2.5.1. System & Safety

During a procedure the patient is prepped, positioned on the surgical table and four 5 or 8 mm trocars placed into his or her abdomen. The robot arms then insert instruments through these trocars and move them about 4 DOF: advancement, rotation and two angulations. Intuitive's EndoWrist instruments have intricate 3 DOF cable-driven wrists at their distal ends, which deliver cutting, grasping, retracting and cauterizing functions and are able to execute complex sutures. This allows the surgeon to regain the two degrees of freedom, normally restricted by the trocars, as well as execute a gripping motion, yielding 7 DOF total. The operator sits remotely at the console, views the laparoscope through stereo eyepieces and manipulates two hand pieces to control the robot arms. Though force feedback is not implemented, the control system provides motion scaling and tremor control. [67] One foot pedal "clutches out" tools, so that the hand pieces can be repositioned when they reach an awkward configuration, and the other switches control between the four arms. Each instrument is tracked with a

barcode and limited to 10 uses. The entire patient-side cart and arms are shrouded with a single-use, sterile drape. In the latest iteration, the da Vinici Si HD Surgical System provides a second console for observation or training.

Figure 18 – da Vinic Si HD, showing dual consoles [65].

Multiple safety layers exist to prevent unintended motions. Should the operator remove his head from the console all tools lock; they are only reactivated by positively engaging the handles and "clicking" both grippers. A "disable" button is located on each arm and, because the surgeon is remote from the patient, a resident or nurse is expected to remain besides the table at all times, ready to disable and manipulate the tools manually. A search of the FDA's Manufacturer and User Facility Device Experience (MAUDE) database [68] turns up relatively prosaic instrument defects and breakages as well as reports of system errors and arm lock-ups, which required conversion to open procedures, reboots and service visits with hardware replacement as well as a few reports of unintentional tool motion outside the camera's field of vision causing harm. However, overall the da Vinci has a good reputation for safety.

2.5.2. Adoption & Financials

Adoption of the da Vinici has grown steadily since 2003, as shown in Figure 19, and hospitals have found its use in advertising campaigns to be effective. According to Intuitive's 2008 annual report [69], 335 systems were sold in 2008, bringing the installed base to 1,111 (825 in North America, 194 in Europe, 92 elsewhere) and 136,000 patients treated, an increase of 60% over the preceding year, primarily for prostatectomy and hysterectomy. In the case of cancerous hysterectomy, the system is reported to reduce average hospital stays by 6.3 and 1.2 days as compared with the open and manual laparoscopic procedures, respectively, which represents a reduction in hospitalization costs. Total revenues of $874.9 million were recorded for 2008, an increase of 46%, comprised of $455.3 million for systems sold and upgraded, $293.0 million for consumables and $126.6 million for system service. Gross profit was $620.8 million and income $204.3 million. Revenue per system sold has steadily increased from $1.18 million in 2006 to $1.34 million in 2008. Usage per unit was estimated at once every three days, with that number expected to increase.

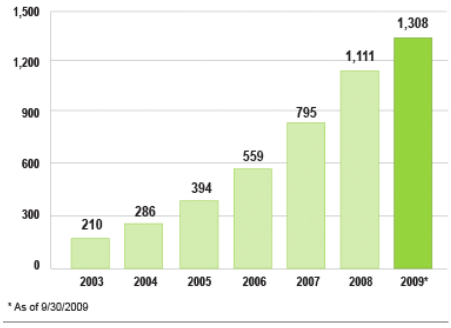

Figure 19 – "Worldwide da Vinci Surgical System Installed Base" [70].

Figure 20 – Billboard located above the Massachusetts Turnpike showing Dr. Ingolf Tuerk from St. Elizabeth's Medical Center, Brighton MA, photo by David L. Ryan, Boston Globe, [71].

2.5.3. Efficacy & Cost

While the da Vinci was initially intended to excel at challenging cardiac and narrow surgeries, where precision is of utmost importance, these procedures carry the highest risk and, consequently, the highest barriers to entry. Instead, to date, the system has found most use in the conduction of prostatectomies, where potential loss of erectile function is a (non-lethal) risk that resonates with patients. Surprisingly, despite many studies, no randomized prospective studies have been conducted to compare da Vinici surgery outcomes with those of experienced surgeons conducting traditional laparoscopic or open prostatectomies. The results of retrospective studies are variable, though the system is popular with clinicians. While the system's engineering and performance is impressive, the costs of acquiring and using the da Vinci system are significant and, potentially, representative of medical care's unsustainable upward cost trend. Notably, the clinician on the billboard in Figure 19 asserts that he can obtain equal or superior results without the robot [71]. Multiple studies demonstrate inconclusive results regarding the clinical benefits of robot assisted laparoscopic prostatectomy (RALP) and sharply question its cost effectiveness.

One retrospective study, conducted at Tulane University Medical Center's Department of Urology, reviewed 78 robot-assisted laparoscopic, 16 retropubic and 16 retroperineal radical (complete removal) prostatectomies conduced over 22 months, with the results reported in [72]. The average robot-assisted procedure time was 262 minutes; however there was a clear learning curve with the first 20 cases averaging 404 minutes and the last 20 225 minutes, a decrease of 42%. In contrast, the manual retropubic and retroperineal procedures were significantly shorter, averaging 202 and 196 minutes respectively. Blood loss was less for the robotic surgery. No significant differences in post-operative changes and outcomes were noted. Highlighting the possibility of medical robotics to be a skills leveler, Burgess et al. state that "many practicing urologists are not adept with advanced pelvic laparoscopic procedures" and thus "robotic technology has the potential to alleviate the technical difficulties associated with pure laparoscopy and thus allow more urologists to offer minimally invasive prostatectomies." While the investigators were unable to examine actual hospital costs, the gross billed charges indicated average operative charges of $25K for robot-assisted surgery as compared to $17K

and $16K for the conventional retropubic and retroperineal approaches. (Capital costs were excluded from this analysis.)

In one paper [73], Hu et al., use data from 2003 to 2007 to compare 1938 minimally invasive prostatectomies[2] against 6899 open procedures. They report shorter hospital stays, a decrease in some in-surgical complications and an equal rate of additional therapy, however the rate of postoperative genitourinary complications increased twofold and there is an increased rate of post procedure incontinence and erectile dysfunction rates. It is noted that this may be due to reporting bias, possibly due to a "heightened expectations." This is drawn from [74] which demonstrated that some patients are dissatisfied with their robotic surgery having expected "better" outcomes commiserate with the system's successful direct-to-consumer publicity. Outcomes improved significantly with surgeon volumes, further indicating a learning curve that lasts longer than the 2 day training session. Reviewing demographics, white and Asian men were more likely to receive minimally invasive surgery, as were patients living in areas of higher education and income. This is postulated to be due to robot-assisted surgery's marketing demographic and access to appropriate surgeons and hospitals.

A large retrospective study was conducted by the University of Texas Southwestern Medical Center [3]. Citing European studies that have shown increasing costs from open retropubic to manual laparoscopic to robot-assisted laparoscopic prostatectomies, Bolenz et al. conducted a detailed, retrospective analysis of the direct costs associated with 643 patients treated by experienced surgeons. Costs were normalized to 2007 rates, and results indicated significantly higher costs for robot-assisted procedures, averaging $6,752 as opposed to $5,687 for laparoscopic and $4437 for open surgery. The primary drivers of the cost were consumables at $2015, $725 and $185, respectively, and operating room time billed at $12.9 per minute, resulting in costs of $2798, $2453 and $1611, respectively. Robot-assisted procedures took significantly longer and a slight learning curve was observed. The robotic procedure employed EndoWrist instruments including two needle drivers, a grasper, a forceps, a Hot Shears and a ProGrasp, each costing $220 per use when averaged over their 10 use lifespan, and a PlasmaKinetics sealer costing $250 per use. Manual laparoscopic procedures used cheaper, disposable tools and open surgery was relatively inexpensive. If the $1.4 million robot purchase price is amortized over 7 years and the $140K annual maintenance costs are divided by approximately 126 cases per year, an additional $2,700 are added to the robot-assisted procedures for a per procedure total of $5,013, more than the traditional open retropubic procedure.

This Texas paper pointedly asks: "Can the robot become cost competitive with the other approaches?" The authors conclude: "To date, there is not enough evidence of a significant improvement in patient care with RALP to justify the high added cost." In a postscript editorial comment, Dr. Markus Graefen seconds this conclusion with: "… the fact that RALP is extraordinarily more expensive than open RP will not change …" and "Robotic surgery is a fascinating approach … however, a growing body of evidence shows that the results of RALP are not superior to other surgical approaches. It is certainly up to urologists to give the patient a realistic view of what he can expect when

[2] Lacking a separate CPT code it was not possible to conclusively, retrospectively identify procedures that were robot-assisted.

prostate surgery is performed. Furthermore … we must be aware of our responsibility to society and to our patients to deliver the best possible care at justifiable cost.”

3. Implications for the Future of Robotic Surgery

As the preceding literature review demonstrates, progress is being made in the development of robotic surgery. However, of the few robots to achieve market success, the Robodoc, Stanmore Sculptor, Piga CT, Spine Assist, da Vinci and Renaissance, all but one still embody the cost and stature of industrial robots. The da Vinci, the market leader, represents both a high capital and disposable cost, while delivering RALP's outcomes that are comparable to those of a skilled surgeon performing either minimally invasive or traditional open prostatectomies. With increasing use in more challenging, minimally invasive procedures, it may become easier to demonstrate efficacy. While Intuitive's success is predicted to continue, the remarkably multifunctional nature of the da Vinci's design makes it inherently expensive, and this will eventually lead to a ceiling on the upward trend of the installed base shown in Figure 19.

Intuitive's ground breaking work in the medical robotics field has led to many discussions as to the cost-effectiveness of robotic surgery, both in literature and the medical community. In February 2010, the Boston-based Center for Integration of Medicine and Innovative Technology (CIMIT) [75] hosted a weekly forum entitled "Current Status of Robotic-Assisted Surgery and the Challenges Ahead." Dr. Bob Nguyen from Children's Hospital presented his personal experience with the da Vinci Surgical System. He spoke positively of increased dexterity, tremor control and the comfortable interface, and asserted that the robot facilitated better suturing and decreased scarring. In contrast with the reports of Section 2.5.3, he estimated that it is 9% cheaper to do surgery robotically, due to reduced hospitalization, and 15% more profitable. This presentation sparked a lively debate where a common theme in the research-focused audience, was the need for increased competition despite many blocking patents, such as the 160+ protecting the da Vinci. Features envisioned for new robots in medicine include self-guidance, integrated ultrasound, autonomous operation inside the body, haptics, heads-up displays, addition of sensors, tools and software to process images, improved tissue joining via automated suturing, laser "welding" and tissue glues.

The work of Intuitive Surgical has introduced clinicians and patients to the potential for robotics to contribute to interventional medicine. In the book, *Advanced Gynecologic Endoscopy* an entire chapter is devoted to asking *Do costs of Robotic surgery matter?* [76]. This provides a summary of the advantages, limitations and costs of using the da Vinci System and concludes that the robotic surgery does not yet, but must pay for itself on a per-procedure basis. Dam, et al. suggest ways to reduce operating costs, including limiting the variety of tools used, training dedicated specialist surgeons to reduce procedure time and steering only complex cases to the robot. However, in the long term "the future of robotics looks bright as robots will become even smaller and easier to handle, surgeons will get better performing robotic surgery, and eventually robots will become cheaper as almost all electronic devices did when they became more mature with many competitors on the market." There is clearly room for disruptive technologies in the medical robotics space.

4. Medical Device Prototype Design Process

Key to the design and rapid prototyping of medical devices is a structured process that encourages creative solutions and is documentable, as will be required for FDA approval. One such is the deterministic design process, described in [77-79]. This evolved from the scientific method in combination with industry best practices. The scientific method proposes a hypothesis, designs and conducts experiments and then modifies the hypothesis accordingly. The deterministic process begins with identification of the (clinical) challenge and careful examination of the solution space. At each step of the way functional requirements (FRs) are identified and potential solutions (mechanisms) brainstormed. Research, analysis and hands on experiments are used to make a selection from amongst the options. Peer review with engineering colleagues and clinicians helps to refine the design and at each step, potential failure points (risks) are identified and solutions (countermeasures) developed. As the design moves from coarse to fine, unknowns are minimized and the design's essential elements are retained; the process is biased towards producing a lean, minimally complex prototype solution on time and on budget. Good record keeping is essential through the process. Each finding and step of the design must be noted and archived. This will form the basis of any IP filings, as well as the design history file which the FDA requires for all medical devices in order to file for approval as well as continued compliance.

This process has been adapted and iteratively optimized for use in the MIT Precision Machine Design course (2.75) which has focused on medical device design for the last 9 years. In this course, student teams successfully take a clinician's challenge to a proof-of-concept prototype in only 14 weeks. During the last four years teaching, particular effort has been made to structure the process and identify those steps particularly pertinent to designing medical devices. Three distinct phases, which roughly break the course into thirds, have been defined and are shown in Figure 21 along with their sub-steps.

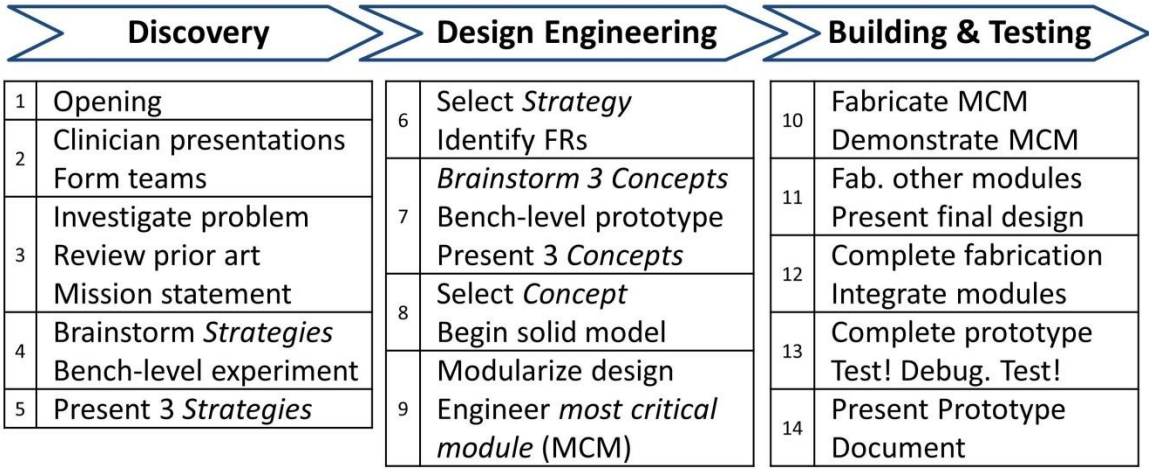

Figure 21 – The three-phase deterministic design process, as taught in the Precision Machine Design course and applied to designing electromechanical solutions to medical challenges. Numbers correspond to the 14 weeks of course.

The first step of the process is to develop a deep understanding of the clinical practice pertinent to the challenge identified. Each summer clinicians who have identified challenges in their practices submits applications, of which a subset is selected for presentation to the course. From these

presentations, student teams of 3-5 persons each are formed, whereupon the *Discovery* phase begins. Firstly, the problem is precisely defined from discussions with clinicians and by first-hand visiting the clinical settings to carefully observe the current procedures and equipment. If practical and permitted, notes are taken along with the capture of video and still images.[3] Interviewing a clinician is also a distinct skill; it does not suffice to simply ask "What can be better?" It is best during the discovery phase to steer the discussion towards function, rather than the form of the current tools or techniques. Experience has shown that initially clinicians often seek minor improvements rather than full solutions, because of a reluctance to completely rethink the tools and protocols that they are familiar with.

Rather than developing a robot or device with which to conduct the entire procedure, à la da Vinci, this design method specifies narrowing the design challenge to a tightly constrained set of tasks. Using the information gathered, the procedure is decomposed into discrete steps, as is demonstrated in Section 5.3, and portioned between the clinician and the proposed robot (or tool). The design team should then conduct a virtual "muda walk" [4] to identify inefficiencies - those tasks which, while essential to the procedure, are time consuming, challenging, limit precision or do not necessarily add substantial value. This is an adaptation of industrial value stream mapping [80] as well as Fredrick's Taylors' Scientific Management [81] that sought standardization and optimization in place of craft production. Given the uniqueness of each patient, medicine is still very much as craft practice; however there is evidence that standardizing some treatment paths, as shown in Figure 27, and protocols to encompass evidence-based best practices can improve patient care. In developing the Robopsy System, Section 5, the CT-guided biopsy procedure was identified as unnecessarily challenging as a result of the current manual clinical technique which underutilizes the CT scan's full 3D positional data. Similarly, the improved morcellator design, Section 6, is proposed as a means to automate the removal of large excised tissue masses through minimally invasive incisions. Coming at the end of a procedure, the task required minimal skill and was time consuming and repetitive. Table 1 provides an excellent guide to parsing out those tasks which lend themselves to robotic integration. Tasks identified as inefficient are then used to generate a broad set of Functional Requirements (FRs) and define a mission statement that concisely summarizes the project's goal. Through, the goal is to maximize the functionality / complexity ratio.

Simultaneously, it is necessary conduct a prior art review to identify existing products, patents and literature pertinent to the current procedure. If affordable, samples of existing devices should be acquired for hands-on testing and disassembly. Utility patents often provide inspiration for mechanism design and, by tracking the inventors and assignees, a history of the development of current devices. However, patent searching proves a greater challenge then identifying products; a 2011 USPTO report [82] identifies *Medical Devices* as spanning 20 classes and numerous sub-classes, covering from bandages to imaging methods to surgical tools. The report's data from 1998 to 2011, plotted in Figure 22, shows a steady increase in patent issuance. Interestingly, the three companies with the highest

[3] In some clinical settings detailed chronometry is not permitted; it is felt that an overt focus on procedure time could pressure clinicians and result in compromised patient care.

[4] The term "muda walk" is commonly used to describe an industrial engineer's physical walk through a factory floor to identify wasted actions.

number of patents issued in 2011, Medtronic Inc. (336), Cardic Pacemakers Inc. (307) and Boston Scientific Scimed Inc. (401), are all operate in the same market space. As afore mentioned, the MAUDE database can also provide insight into current tools' shortcomings. Likewise, as seen in Section 2, engineering literature provides background into past advances in the field as well as developing trends, while clinical publications focus on the validation of new technologies. In addition, they deliver background data on clinical conditions, such as cancer rates, and the current best practices for treatment procedures. Prior art should be frequently revisited as the design process continues.

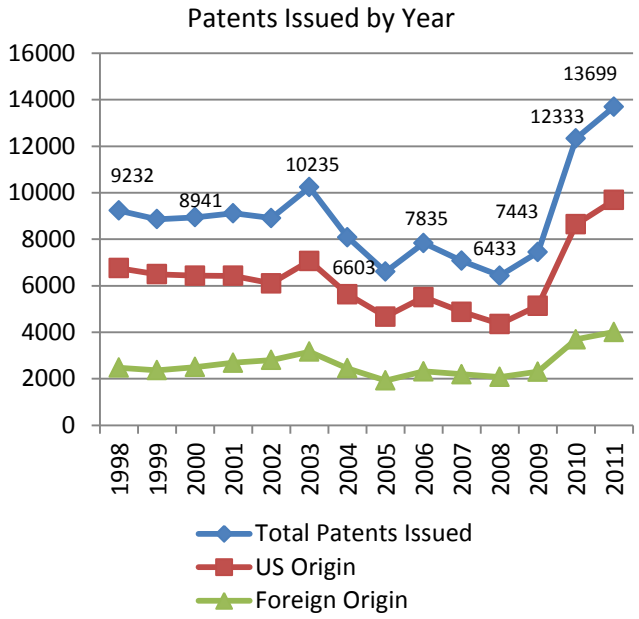

Figure 22 – Foreign, domestic and total US patents issued by year, select data shown from [82].

The next step is to develop possible solution *strategies*. These are intended to be broad approaches, rather than specific mechanisms, of fulfilling the Mission Statement. Clinicians should be encouraged to participate in creative brainstorming. Sketches and calculations in design notebooks are preferred over CAD and Matlab® models which may result in premature "locking down" of a solution path. Further literature review, analyses and bench-level experiments are conducted to evaluate each proposed solution. In house fabrication of test mechanisms enables rapid iteration and controls costs.

With the selection of the strategy the *Design Engineering* phase begins. Based on the detailed problem understanding and the selected strategy, the FRs are enumerated and become more explicit, such as "orient a needle about two angles," and are accompanied by clear specifications, such as the desired torque and ROM. Specifications are often identified by hands-on bench-level testing with measurement equipment, as shown in Figure 32. Next specific mechanism concepts are developed that execute the chosen strategy and fulfill the functional requirements. These are often mocked up and tested and at this point in the design process it is appropriate to begin developing CAD models. With the selection of the desired concept, the basic mechanism and its desired operation are understood.

The next step is to modularize the design, with each module comprising a specific device function. Those modules that are fundamental to device operation and will comprise the core intellectual property (IP), should receive attention first. For example, in the John Hopkins's needle driving system the PAKY and RCM are the most critical modules since they are directly responsible for the placement of the needle into the patient and incorporate novel mechanical designs, while the support arm represents a less critical module and hence a lower design risk. It is essential throughout the process to continually examine the design and operating protocol for potential failure points and from user and patient safety perspectives.

During the *Building and Testing* phase the detailed design and CAD modeling of the most critical module (MCM) is completed. Once the most critical module's fabrication is planned and underway, work can commence on the supporting modules. As the design develops, placing even partial physical prototypes into clinicians' hands elicits far superior feedback than CAD renderings or sketches. As will be shown, testing continually with potential users is essential to differentiating between essential features and those that are either "nice to have" or downright unnecessary. Outside fabrication facilities are often used such as machine shops and, increasingly, 3D printing facilities. The latter is used extensively for speed and to complex geometries, with many integrated features and compound curves, such as those in ergonomic handles. Care must be taken, however, against designing parts that can only be realized with low volume 3D printing; even at the prototyping stage, focusing on manufacturability is critical to producing cost effective solutions. Table 4 provides a summary of various fabrication techniques and their functionality.

Table 4 – Prototype Fabrication Technologies

Method	**Comments**
Machining	Wide range of materials, i.e. polymers, metal Complex parts challenging, expensive Feature size ~0.003 – 0.001" Precise fits and finishes can be specified Labour intensive, hence longer lead times than other processes
Abrasive water jet (AWJ)	Cutting without heat affected zone (HAZ) Limited to 2D geometries Brittle materials pose no challenge Layered composites can delaminate Feature size ~0.010" as a function of thickness
Stereolithography (SLS)	Part built with laser hardened epoxy layers Properties mimic nylon, but lower toughness Prone to embrittlement duet to exposure to normal light Low post processing With post processing feature size 0.003" horizontally & 0.01" upwards Parts require post fabrication sanding and fitting
Fused Deposition Modeling (FDM)	Part built with extruded polymer threads Good toughness Poor feature control
Resin casting	A flexible silicon or urethane mold made is from an existing part or 3D printed prototype and filled with liquid polymer Good for ~10x uses Good feature reproduction, certain geometries challenging, i.e. deep cavities
Rapid Machining	Fast machining of parts directly from CAD in polymers and metals Machining instructions generated automatically Slightly lower tolerances than high-precision machining

With the prototype complete, testing can begin, first in the lab and then in a clinical setting. The first testing should be conducted on phantoms and, while these need not look anatomically correct, they should be crafted to represent the appropriate tissue conditions. Ex-vivo animal organs from a slaughterhouse can also be obtained and used to validate mechanical function. Only once confident in the solution, is it ethically appropriate to conduct a live porcine trial. As an alternative, it may be possible to utilize a deceased porcine or piggy back on the protocol of another researcher's porcine experiment. In vivo tests should attempt to fully simulate the procedure and in doing so will often turn up hitherto unnoticed human factors issues. The basis of this testing is used to identify points where the device does not integrate smoothly into the existing procedure, as was the case with the Robopsy system's interface, and refine and redesign.

The overarching goal of this process is to maximize the exploration of options, while rapidly converging on a solution that exhibits minimal complexity. It is hypothesized that an efficient design process will tends towards the development of efficient solutions. Having reviewed the current trends in medical robotics, it is further suggested that this may be and effective means of developing disruptive technology. This design process was closely followed in the development of the Robopsy System, Section 5, and optimized over through the development of the Medical Device Design Class, Section 7. The improved morcellator, described in Section 6, demonstrates the rapid convergence on a concept from a clinical need and subsequent prototyping.

5. Robopsy – Robotic Biopsy System

5.1. Introduction

The Robopsy (Robotic Biopsy) project began in the Precision Machine Design course in the fall of 2004 working with Steven R.H. Barrett, Conor J. Walsh and Dr. Rajiv Gupta who was training in interventional radiology at Massachusetts General Hospital (MGH). Dr. Gupta observed the need for a better way to conduct CT-guided percutaneous needle biopsies (PTNB) of the lung and, in general, CT-guided insertion of probes into a patient. With training in Electrical Engineering and over ten years' experience at the University of Southern California and General Electric's Research and Development Center, he saw robotic technology as the solution and articulated the project mission statement:

To create a robotic needle guidance system to assist radiologists in targeting lesions during CT-guided lung biopsies.

The current PTNB procedure is iterative and time consuming, even when executed by a clinician with sufficient skill and expertise. Each step of the needle insertion, from skin surface to target point, requires that the clinician alternate between acquiring a CT scan of the patient and adjusting the needle position until it transits from the insertion point to the target location. Each cycle of needle manipulation and scanning necessitates moving the patient into and out of the bore and the clinical team shuttling from the radiation shielded control room to the CT room. Current CT scanners can provide imaging of structures on the order of 0.5 mm as well as 3D coordinates; however, with the current procedure, whereby the clinician measures angles and depths on the CT slices and manually transfers these to the needle during positioning, the target nodule size is effectively limited to approximately 5 mm diameter. The limiting factors are the clinician's dexterity and ability to perceive angles, as well as tissue characteristics that can cause the needle to "spring back" after positioning. The effects of Abbe error on targeting lesions is demonstrated in Figure 23. When aiming at the centre of a 10 cm deep lesion (bariatric patient), a clinician needs to achieve angular accuracy of 3° if the lesion is 1 cm in diameter and 5.5° if the lesion is 2 cm in diameter. In Table 1 dexterity is listed as a human weakness while geometric accuracy and integration of numerical data are robot strengths. The opportunity for a robot to address the targeting challenge while utilising the clinician's judgement to increase procedural efficiency was apparent.

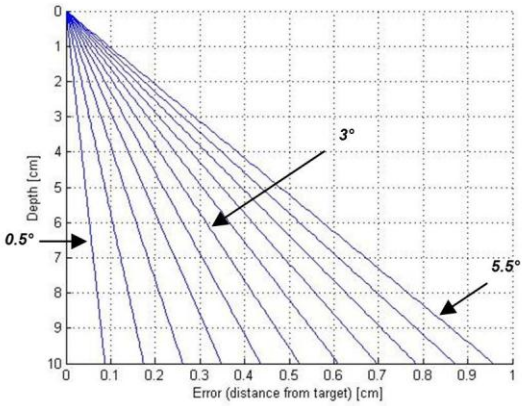

Figure 23 – Abbe Error – As depth increases, small angular errors lead to increasing lateral errors.

5.1.1. Significance

Lung biopsies were identified as one of the most challenging biopsy procedures, due to the care needed to access a desired target through the ribcage while avoiding vessels and cleanly penetrating the lungs' pleura. Any tears of this membrane increase the risk of a post-procedure pneumothorax, full or partial lung collapse. Furthermore, according to the American Lung Association 2012 data [83], lung

cancer is the most deadly cancer in the US, killing more people annually than colon, breast and prostate cancers together, and accounting for 28% of deaths. In 2012 an estimated 226,160 new cases will be diagnosed while 160,340 Americans will die from it; sadly 90% of cases are traceable to smoking. The annual costs of lung cancer treatment are estimated at $10.3 billion. Only 15% of cancers are diagnosed while localised within the lung and for these the 5-year survival rate is 52.6%; for later diagnoses survival rate plummets precipitously. Earlier diagnosis clearly leads to improved survival rates; however, preventative screening of at risk persons is not standard practice, while it is for breast, colon and prostate cancer.

Acquiring a diagnostically significant sample from a small lesion requires practice and success rates vary between institutions and clinicians. Nodules on the order of 5 – 10 mm are considered the minimum size targetable. Radiologists report that the CT-guided lung biopsy procedure is fatiguing, due to the challenge of accurately placing the needle while avoiding surrounding structures. Additionally, it is especially challenging to target specific portions of a lesion, such as those which have been shown to be metabolically active on a positron emission tomography (PET) scan, as well as collect samples from multiple sites in a lesion, which would be beneficial since the central portion often contains inconclusive necrotic tissue. The limits on targeting size leads to "watchful waiting" where by small lesions are scheduled for observation rather than a biopsy. This results in both a worried patient and a missed opportunity for early treatment, potentially with a minimally invasive brachytherapy or radiofrequency (RF) ablation therapy. Both of these procedures also require the guided placement of probes.

A 162 patient study [84] focusing on small solitary pulmonary nodules showed significantly decreasing rates of diagnostic success, defined as true-positives and true-negatives. For nodule ranges of 20 – 16 mm, 15 – 11 mm and under 10 mm rates were 91.5%, 74.4% and 52% respectively. Due to the low accuracy rate, follow up CT scans of lesions less than 10 mm were strongly recommended. Similarly, as depth increased success rates decreased from 95% for depths under 10 mm to 12.5% for depths greater than 81 mm. The overall pneumothorax incidence rate was 28.4%, positively correlated with the number of punctures and depth. It is important to note, however, that equipment and technique was a factor: The investigators employed a single 22 gauge (0.644 mm) Wescott needle which was removed after aspiration and the sample inspected by the cytologists; when the sample was found inadequate the needle was reinserted creating a new puncture. In contrast, the technique at MGH employs coaxial needles which are inserted, the stylet removed and a thinner needle deployed to collect samples; the stylet can be replaced and the needle left in place while the sample is examined. Regardless, this highlights the importance of accurate biopsy needle placement on the first pass.

CT-based screening, with its high resolution 3D data enables the detection of small, early stage lung nodules. The National Cancer Institute funded *National Lung Screening Trial* was begun in 2002 to investigate whether CT-based screening could improve upon X-ray based screening, which has not been shown particularly effective in reducing mortality, and results [85] were published in 2011. An at-risk population of 53,454 current or past heavy smokers received either a helical CT scan or a standard chest X-rays annually for 3 years at 33 medical centres. Data was collected from 2002 to 2004 and patients were tracked until 2009. Over all visits, subject receiving CT scans had a 24.2% positive rate of screening tests versus 6.9% for x-rays. Positive tests resulted in further evaluation and for each group, respectively, 96.4% and 94.5% were false positives, with most detected non-invasively through

observation of non-growth during follow-up. In total, 1060 versus 941 cancers were diagnosed with mortality of 247 versus 309, representing 20% lower mortality amongst the group receiving CT than receiving X-ray screening. Complications amongst those receiving invasive bronchoscopy or needle biopsy were rare, with deaths generally attributable to cancer. Clearly further studies are needed to definitively demonstrate screening's efficacy; however, it is likely that screening will increase, resulting in the detection of more small nodules that require biopsy.

Although CT-guided biopsies are considered safe and can be tuned to deliver low doses, they are recognised as delivering more radiation than other diagnostic techniques, such as X-ray (lower dose) or ultrasound (no dose.) As was seen during a detailed biopsy study, Section 5.3.1, radiologists focusing on the target are frequently unaware of how many repetitive steps this actually entails. There is a growing public and medical concern regarding radiation doses, particularly the cumulative effects, as evidenced by a recent article entitled "Americans get most radiation from medical scans" [86]. Thus any technology lowering the number of scans is likely to be positively received, though this savings cannot be directly monetized.

5.1.2. Frequency of Percutaneous & Image Guided Approaches

In a recent Radiology paper [87] Kwan et al. used Medicare data to study the effect of "advanced imaging technology" on biopsy approaches and practitioner specialty between 1997 and 2008. The paper shows modest annual growth rates of 3% in the total number of biopsies and an 8% increase in percutaneous approaches, from 59% to 67%, as a portion of total biopsies for all regions. Percutaneous approaches were consistently employed more than 50% of the time in bone, breast, kidney, liver and pancreas, with chest just topping 50% in 2008. For most procedures CPT codes do not distinguish between image-guided and non-image guided procedures, with the exception of fine needle aspirations (FNAs), where fluid rather than a solid sample are collected often in conjunction with a biopsy, for which an increase from 54% to 77% is reported from 2004 to 2008.

A reliable proxy for the use of image guidance is the biopsy practitioner and the overall percentage of biopsies conducted by radiologists increased from 48% to 66%, while those by general surgeons and pulmonologists decreased. A chart showing breakdown by anatomical region is reproduced in Figure 24. In addition, the Kwan et al. propose that while imaging technology is enabling less invasive biopsies, since the overall growth rate is modest, it is not encouraging unnecessary biopsies. While CT data is displayed to the clinician as a picture that he or she uses to confirm the needle position as it is placed into the patient, the underlying data is coordinate based, thus any increase in the use of imaging technology with interventional procedures also increases the potential for robotic assistance which could employ that spatial data to assist the practitioner.

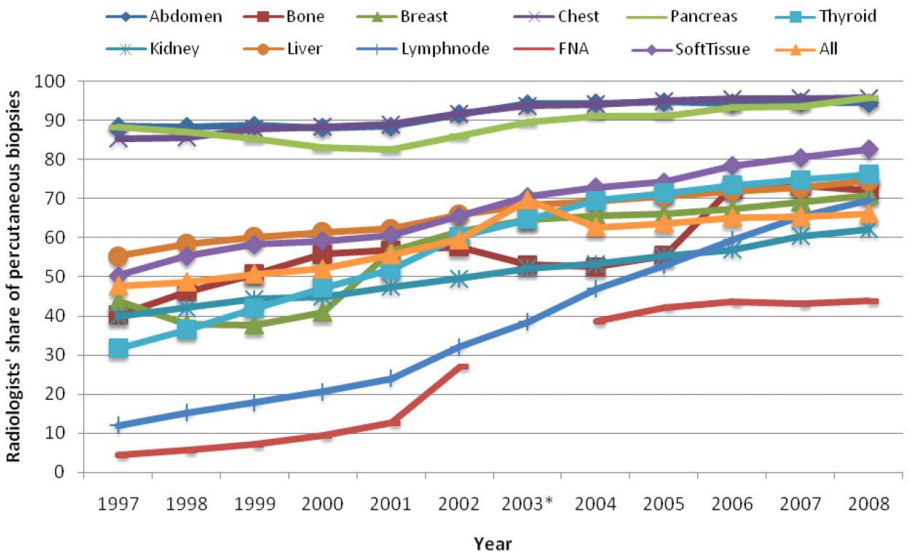

Figure 24 – Graph shows relative share of all biopsies performed according to specialty from 1997 to 2008 [87]. (Data in 2003 were affected by a coding discrepancy for FNAs.)

5.1.3. Project Overview

Design of the Robopsy system followed the process described in Section 4. Initially a handful of biopsy procedures were carefully observed and detailed notes taken; these provided the guidelines for the design process. This was followed up with a 10-case observational study and a later 50-case retrospective study. A thorough understanding of the PTNB protocol enabled precise identification of inefficiency and minimization of the proposed robotic solution's DOF, needle gripping, angulation and insertion. From this strategies were identified and a concept developed comprising a low cost, lightweight, disposable robot, a controller and a clinician interface. Over three generations the design progressed from a 3D printed prototype with a simple motion control interface to a prototype with a potential production partner and an image guided, point-and-click graphical interface. Testing has been conducted on custom thoracic phantoms as well as two in-vivo porcine models.

5.2. Prior Art Review

The first step in developing a solution to assist in the placement of biopsy needles was to review existing devices, both in the market and patent literature. Of the robots described in Section 2.3, the PIGA CT, described in was not yet visible in the market when this project was conceived; however the CT Bot and Light Puncture Robot were identified as pertinent. Both employ a patient-mounted design which partially compensates for respiratory motion and minimizes the structural loop from the patient through the robot to the needle's entry point and represent a more appropriate scale architecture. Additionally, since many percutaneous procedures are conducted with local anesthetic and little to no sedation, robots which position the needle with respect to the floor have the potential to cause significant harm if the patient changes position while the needle is rigidly held. Mounting to the patient reduces this risk as well as simplifies robot-patient registration. A review of patent literature and existing products turned up few effective active devices to aid in percutaneous biopsies. However, two passive laser-based guidance systems were identified, shown in Figure 25. Both operate in a similar manner whereby the clinician scans the patient, measures both the in-plane and off-plane angles and inputs

them manually, directing a laser beam to align to the compound angle. The emitter is them moved so that beam's incidence point on the skin pierces the desired insertion point. Finally the needle is inserted along the beam, nominally in a single pass.

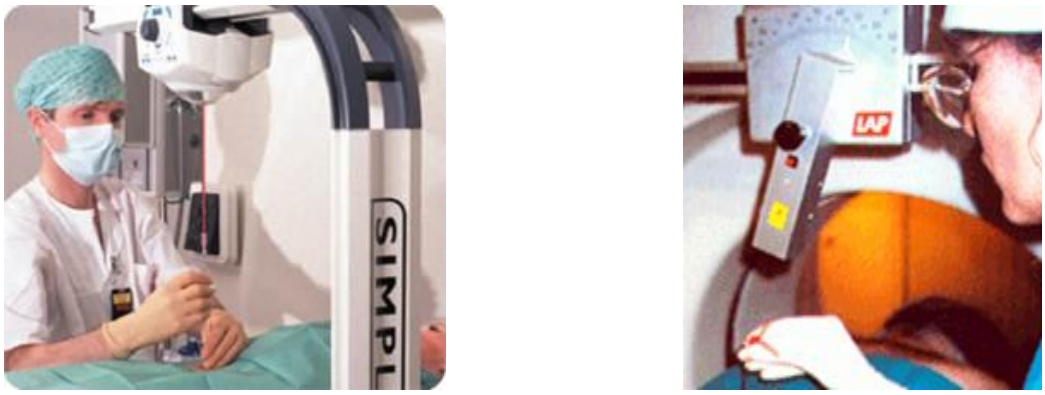

Figure 25 – Left: The SimpliCT CT from Neorad AS, Oslo, Norway, mounts to a floor based stand, photo circa 2005[88]; in later models the system was mounted to an overhead gantry. Left: The PatPos from LAP GmbH Laser Applikationen, Lueneburg, Germany, attaches to the face of the CT machine, photo circa 2005 [89].

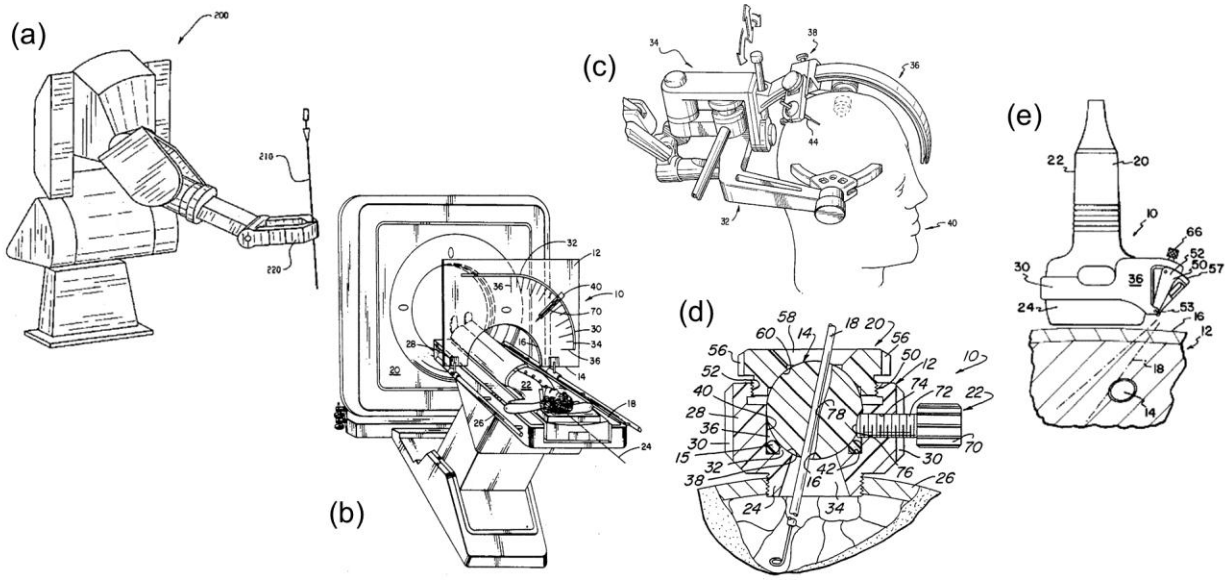

Figure 26 – Sample probe insertion patents: (a) "Tactile feedback and display in a CT image guided robotic system for interventional procedures" [90]; (b) "Biopsy needle guide for use with CT scanner" [91]; (c) "Biopsy guide" [92]; (d) "Biopsy guide" [93]; (e) "Multiple angle disposable needle guide system" [94].

Reviewing patents for devices specifically designed to assist with the biopsy procedure, excluding those associated with the Robots discussed in Section 2.3, yielded a selection of designs of variable practicality. There are a few very broad patents for "remote surgery systems" that fail to describe any physical embodiment such as "Computer controlled guidance of a biopsy needle" [95], with a CT, MRI or ultrasound vision system. Other patents are more specific, such as "Tactile feedback and display in a CT image guided robotic system for interventional procedures" [90], which appear to be scaled-down

industrial robots with haptics and integrated imaging and planning. There was a dearth of methods of compensating for breathing motion. The majority of biopsy assistance devices were passive guides. The "Light beam locator and guide for a biopsy needle" [96] proposes a Cartesian frame to which lasers are mounted that project intersecting beams to "mark the location of the tumor and to guide the biopsy needle." The "Biopsy needle guide for use with CT scanner" [91] can be best described as giant Plexiglas protractor mounted over a patient. Passive stereotactic frames mounting to the head for brain biopsies were also noted such as "Biopsy guide" [92], and one device was found, "Biopsy guide" [93], which consists of a ball shaped needle guide and socket that screws into a burr hole drilled in the skull; the ball is oriented, locked into place and needle passed through its hole into the desired target. Multiple products and patents exist that combine a ultrasound probe with adjustable or multi-position needle guides, for example the "Adjustable needle guide apparatus and method" [97] and the "Multiple angle disposable needle guide system" [94], assigned to CIVCO Medical Instruments, Kalona, IA.

5.3. Procedural Analysis

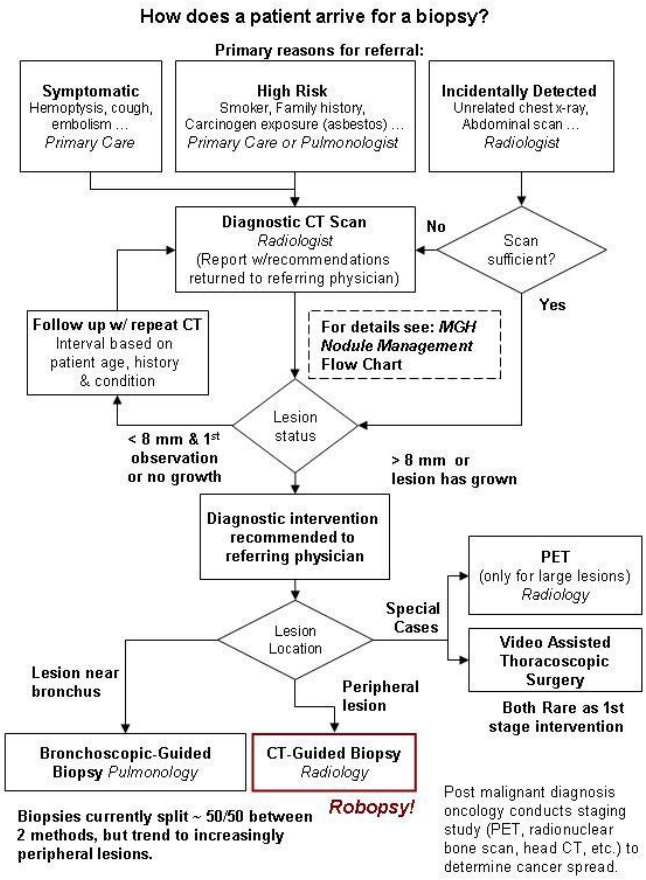

Figure 27 – Flow chart showing the process by which a patient arrives for a biopsy procedure at MGH, with the point where robotic assistance is proposed highlighted.

Concurrent with the prior art review, a detailed study of the CT-guided lung biopsy procedure as conducted at MGH was undertaken. The first step was to understand MGH Radiology's process for managing cancerous nodules, which is summarized in Figure 27. Typically nodules are first found either incidentally or due to screening of an at risk patient. New nodules smaller than 8 mm in patients with no history of cancer are subject to "watchful waiting" and scheduled for follow up imaging. Not all nodules are cancerous; some are bacterial infections, fungus balls or scar tissue from past infections. Larger nodules or those in at risk patients are scheduled for a diagnostic intervention, via a PTNB, bronchoscopic-guided biopsy or, less frequently, video assisted thorascopy. Cases are split 50/50 between PTNB and bronchoscopy, with the former more appropriate for peripheral lesions and use of a guidance system. It is important to note that MGH is a "quaternary care center," medical parlance for a hospital that is equipped to handle everything from severe trauma to mystery infections requiring containment. Therefore, MGH receives a significantly higher portion of the region's difficult biopsies and has a protocol that may be more time consuming, but is

appropriate for biopsies that are small and/or deep and in compromised patients. Quoting one radiologist while conducting a difficult manœuvre, "I have no choice; if I don't do the biopsy today [the patient] won't get a biopsy and a diagnosis." Additionally, radiologists at MGH are specialized; there is a department devoted to interventional thoracic (chest) radiology, and the radiologists are less constrained by time or equipment demands than their colleagues at community institutions. Therefore, in designing the robot-assisted biopsy protocol and interface, there is the potential to incorporate some their "best practices" so that even less experienced or more time-constrained users can more efficiently and reliably conduct their procedures.

5.3.1. Biopsy Observation & Task Partitioning

PTNB lung procedures were personally observed at MGH and detailed notes taken beginning with the patient's entrance to the CT room and concluding with their exit. The scanners used were Siemens Somatom 64 slice scanner. From this observation the procedure was decomposed into the discrete steps, shown in Table 5. Figure 28 is a schematic showing the setup, with the patient in the scanner, as well as a CT slice of a phantom showing how an intervention is planned.

Table 5 – Manual Biopsy Protocol Steps

1. Prior to the patient arriving, the clinician reviews a previous x-ray or a CT scan to locate the nodule, roughly plan the insertion path and select the correct patient positioning. The four common patient positions are: prone (face down), supine (face up) and left and right lateral decubitus (on side), all with the head pointing into the scanner bore.
2. Patient arrives, gives consent, and is placed on the scanner bed and lightly sedated intravenously.[5] Dangling limbs are secured with rolled towels, Velcro straps and/or tape.
3. An initial "scout" scan, with 5 mm slices and approximately 30 cm in length, is acquired and used to confirm the approximate planned trajectory. The patient is withdrawn from the bore.
4. A Fast Find grid, tissue paper printed with metallic lines and manufactured by the Webb Manufacturing Corporation, Philadelphia, PA, is adhered to the patient over the approximate insertion zone. In a CT slice these lines show as a slice as a series of dots, as seen in Figure 28, and provide transverse coordinates. The patient is inserted into the bore.
5. With the grid attached, a detailed, 2.5 mm slice thickness "planning" scan is taken. The clinician then uses this and onscreen drawing and measuring tools to explore various entry points and trajectories. Angles measured in a single scan slice are referred to as "in-plane" while the "off-plane" angles are approximated by flicking through multiple slices. Normally, the scanner gantry is tilted until the desired trajectory can be visualized in a single slice. Trajectories perpendicular to the skin surface are preferred.
6. The insertion point selected on the scan is transferred to the patient by reading the axial position from the point containing slice's DICOM headers, advancing the bed to this position,

[5] Not all hospitals use sedation, preferring to remain in communication with the patent. These hospitals follow a "breath hold" technique whereby patients are instructed to inhale and hold their breath during scanning and needle insertion. MGH, however, has found it more reliable to prevent the patent from moving and rely on the clinician to manually perform "respiratory gating."

and finding the intersection between this scan plan, indicated by the bore's lasers, and the appropriate line on the grid. The point is marked with ink and the grid removed, the area sterilized and the patient draped.

7. Lidocaine (local anesthetic) is injected into the insertion point and the short needle left in position, marking the entry point and the trajectory's' approximate compound angle. The patient is scanned and, if necessary, the injector needle's angle is adjusted and the patient rescanned. Occasionally the needle is withdrawn entirely and repositioned by 1 – 2 mm laterally.
8. The injector needle is removed and a small incision is made at the entry point. This facilitates the biopsy needle's entry and prevents entrainment of epithelial cells into deeper tissue, which could cause a growth. A 19 gauge (0.912 mm) coaxial biopsy needle is partially inserted at the skin, replacing the injector needle, and the patient is scanned again. Even though the collection of consecutive slices comprise a 3D coordinate system, when working "out of plane" over multiple slices clinicians were observed to approximate angles, rather than find them geometrically. This was identified as a significant source of additional scans.
9. The needle is advanced in an iterative process whereby scans alternate with adjustments of the needle. The skin serves as the pivot point and occasionally the needle is rotated so that its bevel induces a slightly curved trajectory in a particular direction. The biopsy kit is furnished with a ruler that is used to set a sliding collar on the biopsy needle to the correct depth. Generally, the clincian perfroms "respiratory gating" whereby patient is scanned and the needle is angled and inserted at the same point in the patient's respiratory cycle. Some clinicians reported that twisting the needle during insertion impoves stability in muscle tissue.
10. Depending on clinician, insertion may be stopped at the pleura so that the stylet can be removed and additional Lidocaine injected. Crossing the pleura is generally accomplished with a single swift jabbing motion; this avoids "tenting" which increases the risk of pneumothorax.

Potential for Robotic Assiatnce

11. Once the needle reaches the target the stylet is removed and a longer 22 gauge (0.644 mm) needle attached to a syringe and inserted. Fluid aspiration is accomplished by making small jabbing motions while drawing back on the syringe. Samples are squirted onto a slide or into a vial and fixed. A tissue sample may be collected by deploying a 20 gauge (0.812 mm) side cutting "biopsy gun." The samples are then viewed either onsite or in the hospital's pathology lab.
12. Once the pathologist confirms that a diagnostically meaningful sample has been obtained, as opposed to fluid or unclear tissue, the biopsy is complete. One more scan is taken to verify patient condition, then the needle is removed, a bandage applied and the patient flipped onto a gurney so that they are lying over the insertion site so as to apply pressure. Experience at MGH has shown that enforcing this position decreases the incidence of pneumothoraxes.
13. The patient receives two follow up X-rays to check for pneumothorax before being released.

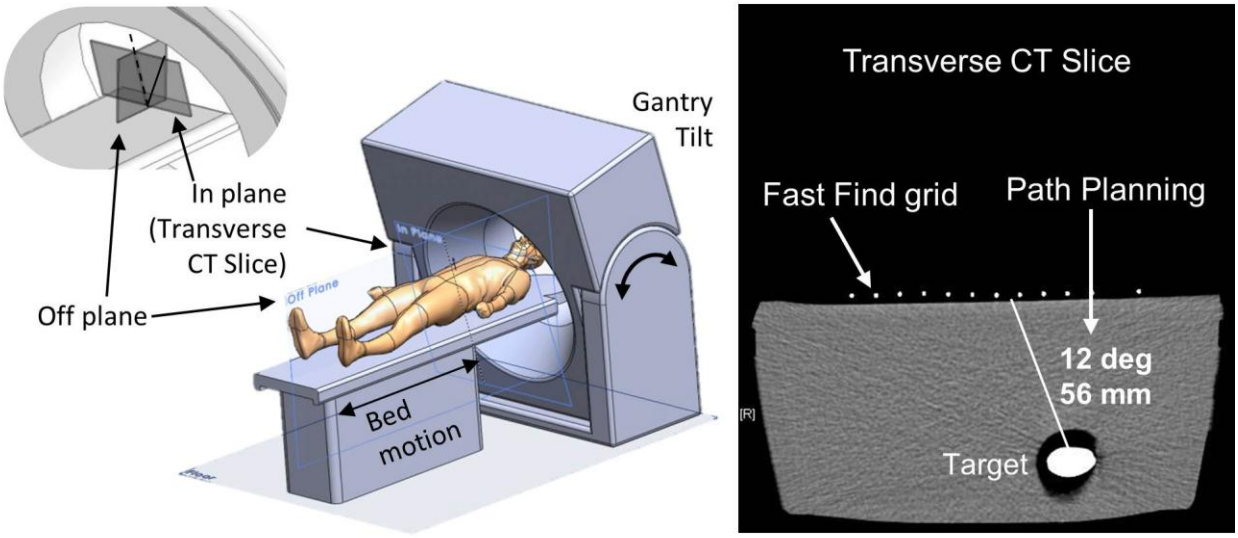

Figure 28 – Schematic of patient in CT bore. “In-plane” angles are measured in the CT slice while “off-plane” angles project across multiple slices, on and out of the bore. The CT display provides drawing and measuring tools to plan the intervention from the grid, visible as a series of dots, to the target.

First hand observation provided a thorough understanding of the biopsy procedure process flow and suggested establishing metrics regarding procedure time and needle manipulations, both inside and outside the pleura, and radiation dose addressed with a more rigorous study, Sections 5.3.2 and 5.3.3. After decomposing the procedure into specific steps, the next design step was to identify those where robotic assistance could increase procedural efficiency and to partition tasks between the robot and the clinician. Target identification and intervention planning appeared to be conducted satisfactory by the clinician using the grid and the on-screen tools. However, Steps 7 – 10 were identified as challenging and time consuming, with the clinician performing tasks that Table 1 identified as more appropriate for a robot and not fully exploiting the 3D data. Finally, while clinicians did sometimes experience difficulty in acquiring histologically significant cell samples, the actual time spent sample collecting was minimal and did not require super-human dexterity. Improving yield would require redesign of the aspiration needle and biopsy gun, a separate project. Therefore, the scope of the Robopsy project was limited to the placement of the biopsy needle from insertion point on the skin surface to target positions.

5.3.2. 10-Case Observational Study

As a follow on to the initial biopsy procedure observation, later in the summer of 2007 a series of 10 procedures were observed at MGH. All were carried out by either a member of the thoracic radiology staff or a fellow under their direct guidance. Each step was recorded along with timing and the dose report which was printed out after each procedure. The following pertinent metrics were identified and the results are given in Table 6.

- Scans to target – The total number of scans from scout to scan showing the needle in position. This roughly correlates with radiation dose.
- Time to target (min) – Measured from the moment that the first scan was taken to the time when the needle is confirmed in target and it is sample time.

- Insertion Points – The number of times the insertion point was selected (minimum one). Generally, the adjustments were small, on the order of a few mm, and made with the injection needle, not the coaxial biopsy needle.
- Manipulations Outside Pleura – The number of discrete needle motions executed in order to reach the pleura. A single orientation and insertion counted as one motion.
- Manipulations Inside Pleurea – The number of discrete motions executed from the pleura. These are liable to cause tearing and pneumothorax.
- Pathology wait time (min) – This was the time spent waiting between sample acquisition to the pathologist's arrival to review the sample; this contributor to procedure time was not directly controllable by the radiologist.
- Procedure time (min) – This was measured from the moment that the first scan was taken to the moment that the needle was removed and bandage applied.

Table 6 – Results of 10 Cases Observational Biopsy Study

Procedure	Date	Description	Scans to Target	Time to Target (min)	Insertion Points	Manipulations Outside Pleura	Manipulations Inside Pleura	Pathology wait time (min)	Total Time (min)	% Time to target
1	2-Jul-07	Posterior, right lung	9	29	3	3	1	16	56	52%
2	9-Jul-07	Anterior, right lung, above breast	18	52	3	8	3	18	97	54%
3	9-Jul-07	Right lateral decubitus, left lung	11	32	2	3	1	26	82	39%
4	11-Jul-07	Anterior above breast, right lung	11	35	4	5	1	24	94	37%
5	17-Jul-07	Anterior, left lung	13	39	1	5	3	15	73	53%
6	18-Jul-07	Posterior, right lung	11	28	2	5	1	18	70	40%
7	23-Jul-07	Prone, left lung superior	14	41	1	5	2	10	79	52%
8	23-Jul-07	Prone, left lung superior	11	31	1	6	1	na	51	61%
9	16-Jul-07	Prone, central lesion	20	na	1	6	2	na	51	na
10	21-Jul-07	Right upper apex, posterior	15	30	2	11	1	na	67	45%
		Range (min):	9	28	1	3	1	10	51	37%
		Range (max):	20	52	4	11	3	26	97	61%
		Averages:	**12.3**	**35.9**	**2.1**	**5.0**	**1.6**	**18.1**	**75.25**	**48%**

The mean observed time to target was in excess of a half hour; nearly 50% of the time was taken up with simply placing the needle into the target, which corresponds to an average of 12 scans, not counting the scout scan.. On average, 5 discrete motions were observed before crossing the pleura after which there is only an average of 1.6 motions. It is necessary to note that in cases 1-7 there was up to a 26 minute intra-procedure delay while waiting for pathology; by the time of the last three biopsies a pathology station had been installed in the radiology suite, thus reducing this delay. Interestingly, despite keeping careful notes through the procedure, in 6 out of 10 cases scans were recorded on the dose report that could not be linked to specific recorded actions. These "extra" scans, which passed unnoticed in the observer's notes, may have been repeats due to slight adjustments of the CT

parameters; nevertheless this indicates the lower priority given to limiting patient radiation dose than precise targeting.

5.3.3. 50-Case Retrospective Biopsy Study

In-person observations were time consuming and disruptive to the clinicians, therefore a more rigorous retrospective study was conducted and the results are reported in [98]. Using MGH's picture archiving and communication system (PACS), 50 consecutive procedures from 2007 were retrieved and the scans read in order by a trained radiologist. The time stamps provided sufficient information to collect much of the same data as during direct observation. The procedure was divided into 5 steps: trajectory planning, needle placement, extrapulmonary (outside the pleura) needle insertion, intrapulmonary (inside the pleura) needle insertion and sampling and follow-up; for each the number of scans was tracked. The effects of patient characteristics (age, gender, history of lung surgery), procedure characteristics (needle angle to pleura, patient position) and lesion characteristics (size, depth, lobe) were investigated. In addition, the diagnostic success rate, pneumothoraxes and post procedural insertion of chest stubs were tracked. Total patient radiation dose was calculated. To the authors' best knowledge, while previous studies investigated diagnostic success and complications, none sought to correlate patient, procedure and lesion characteristics with number of scans, especially when concerned about radiation dose.

The population studied ranged from 32 to 89 in age and comprised 26 women and 24 men. The procedures were conducted by 5 radiologists at MGH with 5 to 26 years' experience using a Siemens Somatom Sensation 64 helical scanner and following a standardized procedure for scanner settings and procedural steps. Lesions varied in size from 0.7 (near the limit that can be biopsied) to 7.9 cm with a median of 2.1 cm and varied in depth from skin surface from 2.7 to 15.2 cm, with a median of 7.3 cm. As expected, given the wide ranges of lesion characteristics, the number of scans per procedure also varied greatly, with a range of 11 to 38 with a mean of 21. Procedure time averaged 1 hour. Of the total scans, planning accounted for 18.5% of the scans and insertion 52.9%, which together yielded 15 scans to compare with the mean of 12.3 from the prospective study. As expected, smaller and deeper lesions and shallower pleural approach angle were all associated with increased scanning. With decreasing lesion size and increasing depth the number of (undesirable) needle manipulations after crossing the pleura increased was seen to increase.

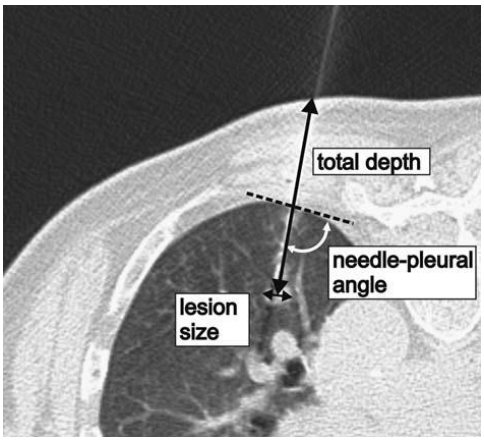

Figure 29 – A representative CT scan showing the parameters that were recorded from the images [98].

Radiation dose was evaluated using the CT dose index ($CTDI_{vol}$) reported in milliGray (mGy), which is the approximate mean dose delivered to a volume of a standard cylindrical phantom, and the dose length product (DLP) which is this value multiplied by the scan length. The effective dose E in milliSieverts (mSv) is used to quantify risk and was found using the ImPACT (Imaging Performance Assessment of CT Scanners) CT Patient Dosimetry Calculator, a Microsoft Excel based tool from the Imaging Performance Assessment of CT scanners (ImPACT) Group at St George's Hospital, Tooting,

London [99]. This tools overlays scans on the appropriate region of a model patient and applies scale factors to account for organs' differing radiosensitivity and reports E as a single number. Also calculated was the effective skin dose (ESD) in millisievert (mSv), which is pertinent since a CT-guided biopsy concentrates scans in a relatively small area. For the entire study, an average E of 14 mSv and ESD of 249 mGy with a maximum of 534 MGy were reported. For reference, a dose of 2 Gy to the skin will cause visible damage; therefore dose does remain in a safe range. This paper concludes, "Ultimately, the results of this study illustrate the iterative nature of CT-guided interventions. This information highlights the need for hospitals to set low tube current and voltage levels for their CT-guided intervention protocols to minimize the radiation dose per scan, and also to explore the use of devices to aid needle placement to reduce the overall number of CT scans required." Such devices would be most beneficial is targeting small and deep lesions while increasing procedural efficiency.

5.3.4. Financial Consideration

Cost is also an important factor and at MGH CT scanner time is booked in 20 minute blocks with each block costing approximately $250 dollars, for a total of $750 per/hour. Although, as observed, they can run shorter, percutaneous lung biopsies are scheduled for two hour time slots and are reimbursed at rates between $560 (Medicare) and $1000 (average). Smaller, deeper lesions and multiple sample sites correlate with longer biopsies. It is important to note that charges billed by hospitals to payees are not necessarily paid in full, nearly all payees negotiate rates with self-pay patients often also receiving a discount. Based on the results of this study, it was estimated that by shortening the lesion targeting phase and aiding sample collection by stabilizing the needle it might be possible to consistently shave 20 minute off scheduled procedure time. This slot can be filled with another revenue generating non-interventional scan reimbursed at an average of $276. This informed the design process to focus on minimizing the disposable components' costs.

5.4. Strategies, Functional Requirements & Concept Development

5.4.1. Strategy Selection

With the needle placement procedure thoroughly understood, and the tasks portioned between the clinician and the robot the following broad FRs and corresponding 6 DOFs for the robotic device were identified, in order of operation:

1. Needle gripping (1 DOF)
2. X-Y position of needle tip about the patient's abdomen (2 DOF)
3. Needle inclination about two axis compound angle (2 DOF)
4. Axial needle insertion (1 DOF)

Firstly, there must be a way, either manual or automated, of gripping the needle. Secondly, the tip must be placed correctly at the insertion point, which may or may not need adjustment, as was seen during the biopsy observations. Thirdly, with the needle positioned, it is inclined about a compound angle so that it is aimed at the lesion. Finally, it is inserted to the lesion, with angular adjustments if needed. A 7^{th} degree for freedom was identified, corresponding to rotation of the needle during insertion, however this was eliminated since no clinician indicated that it was essential.

Using these FR's and working with the two other mechanical engineers in the team two *strategies* for a patient-mounted robot were developed: a Cartesian frame and a gimbal-like mechanism, both

shown in Figure 30. The strategies are notably broad; at this stage the selection of actuators or detailed mechanical design would have been inappropriate.

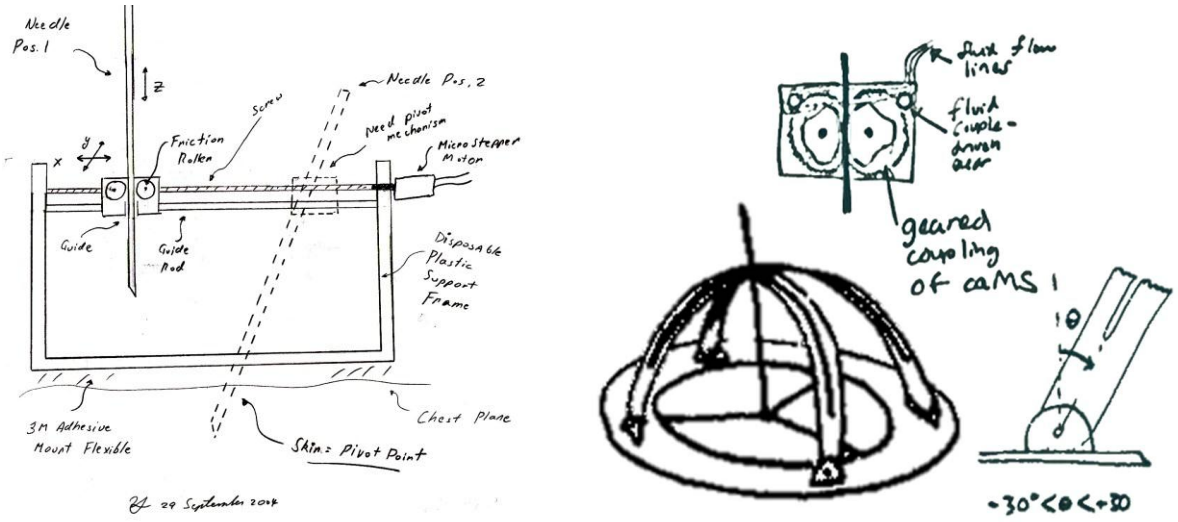

Figure 30 – Left: Cartesian frame for x-y translation with roller driven needle. Right: Two hoop, gimbal-like mechanism with overlapping slots, through which the needle projects.

These represent two significantly different operating modalities:

In the first strategy, a carriage with two rollers grips and secures the needle to fulfill FR #1. Translating this carriage about X-Y, with belts, screws or another mechanism, specifies the insertion point and fulfills FR #2. Once the needle is in the desired position, it is lowered into the skin surface. This becomes the pivot point with subsequent motion of the carriage now causing the needle to angulate and fulfill FR #3. Finally, with the correct compound angle specified, the roller drive is used to actuate the needle to the target, fulfilling FR #4.

In the second strategy, a spherical device is built around a single pivot point. A pair two hoops are arranged so that the rotational axes are perpendicular. Each is slit in the middle so that the needle can be contained in the intersection of the slots. By angulating the two hoops, the needle can be made to describe a compound angle, fulfilling FR #3. This was inspired by various designs for robots wrists; particularly those of Mark Rosheim's seminal *Robot Wrist Actuators* book [101] and various spherical actuators for pointing radar dishes. FR #1 and #4 would be addressed with the design of a "carriage" riding in the dual slot that comprises a method of gripping and inserting a needle. In this design there is no method of

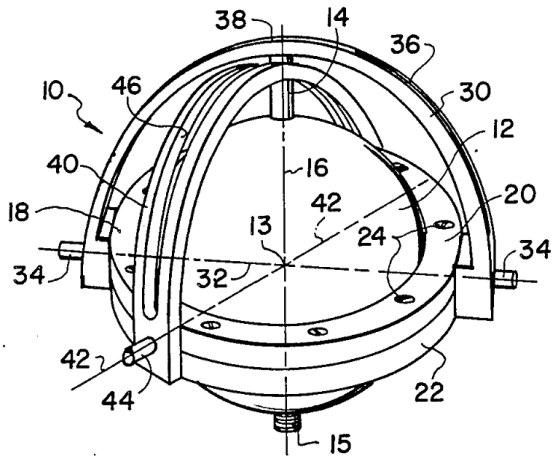

Figure 31 – "Spherical Wrist Joint" [100] developed in 1980's at Rensselaer Polytechnic.

selecting the insertion point, other than gross positioning of the robot on the patient.

Based on study of multiple procedures and clinician interviews, it was determined that positioning of the insertion point was not a critical requirement. In Table 6 the insertion point was moved on average 1.2 times per procedure; however it was often not strictly necessary. Therefore, in accordance with the minimalist design philosophy, the 2 X-Y position DOFs were eliminated and the second strategy selected, as most likely to lead to an appropriate scale device. In the cases where moving the insertion point was critical; this task could be accomplished by the clinician repositioning the entire robot. This reduced the total to 4 minimally essential DOF and the focus was narrowed to the development of a low cost, lightweight and disposable device to be placed directly upon the patient, independent of the CT machine. Target lesion size was selected as 5 mm.

5.4.2. Functional Requirements & Concept Development

With the double hoop wrist strategy selected, a concept system evolved as the functional requirements were expanded upon and further detailed in Table 7. Details of the device's design are presented in a 2005 ASME Design Engineering Technical Conference paper [102], which showed the first prototype, and a 2008 ASME Journal of Medical Devices article [103], which built upon this and showed the second prototype. Much of the following material is drawn from these two papers.

Table 7 – Robopsy System Functional Requirements

1. Sizing – Fit inside a 70 cm diameter CT machine bore, between the patient and top of the bore, while not restricting access to the patient.
2. Pitch & Roll – Angulate the needle about 2 DOF with the center of rotation placed at the skin surface. A cone of ±25° was identified as the workspace addressable in 1° increments. An approximate torque of 60 N-mm was observed during the testing shown in Figure 32.
3. Insertion & Retraction – Place and withdraw the needle in 1 mm increments with a maximum force of 10 N.
4. Radiolucency – Minimize CT scan artefacts (distortion) within the region of interest (ROI).
5. Maintain Sterility – Design for disposability, select sterilizable materials and components and sheathe as appropriate.
6. Chest Motion – Maintain needle in fixed reference frame with respect to rising and falling chest.
7. Organ Motion – Provide for selective needle gripping to accommodate motion. Observations indicated a range of motion up to 25° with a fully inserted needle.
8. Intuitive Interface – Provide the clinician with an operating procedure that enables straightforward integration with the current procedure.
9. Safety – Reject unintentional motions and enable rapid stoppage, removal and conversion to a manual procedure.

Normal CT bores are sized at 70-80 cm so as to provide a close fit around average patients (and a significantly snug fit around bariatric patients) so as to maximize image quality. In general, needles of 10 – 15 cm in length projecting from patient do fit within the bore. Therefore, it was important to minimize device size and a nominal diameter of 10 cm was selected as the maximum that could be accommodated. In addition, larger devices such as the CTBot and the Light Puncture Robot, despite the straps, were seen as challenging to reliably mount on the curved surfaces of a patient.

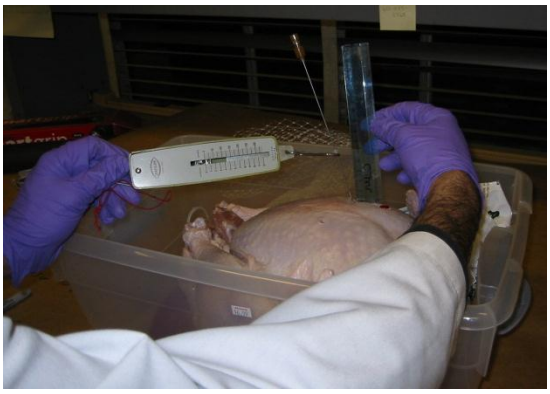

Figure 32 – Measuring force required to angulate a needle previously inserted into a turkey breast.

Limited data is available on the actual forces during needle manipulation and insertion. One paper [104] reports on the placement of a 1.27 mm needle into ex-vivo bovine livers and reported an average puncture force of 2.3 N. 10 N was estimated as an upper bound on the maximum insertion force. In order to determine the force needed to orient a needle during insertion testing was conducted in a turkey breast. As shown in Figure 32, a 19 gauge (0.912 mm) needle was inserted to depths of 10, 50 and 100 mm and the lateral force, at the fixed distance from the insertion point, to orient the needle measured with a spring scale. At the deeper depths of 25 and 50 mm torques of 25 and 60 N-mm were observed.

Based on observation and discussion with clinicians, a 50° cone was determined to be a reasonable maximum range of motion. This is beyond the maximum tilt of any CT machine gantry. Clinicians strive to insert the needle as perpendicular to the skin as possible, both to aid in imaging and minimize the risk of pleural tearing. Angles of greater than 30° are needed only when no other unobstructed path to a target is available; this rarely occurs. In keeping with the design philosophy that eschews adding complexity, it was decided to focus on the majority of procedures.

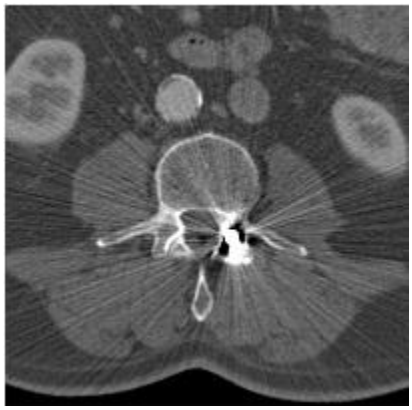

Figure 33 – Artifacts emanating from a pellicle implant, without correction [105].

Avoiding metallic elements in the image range is essential to preserving image quality. As the CT beam emitter and detector rotate around the patient, they take a series of images which are subsequently reconstructed into a single slice image. Any errors in this are referred to as *artifacts*, excellent coverage of which is provided in [105]. Some are due to the physics of how X-rays are absorbed by the body and scanner emitter and detector operation, but the most severe artifacts with regard to this project are caused by metal objects, whose density exceeds the range of normal tissue, in the scanned region. These effectively wash out and show up as white patches with radiating streaks that distort and obscure the image, as seen in Figure 33. Some software correction is possible to remove streaking; however this cannot address the localized degradation. Incidentally, with long slender objects a streak will appear to emanate from the object's tip. In the case of biopsy needles, radiologists use this streak to preview the needle's straight line trajectory. The best practice is to keep metal outside the ROI and this led to the decision to manufacture the robot structure entirely from polymers. In addition, this left the design space open for the potential later development of an MRI compatible robot, though MRI compatible actuators are still in their infancy and expensive.

Sterility can be addressed through a combination of disposable components: those that can be sterilized, and those that require protective sheaths, similar to the sheaths used to cover the da Vinci's

arms. The major sterilization methods employed in medical devices include steam autoclave for reusable devices and ethylene oxide and gamma irradiation for packaged disposable devices. The selection of radiolucent polymers also facilitated the decision to make the end piece's structure low cost, lightweight and single use.

Patient motion, both gross and that of internal organs also causes artifacts, hence the use of a robot to manipulate the image should not interfere with application of the "breath hold" technique during scanning or needle manipulation. In addition, a sufficiently light robot placed on the patient should rise and fall with respiration, as well as move with him or her in the case of a gross motion, such as a shift in position. In addition, the need for a complete releasing of the needle was identified by Dr. Jo-Anne O. Shepard, Division Chief of Thoracic Radiology at MGH, as critical. In the fully inserted state, needles were observed to "waggle" from side to side by approximately 20° due to internal, respiration-driven organ motion. No contemporary device was found to truly have this feature. While the PIGA does grip and release a plastic bushing, through which the needle is inserted, the needle is intended to be inserted in a single pass. The Light Puncture Robot provides for step-wise insertion; however it is not clear that free motion is permitted when the needle not gripped. Being able to release the needle on command would also afford the clinician free access to manipulate the needle during sample collection, as well as permit easy conversion to a manual procedure.

In order for robotics to gain wider acceptance in lower value procedures, with significant potential for efficiency improvement, the philosophy of appropriate scale should also apply to the clinicians' interaction with the device. So while providing an "extra hand" to perform the tricky manipulations inside the bore, the interface should enable the user to follow current procedure as closely as possible. Additionally, minimizing the disturbance between the clinician and patient will enable easier conversion to a manual procedure in the case of device failure.

With an understanding of the functional requirements, the design was separated into three modules, with the first identified as the most critical.

Table 8 – Robopsy Modules

1. Robotic Actuator – The device that sits directly on the patient inside the CT (MCM)
    a. Base structure and double hoop angulation sub-module (2 DOF)
    b. Needle gripping and insertion sub-module, the "carriage" that is carried by the hoop. (2DOF)
2. Control Box – Connected to the device and remote from the patient, nominally on a cart beside the CT bed.
3. Clinician Interface – This comprises a software graphical user interface (GUI) as well as a hardware interface, such as a joystick, stylus or mouse.

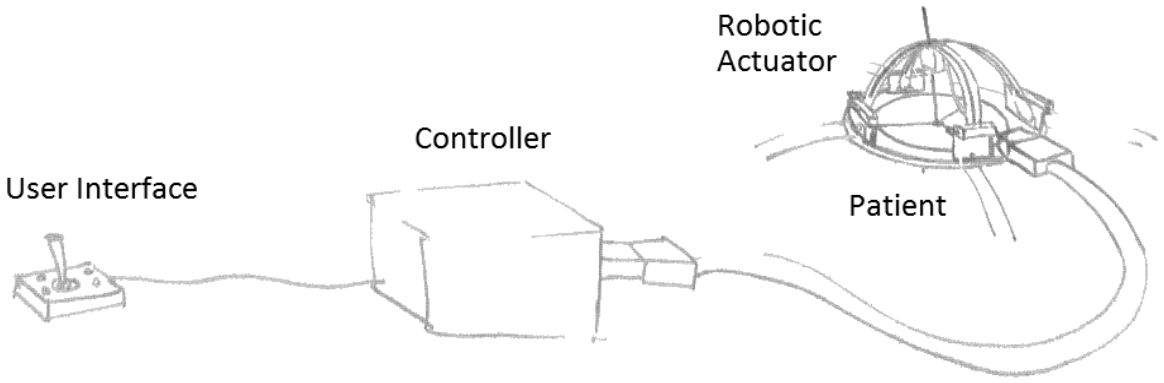

Figure 34 – Robopy system concept and modules.

5.4.3. Actuation Modality

Before progressing with the structural design, it was necessary to select an actuation means. Various options are presented in Table 9 encompassing two basic modalities: Remote and Local. The former would generate force within the controller and transfer it to the device and while the latter placed electric motors directly onto the device. The remote options could, potentially, have resulted in a more economical design, by placing more expensive components in the controller, the drawbacks outweighed the benefits: While pneumatics are clean and easy to connect, they have poor positional control, a challenge only overcome by Innomedic after years of work. Hydraulics, using incompressible fluids, provide better position control; however their resolution is limited due to friction in the seals which must be tight if leakage, unacceptable in a medical environment, is to be avoided. This was extensively explored in [106], the authors masters' thesis, with negative findings. Both hydraulics and pneumatics would require a hose with a minimum of 4 lumina, 8 if a dual acting configuration were sought, the stiffness of which would be a concern when placing the device. Both flexible drive shafts and cable drives could be constructed of sterilizable materials; however they are typically bulky, suffer from windup and are better at delivering unidirectional torques. Therefore, it was decided to place 4 micromotors directly on the device with a single, flexible cable connecting to the controller. Further discussion of the actuators is provided in the context of each prototype.

Table 9 – Actuation concepts for the robotic device

		Cleanliness	Flexible Transmission	Positional Accuracy	CT compliance	Serializability
Pneumatic	Remote	✓	?	X	✓	?
Hydraulic	Remote	X	X	?	✓	?
Flexible drive shaft	Remote	✓	X	?	?	✓
Cable drive	Remote	✓	X	?	?	✓
Micro motor	Local	✓	✓	✓	X	?

5.4.4. Prototype Overview

Three generations of the Robopsy robot, called *Alpha*, *Beta* and *Gamma*, were constructed and are show in Figure 35. All prototypes were modeled with SolidWorks CAD software, Waltham, MA. The first two devices were created with SLA rapid prototyping, using a local vendor and assembled and tested at MIT. Both micro stepper and micro servo motors were tested. The third prototype was developed in partnership with Saia-Burgess Dresden GmbH, Dresden, Germany, part of the Johnson Electric group, Hong Kong [107], which custom designed a stepper motor and integrated it into the design. The third prototype was resin cast from urethane molds. All three control boxes were designed and assembled at MIT. Each prototype was demonstrated to clinicians, tested and refined.

Figure 35 – Three generations of Robopsy devices and controllers: alpha, beta and gamma.

Conversations with clinicians indicated openness to a robotic biopsy assistant, provided they remained in control and the learning curve was short. This contrasted with systems such as the da Vinci where extensive training is commensurate with complexity. Developing and refining a user interface proved as challenging as the mechanical design. The goal was that one the device was placed on the patient, the clinician would be "fly-by-wire" from the control room, updating the image as needed, until the needle was successfully located in the target. The first two graphical user interfaces (GUIs) were programmed in Microsoft Visual Basic 6, which permitted basic graphics and rapid prototyping, and required the clinician to be the bridge between the CT display and the robot interface. The second was used with the Beta prototype in both phantom trails and a porcine trial. The third interface was developed and as joint project with the German Cancer Research Center (DKFZ) Division of Medical and Biological Informatics in Heidelberg, Germany. This direct point-and-click control and was used, again, in both phantom trails and a porcine trial.

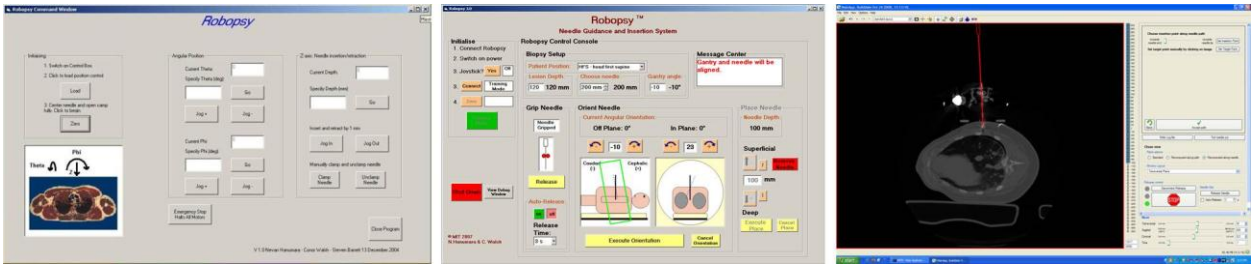

Figure 36 – Three generations of Robopsy interfaces showing progress to point-and-click guidance.

5.5. Alpha & Beta Prototypes

5.5.1. Structural Design

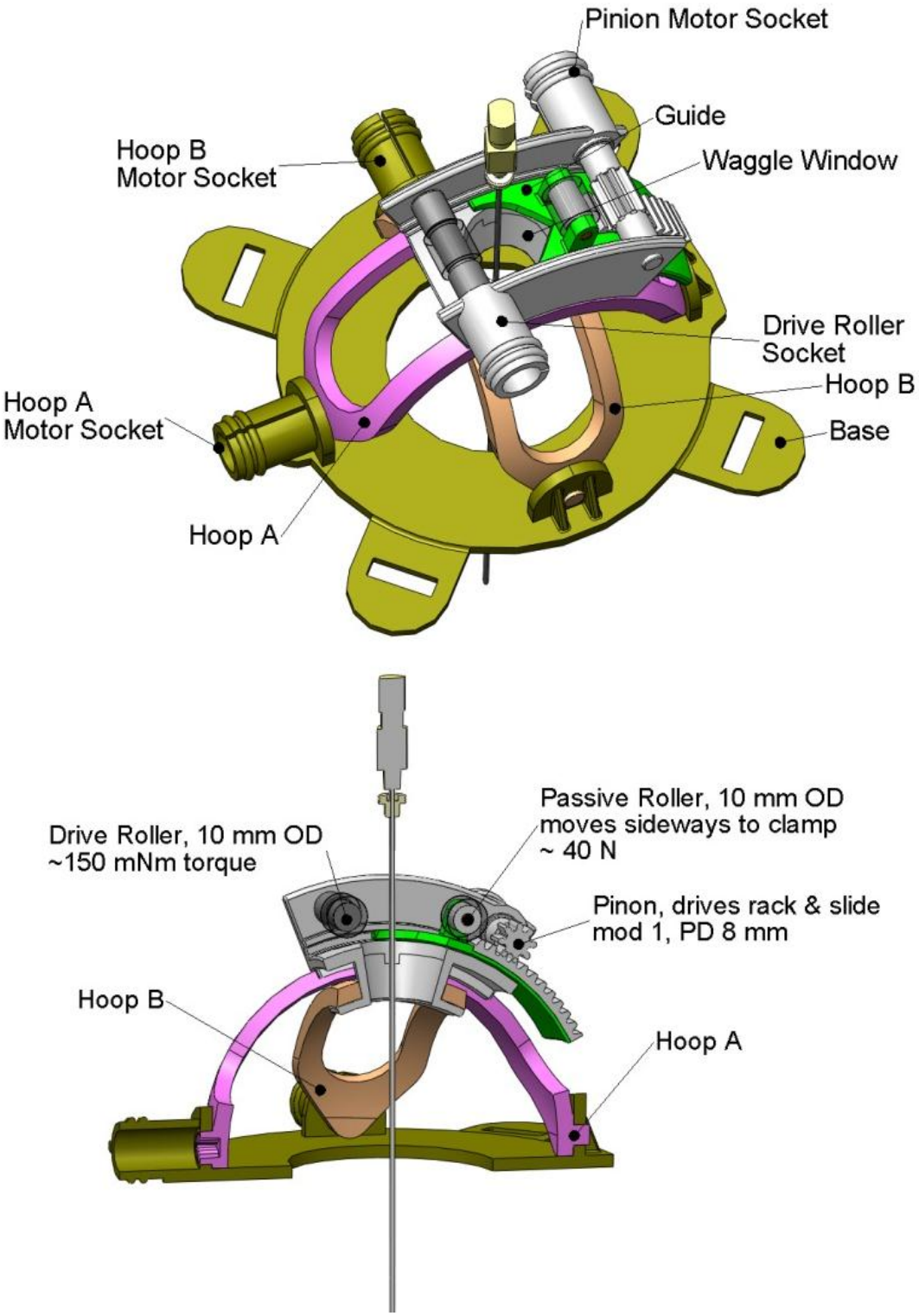

Figure 37 – Alpha prototype SolidWorks CAD model showing components with the needle unclamped.

The alpha prototype, shown in Figure 37 and Figure 38, encompassed all of the major design features. The structure was 3D printed polymer and weighed 200 g, including the motors but excluding the wiring harness. This is significantly less than the CT Bot's 3 kg. The base plate is intended to rest directly upon the patient and was equipped with tabs which could be taped down and slots for straps. Later in the process, tape was found to be more satisfactory and a two sided, starfish-shaped adhesive pad developed, discussed in Section 5.5.1. The nominal diameter of the device is 10 cm, which made it easily handleable and able to accommodate motors of sufficient torque. This sizing was maintained in all 3 prototypes. For future embodiments, an array of bases with geometries fit a particular region of the body was prevue.

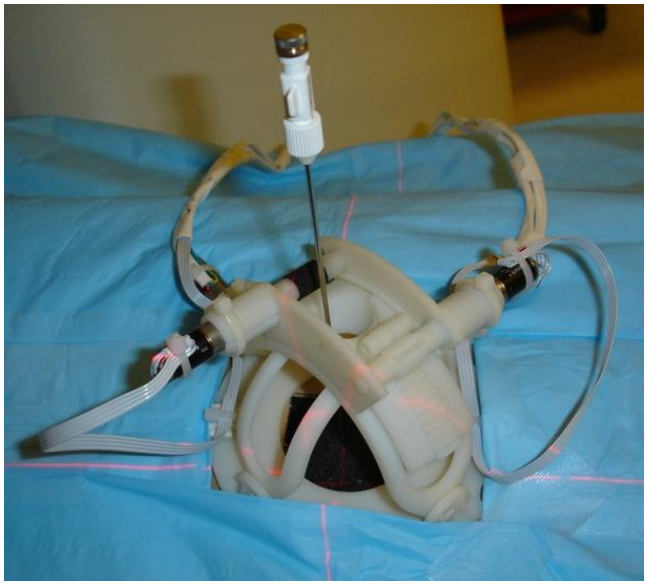

Figure 38 – Detail of Alpha prototype with CT machine's alignment lasers visible.

The two hoops snapped into raised tabs on the base and shared a central pivot point. Two motors fit into sockets and directly drove the hoops. The nominal needle pivot point was located at the intersection of the hoops' axes. Ideally, this would be located right on the skin surface; however it was lifted by 8 mm, the motors' 5 mm radius plus their 3 mm thick sockets. In practice, the actual pivot point is indeterminate and located somewhere inside the dermal tissue. Restraining the needle to pivot at a specific point was not seen as desirable and liable to cause tissue tearing and needle bending. Placing the motors in a vertical configuration with a bevel gear drive would have facilitated a more compact configuration, but would also have increased part count and interfered with the envelope of the carriage's movement.

The carriage rides in both hoops' slots and was aligned with the upper hoop, while the lower hoop provided the second DOF, thus the compound angle was described. Inside the center of the carriage is a 25° cone shaped opening, termed the "waggle window," through this the needle passes and is free to move when not gripped. Various needle gripping and insertion methods were considered, including drill chucks and propelling pencils, but the simplest was found to be a 2-roller friction drive. The driven roller is mounted to the carriage while the opposing roller is free spinning and attaches to a curved slide, which rides in slots in the carriage and is driven by a rack and pinion. As the slide closes from one side, moving the lower hoop a corresponding 12.5° centers the needle in one direction, while a scalloped guide, incorporated into the slide so that it advances ahead of the roller, centers the needle along the rollers axes. A more complex mechanism that would close from both sides was brainstormed, but eschewed in preference for a drive motor mounted to the carriage. The slide is curved concentric with the top hoops to ensure that the rollers provide a griping force that is tangential to the needle axis and does not tend to cause misalignment. This clamping mechanism allows for a range for circular needles to

be inserted, including ablation probes. Opening the slide leaves the needle free for immediate device removal and conversion to a manual procedure.

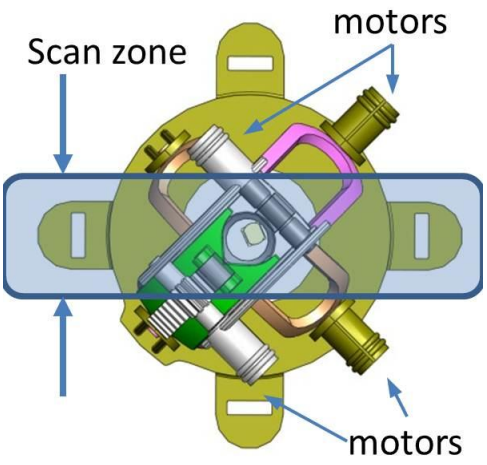

Figure 39 – Top view of Alpha prototype showing metallic free scan plane.

The plastic structure was designed to be disposable, following the principles of DFMA (Design for Manufacture and Assembly) of Boothroyd, Dewhurst and Knight [108], with the intent that in a production all parts would be injection molded, with the minimum of side pulls and complex mold geometry, and snapped together during assembly without adhesive or screws. No separate bearings were used; plastic-on-plastic sliding contact was satisfactory for the forces and desired lifespan. The final part count was as follows: Base, hoops (2), carriage, pinion, slide, rollers (2), rubber roller covers (2), micromotors (4), wiring harness. CT compatibility was addressed in the same manner as with Johns Hopkins PAKY, by positioning the motors so as to leave a 2 cm metallic free zone in the center of the device, as shown in Figure 39. It is necessary to align the device as shown with the taps parallel to the scan plane and the hoops at 45° angles so that the device's kinematics are defined in relation to the CT machine's coordinate system.

This prototype's components were printed by, Vaupell Rapid Solutions, Hudson, NH, in Somos 14120 photopolymer resin from DSM, Elgin, Il which produces tough, white parts with mechanical properties similar to ABS. All critical components sizing was validated with SolidWorks' COSMOSWorks using a Young's modulus of 2.46 GPa and a UTS of 45.7 MP, which are comparable to the properties of engineering plastics that would be used in a production device. The SLA parts required light sanding on the points with sliding contact. During assembly the hoops were first aligned so that the carriage can be snapped into both slots, then the lower hoop is rotated 90° and they are both snapped into their respective tabs. The slide is fitted to the carriage, the passive roller snapped in and the driven roller and pinion slid into their sockets. All driven elements (hoops, roller and pinion) had tapered, star-shaped bosses which mated with couplings bonded to the motors' shafts. Once the motors were fitted into their sockets and clamped with zip ties the entire assembly was secure.

5.5.2. Torques & Motor Selection

Torque requirements for the motors were determined from the specifications, the robot geometry and masses, as shown in Figure 40, and the associated equations. Using the maximum desired insertion force of 10 N and a nominal drive roller diameter of 10 mm, a necessary drive torque of 50 N-mm was determined. By assuming a frictional coefficient of 0.25 between the roller's rubber cover and the needle, the necessary max pinion torque was estimated to be 160 N-mm. The slide and pinion gear teeth were designed to deliver a 40 N gripping force. A pitch angle of 20°, a pitch diameter of 8 mm and a width of 10 mm was selected. Using the DSM material's properties, a mod 1 gear pitch provided a reasonable factor of safety balanced with sufficient pinion teeth (an 8 tooth pinion is near the minimum) for smooth motion. Likewise, as shown in Figure 40 B, the torques necessary to orient the lower hoop B and carriage were estimated with the carriage at a maximum angle of 30°. Using a carriage mass (*m*) of

~100g including motors, a plastic-on-plastic frictional coefficient (μ) of 0.25, a radius (*l*) of 50 mm and an estimated preload of 0.6 N between the hoops and carriage and a measured torque of 50 N-mm necessary to orient a needle at a depth of 10 cm, the torque required to actuate a hoop B and the carriage was estimated to be in the range of 100 N-mm.

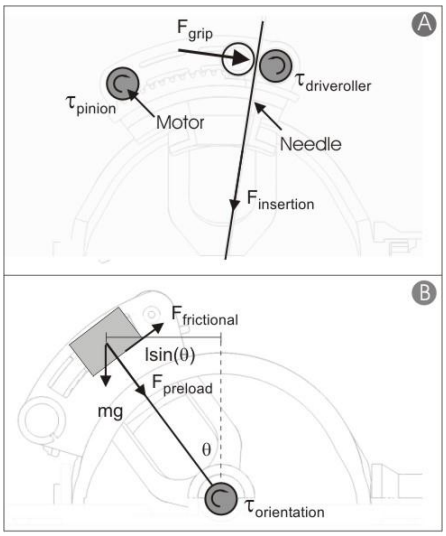

$$\tau_{driveroll} = F_{insertion} \times r_{driverroll} = 10N \times 5mm = 50Nmm \quad (1)$$

$$\tau_{pinion} = F_{grip} r_{pinion} = \frac{F_{insertion}}{\mu_{roller}} r_{pinion} = \frac{10N}{0.25} 4mm = 160Nmm \quad (2)$$

$$\tau_{orient} = \tau_{mass} + \tau_{frictional} + \tau_{needle} = \left(mg\sin\theta + (mg\cos\theta + F_{preload})\mu \right) l + \tau_{needle} = [(0.1kg)g\sin 30 + [(0.1kg)g\cos 30 + (0.6N)](0.25)] \times \times (0.05m) + 0.05Nm = 0.1Nm = 100Nmm \quad (3)$$

Figure 40 – Estimating the torques for needle clamping, orientation and insertion [103].

For the purpose of sourcing and mounting efficiency, it was decided to use the same actuator for all axes, therefore the limiting peak torque was approximately 160 N-mm. The Alpha prototype employed 10 mm diameter model AM1020 bipolar stepper motors with 256:1 ratio gearboxes from Arsape, part of Faulhaber GmbH, and represented by Micromo, Clearwater, FL. The gearboxes were rated to output 100 N-mm of torque continuously (200 N-mm intermittent), which is within the device's requirements, with a speed of approximately 360°/s, which ideally translates to a 1 s needle clamping time and a 20 mm/s insertion rate. Steppers are inherently position controlled, albeit without feedback, and the bipolar design needs only 4 wires. Additionally, in the case of a broken connection, they stop immediately without the chance of spinning wildly, as can happen with servos. For the clamping axis, overdriving the servo and deliberately allowing steps to skip provided sufficient clamping force. Four 4-conductor telephone cables comprised the wiring harness, with each plugging into the control box. Inside the control box was a power supply, four stepper drivers and a USB addressed motor controller from Arcus Technology, Livermore, CA. Components were sourced from NetMotion Inc., Santa Clara, CA. With all prototypes a long cable was run from the control box next to the patient, under the control room door to a laptop running the interface, shown in Figure 42. With no direct sensing of position, during initialization the device must be manually or automatically homed and zeroed.

5.5.3. Alpha Interface

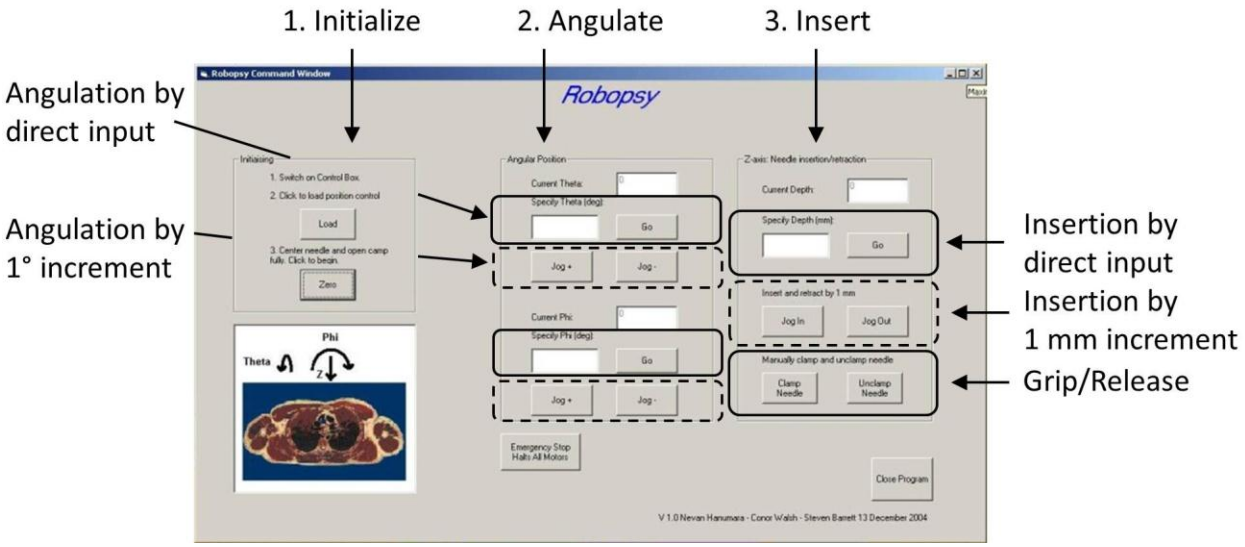

Figure 41 – Basic Alpha interface, used to confirm device operation.

The first interface, shown in Figure 41, provided direct slave control over the robot and minimal feedback to the clinician. After planning the intervention, plugging in the robot and powering the control box, the Altera controller was activated via by clicking the "Load" button. Now the robot could be secured over the insertion point, the hoops centered and the slide opened manually. Clicking the "zero" button energized the four motors and set the counters to zero. The interface displayed a (rather gruesome) cross section of a patient's lungs and indicated the off-plane (theta) and in-plane (phi) angles, explained in Figure 28, as well as the depth (Z). Gripping and releasing was controlled manually via the "Clamp Needle" button. Beginning with the needle gripped in the upright position and gripped, the next scan would be used to find the in-plane and off-plane angles. Then after drawing the desired trajectory on the CT display, the difference between the needle's current angles and the desired angles would be measured. These were then typed into the "Angle Position" box and the "Go" button clicked. For finer adjustments the interface provided 1° "Jog" buttons. Likewise, the distance from the needle tip to the target was measured and the needle inserted by either direct input or 1 mm increments.

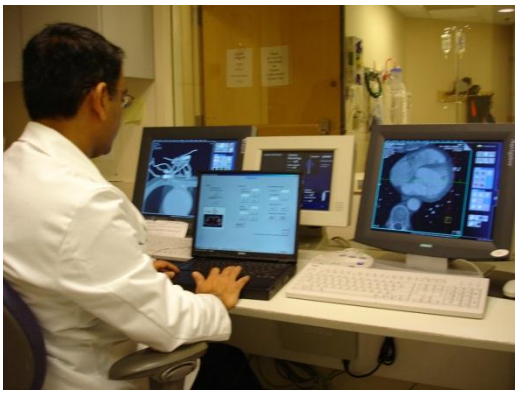

Figure 42 – Operating the Alpha prototype from the CT control room.

5.5.4. Robot-Assisted Biopsy Protocol

Throughout the interface design process the words of Henry Dreyfuss (1904-1972) were kept in mind: "If the point of contact between the product and the people becomes a point of friction, then the industrial designer has failed," [109] as well as the guidelines provided by Don Norman [110] and Sanders and McCormick [111]. In all three generations of the interface, minimizing features and coordinating with existing clinical protocol was stressed. Working with the first interface, the following

general “Robopsy Assisted” protocol was outlined, with the intent of ensuring that all motions were made in “near real-time,” i.e. based on a recent image, while minimizing the number of scans.

Table 10 – Robopsy Assisted Biopsy Protocol

1. With the insertion point selected, the device is placed onto the patient, centered over the insertion point and powered up and initialized. The needle is placed and clamped in the upright position. The patient is then returned to the scanner bore along with the device and the clinician returns to the control room.
2. A scan is done in which the needle is visible; this effectively registers the needle position.
3. The path is drawn from the needle tip, which coincides with the insertion point, and the difference in-plane and off-plane angles measured. These are inputted into the interface and the device moved to the desired compound angle.
4. Another scan is taken and the needle’s orientation is verified; if not correct, it is adjusted and another scan taken.
5. If no adjustments are needed, the depth from the needle tip to the target is measured and the device actuated towards that depth.
6. If desired, an interim scan is taken before the needle crosses the pleura and additional Lidocaine injected. Any final angular adjustments are made at this point. When not being actuated, the needle is unclamped and permitted to waggle freely.
7. The distance is measured from tip to the target again, and insertion is completed. The needle’s successful location in the target is confirmed with a final scan, then the patient is removed from the bore and sample acquisition commences in accordance with current procedure. At the clinician’s discretion, the needle can be stabilized with the clamp.
8. Optionally, should samples be desired from multiple positions, Steps 2 – 6 can be repeated, with care taken to not tear the pleura.

5.5.5. Alpha Validation Testing

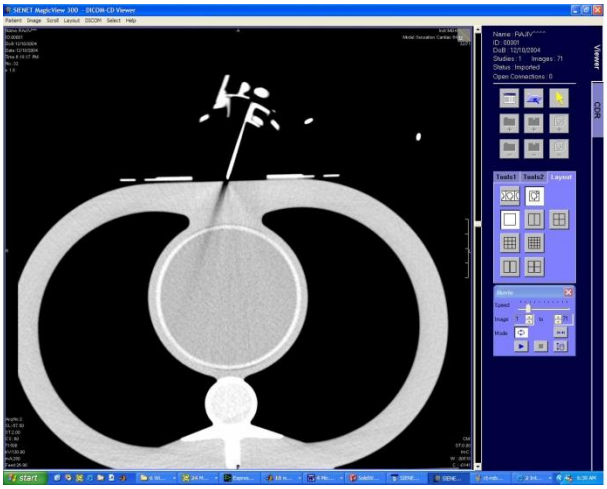

Figure 43 – CT image of Apha prototype on thoracic phantom. The robot is visible but the needle is not distorted.

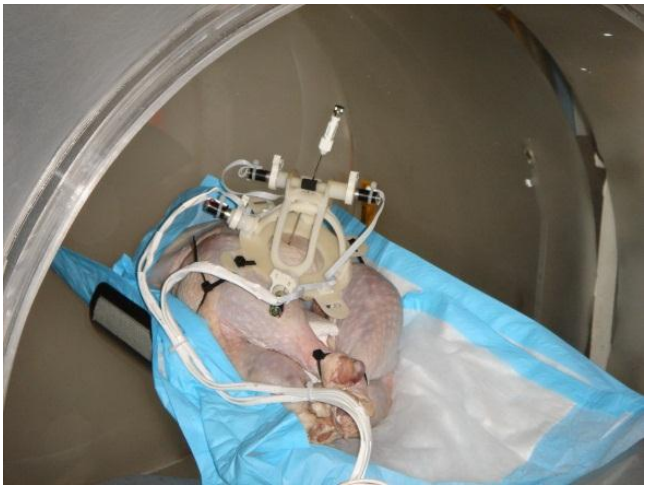

Figure 44 – Testing with turkey tissue. Plastic ties strap the robot to the turkey.

The first testing of the Alpha prototype device, shown in Figure 43, was conducted in December 2004 on a thoracic phantom and a foam block using an MGH Siemens Somatom Sensation 64 CT. This focused on confirming the device’s mechanical functionality as well as the central region’s radiolucency.

As seen in Figure 43, when the robot is correctly aligned, the polymer structure is visible, but no artifacts cause distortion. Subsequent tests were conducted in September 2005, shown in Figure 44, on a store bought turkey with metallic spheres placed inside the cavity as targets. This test was conducted at the MGH Volume CT lab, an experimental facility with a flat panel CT scanner. Partial success was achieved in targeting the spheres, however the turkey tissue proved a poor analogue for human tissue, so future tests employed a gelatin phantom.

5.5.6. Beta Prototype

Testing of the alpha prototype eventually proved destructive, with the SLA material embrittling from exposure to light. Therefore, a new prototype was fabricated, shown in Figure 45. This prototype had the same base dimensions, with minor design tweaks, including a longer motor, a function of switching to micro servos with encoders. The wiring harness was improved with the introduction of "super flexible" wire and better cable management. A ring-like guide was added to the center of the base to facilitate its positioning over the desired insertion point and minor adjustments were made to the carriage geometry.

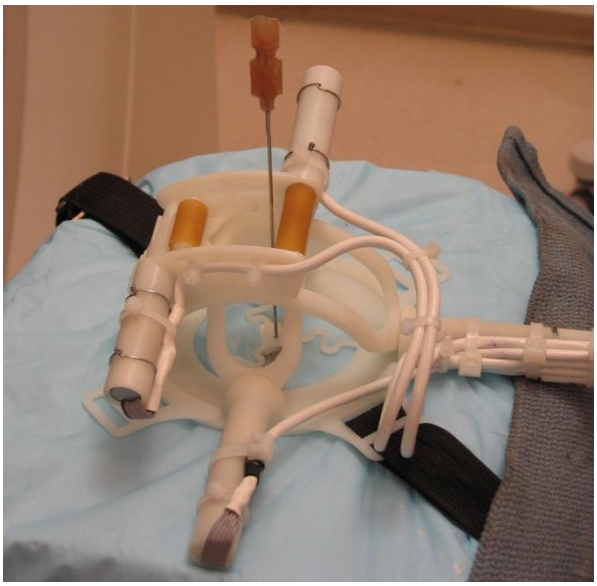

Figure 45 – Beta prototype, shown atop a foam block inside a CT scanner.

The control box was upgraded with the use of an industrial 4-axis control board, model DCM-2143, from Galil Motion Control, Rocklin, CA. This board was addressed via Ethernet or RS232 and Galil graciously donated their control software and Active X toolbox for development use. This board is both able to receive motion commands as a slave and autonomously run programs, though the latter capability was not used. It also accepts a range of add-on driver and breakout boards and in the Beta prototype it was coupled with a Galil servo control board, model AMP-20413. Both boards were sourced from Automation Solutions Atlantic, LLC, Beverly, MA. As an experiment, Faulhaber micro servo motors, model 1024, were selected for this prototype. These 10 mm diameter motors were fitted with the same 256:1 gearbox and an HEM 1016 magnetic encoder for a total package length of 60 mm. The motors have a recommended maximum 1.28 N-mm torque which with 60% gearbox efficacy brings the deliverable torque to 200 N-mm. The recommended maximum speed is 47 RPM after reduction, which meets specifications.

Via the controller, the hoops and drive roller were operated under closed-loop position control. To grip the slide was commanded to an overshot position and the gripping force controlled by sending a current limit command Galil board, which effectively limited the torque. Maximum insertion force was also modulated this way. Using absolute encoders in this size scale was not feasible, therefore a homing procedure was specified and the current limit command used to modulate the force applied to the structure, during this operation step. Each axis required two wires for the motor and four for the encoders, totaling 24 individual leads. To alleviate stiffness issues, 27-conductor Superflex wire from

Cooner Wire, Chatsworth, CA, and a pair of D-Sub connectors was used to connect the robot to the control box, which was made from a standard project box.

5.5.7. Beta Interface

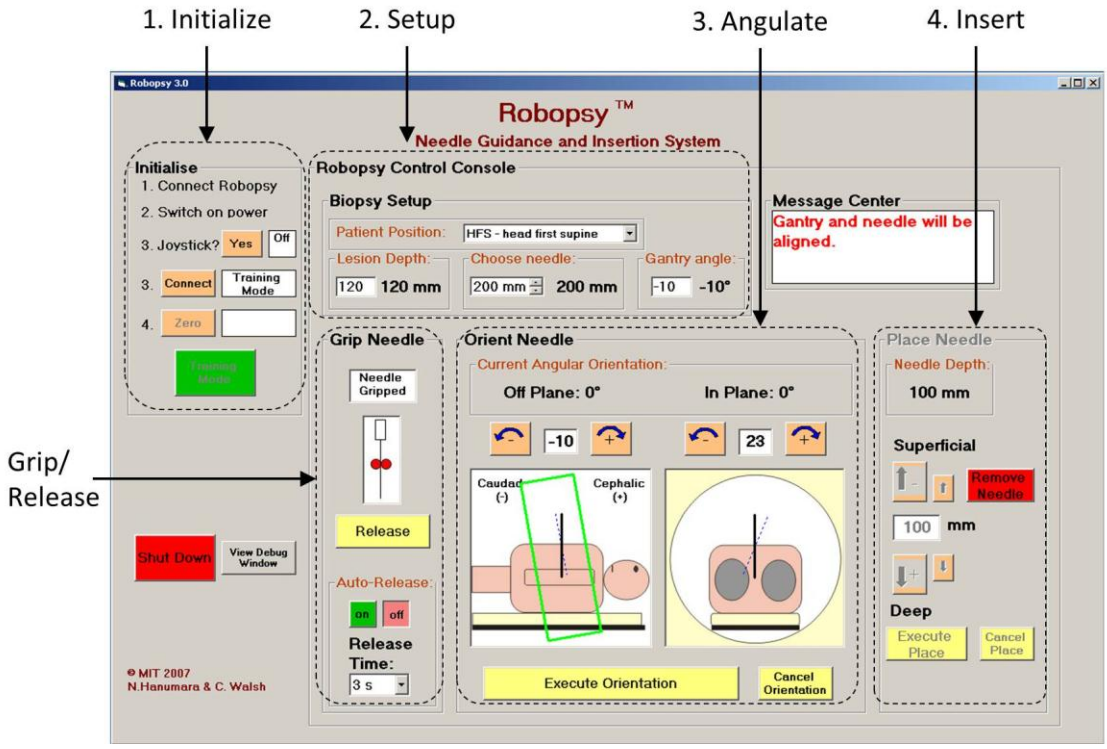

Figure 46 – Beta interface, which guides the clinician through the procedure and provides graphical feedback of needle planned and actual position with respect to the stylized patient graphic.

Testing with the Alpha interface confirmed the device's functionality, but also highlighted several weaknesses: Radiologists had difficulty in translating the angles measured on the CT display to the "theta" and "phi" of the Robopsy interface. Moreover, selecting the correct length needle, 5 cm longer than would be needed for the conventional procedure was challenging. Surprisingly difficult was bridging the gap between the coordinate systems used by engineers and radiologists. While engineers can intuitively think in compound angles and coordinates, a radiologist positions a needle with respect to a patient's body. It became clear that it was important to provide the same in-plane and off-plane views. Therefore, the second interface, shown in Figure 46, was developed with the goal of providing a 1:1:1 mapping between the view of the patient visible through the control room window, the CT display and the Robopsy interface. The design of this interface was described in the proceedings of the 2007 EMBS conference [112].

The Beta interface guided the clinician through the procedure and provided a stylized representation of the patient and the needle's position. Panel 1 prompted the clinician to plug the robot into and power up the control box, indicate whether he wished to use a joystick, establish a connection with the controller and then perform the powered homing procedure. This entailed driving the hoops to their limits of travel then returning them to a central position and opening the slide. At this point the

robot was ready to be placed on the patient and secured at the insertion point. In Panel 2 the patient position on the scanner was selected (head first supine, head first prone, etc.) which caused the cartoon graphic to change along with the labels for +/- sign conventions, caudad (towards posterior) and cephalic (towards head). Entering the measured distance from insertion point to lesion resulted in the interface adding 5 cm and rounding up to the minimum acceptable needle length. Entering the gantry angle updated the green box on the patient cartoon. Only once the required information was entered in Panel 2 did Panel 3 become active, thus the possibility for erroneous actions was decreased.

Panel 3 provided control over the needle angulation. The needle's position was displayed as a solid line and clicking the arrow keys or entering an angle or depth value generated a preview blue dashed line on both the off-plane and in-plane (transverse) views. The current position was represented by the black line. This preview could then be accepted with the "Execute Orientation" button or cleared with the "Cancel Orientation" button. Since the hoops are oriented at 45° to the scan plane, the commanded in-plane and off-plane angles were transformed to robot commands and motor steps with Equation (4). Included in the position of Hoop B was an adjustment *ClampStep* to account for Hoop B's movement in sequence with the slide during clamping.

$$\begin{aligned} HoopA_{stpes} &= \left[-InPLane\cdot\cos(45^\circ) - OffPlane\cdot\sin(45^\circ)\right] steps/\deg \\ HoopB_{stpes} &= \left[InPLane\cdot\sin(45^\circ) - OffPlane\cdot\cos(45^\circ)\right] steps/\deg + ClampStep \end{aligned} \tag{4}$$

The clamping and unclamping was automated, though the clamp could be activated manually, such as when a sample was being collected as a means of steadying the needle. As before, the insertion control was decoupled from orientation so as to prevent compound angulation and insertion motions. Clinician response to this interface was improved and it was used in both a phantom and a porcine trial.

In response to questions as to whether haptics could be added to the system, this interface also served as a test bed for incorporating joystick based control. The hypothesis was that, rather than clicking and measuring on the screen, tilting a handle in the same direction as the needle would be intuitive, as was done with the Sensei X catheter. Surprisingly, user testing promptly demonstrated that this was a hindrance to the workflow, rather than an asset. Radiologists are comfortable working in a 2D space and flipping through multiple slices to approximate a 3D view, as well as tilting the gantry. Clinicians were more comfortable with continuing to specify in-plane and off-plane angles than remotely "driving" the device. Therefore, this option was removed. This example demonstrates the importance of continuous user feedback through the design process. Interest did remain in being able to sense penetration through various tissue layers, however the design and production costs of implementing force sensing into the robot would be substantial and not justified given the near real-time feedback and ability to precisely control depth. Additional feedback could be effected by adding a camera to the control box, and feeding the image back to the interface to provide visual confirmation of the robot's function, allow for remote patient monitoring and, possibly, assist with respiratory gating.

5.5.8. Beta Phantom Testing

With the fabrication of the Beta prototype and interface, a uniform and sanitary thoracic phantom was constructed from Vyse ballistic gelatin, used to simulate human flesh for armaments testing, from Gelatin Innovations, Schiller Park, IL. The gelatin was cast around plastic pipes, which mimicked the patient's ribcage, with 2 to 20 mm radiopaque glass beads underneath, which served as targets. A layer of thin (shelf liner) foam served as the skin. Mechanical and interface testing with this phantom design in January 2007 prepared for subsequent porcine testing. Testing followed the protocol defined in Table 10. For each insertion attempt, the total positioning and insertion time and number of scans were recorded. This data was compared to manual lesion targeting trials, following standard protocol, with the same phantom. Rigorous analysis, however, was not conducted during this test. In general, it was found that the gelatin provided reasonably realistic resistance to angulation, but clinical opinion indicated that it was too easily cut by the needle. The container's clear sides and the gelatin's translucency enabled direct observation. The glass beads, while indeed visible in the CT, displaced when targeted by the needle, leading to a lack of clarity in evaluating targeting. Therefore, in future phantoms they were replaced with penetrable materials. Overall, phantom testing with the Beta prototype indicated that, under ideal conditions it may be possible to complete a procedure with only 4 scans: 1. Planning; 2. Post device placement for needle registration; 3. After angulation; 4. After insertion to confirm correct placement in lesion.

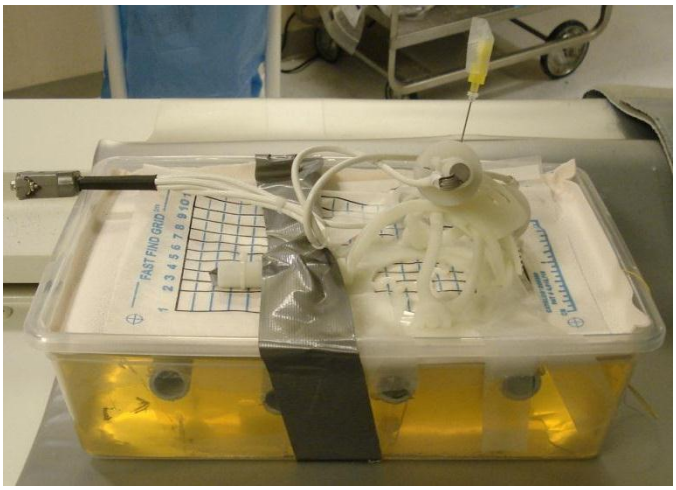

Figure 47 – Testing on a ballistics gelatin thoracic phantom with positioning grid and robot.

5.5.9. User Feedback

Early contact with clinicians not affiliated with a project is essential for obtaining candid feedback to guide the design (and potentially the commercialization) process. In November of 2006 the Robopsy Beta system was privately exhibited at the Radiological Society of North America Annual Meeting in Chicago, IL. The trip was organized by a company with a potential interest in the technology and the prototype, under joystick control, was demonstrated to 40 – 50 select clinical radiologists, with a portion considered key opinion leaders (KOL). Along with a request for general feedback the following guiding questions were asked:

1. Do you see this device adding value to CT-guided biopsy procedures?
2. For what type of procedures would you use this device?
3. How much do you think this device should be priced? For hardware? For the consumables?
4. Future enhancements?

Though the demonstration format did not allow for a statistically controlled or analyzed study, notes were taken and the results summarized:

- Most radiologists thought the device would be valuable to help save time going back and forth between the scanner and control room. The reported length of time for lung biopsies varied depending on the expertise of the doctor doing the procedure, but most felt that the MGH slot of 2 hours was too long.
- Some clinicians commented that while they had the expertise to target lesions without the assistance of a mechanical device, "less experienced" radiologists might benefit.
- Responses varied as to whether patient radiation dose was of sufficient concern for reducing it to be perceived as a benefit.
- Potential hospital targets included both small community establishments where clinicians have less confidence and practice in performing biopsies, as well as those familiar with high tech devices.
- Procedures that would benefit from this device included lung, kidney, liver, pancreas, adrenal glands, RF ablation, prostate seed placement. Breast biopsy was never mentioned since ultrasound is the most commonly imaging modality and lesions are relatively accessible.
- All clinicians wanted to see animal and, later, human studies using the device along with clear date on accuracy.
- Pricing was explored with a range of $50 – $300 for consumables; $200 was perceived as reasonable. Acceptable pricing for the control hardware was less than $5000; this, however, is a significantly lower number than is typical for comparable systems, such as Mazor's Renaissance.
- Mounting to a patient with straps was seen as a challenge, especially with bariatric patients; adhesives appeared to be a better option.
- A future enhancement could also be the addition of limited haptics or an indicator to allow clinicians to feel changes in tissue as the needle was inserted.
- Pertinent to the question of whether to make the robotic end piece entirely consumable or in two parts, with the motors and wiring harness salvaged, was in part answered by the assertion that any complexity in the assembly procedure would be negatively perceived.

5.5.10. Robot Mounting

Adequately securing the prototype was an ongoing challenge. Testing indicated that the straps did not provide a particularly secure mounting. Moreover, placing the straps around an actual patient, after they had been appropriately positioned, the intervention planned and the insertion point marked on the skin, would be a significant disturbance to procedural flow. Nor did taping down the device tabs prove satisfactory. Therefore, a starfish shaped adhesive pad was developed, inspired by Nexcare Active Strips, from 3m Medical, St. Paul, MN. Personal experience showed that (only) these adhesive plasters, by virtue of their foam backing and particular adhesive chemistry, adhered reliably, resisted moisture and peeled

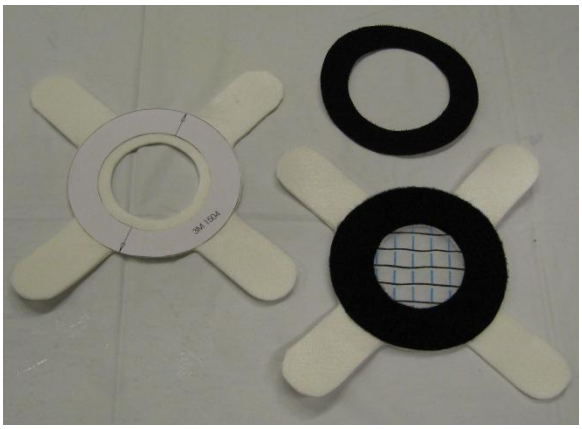

Figure 48 – Adhesive pad without and with Velcro and alignment grid.

off hair painlessly. The same material was sampled from 3M and various durometers tested. Adhesive tape 9781, a PVC foam, coated on one side with an acrylic adhesive and totaling 0.6 mm in thickness, was selected for its moisture resistance and high conformability. When cut into the starfish shape, the legs can be stretched during application to the skin, resulting in tensioned grip. During the 2007 porcine test, the material was found to satisfactorily attach the device over the bristle of an unshaved porcine, as seen in Figure 52. Both bonding the pad directly to the base of the device with a double sided tape, also from 3M, and using a Velcro interface and integrated locating grid were prototyped. With the latter, the pad would be placed right before the planning scan and the integrated grid used to locate the insertion point on the patient, whereupon the skin would be nicked and the robot Velcroed to the pad, with the possibility of adjusting the insertion point, without having to peel off and replace the pad. However, the Velcro base limited the grid's size and unless the insertion point was luckily in the center of the grid, the device and the pad would not align, resulting in unsecure attachment. Providing replacement pads for the occasional adjustment was a more efficient solution for the occasional remounting challenge.

5.5.11. In-Vivo Porcine Trial with Beta Interface

The first live porcine test of the Robopsy system was conducted at MGH in July 2007 on a Siemens Somatom Sensation 16 scanner. All MGH regulations pertaining to animal testing were observed, the testing protocol was approved by institutional review and a veterinarian monitored the procedure for compliance. Images of the test are shown in Figure 49. The porcine was anesthetized, intubated for positive ventilation and placed in a head first, left decubitus position. Rather than surgically implanting targets or using a porcine that was positive for cancer, a handful of artificial targets were created with a mixture of agar and 37% iodine CT contrast agent. An initial scan was conducted and this was injected with a 22 gauge (0.64 mm) needle, as seen in Panel B, and hardened into blobs visible under CT.

After taking another scan, a target of approximately 2 cm was selected and, subsequently, the test followed the protocol described in Table 10. The insertion path was planned, the skin nicked and the robot homed and placed; the adhesive base was attached, and satisfactory performance was confirmed. The second scan was taken with the needle clamped in the upright position. Using the CT display, the angles between the needle and the trajectory from the tip/insertion point were measured, as was the depth. The needle was angulated and inserted and a third scan acquired. From this a 3° angular correction and 4 mm further insertion were needed. This was executed and the needle was confirmed touching the target in the fourth scan, as seen in Panel (f).

The primary goal of this test was to in-vivo validate the system operation; with only a single porcine it was not possible to conduct a significant comparison between the manual and Robopsy assisted test and time was not kept. During testing the device was observed to rise and fall approximately 2 cm with respiration and the needle to oscillate by 10° when unclamped, thus highlighting the applicability of the patient mounted model as well as the “waggle window.” Targeting was accomplished with the expected 4 scans, as compared with the over a dozen observed during the observational study in Section 5.3.2.

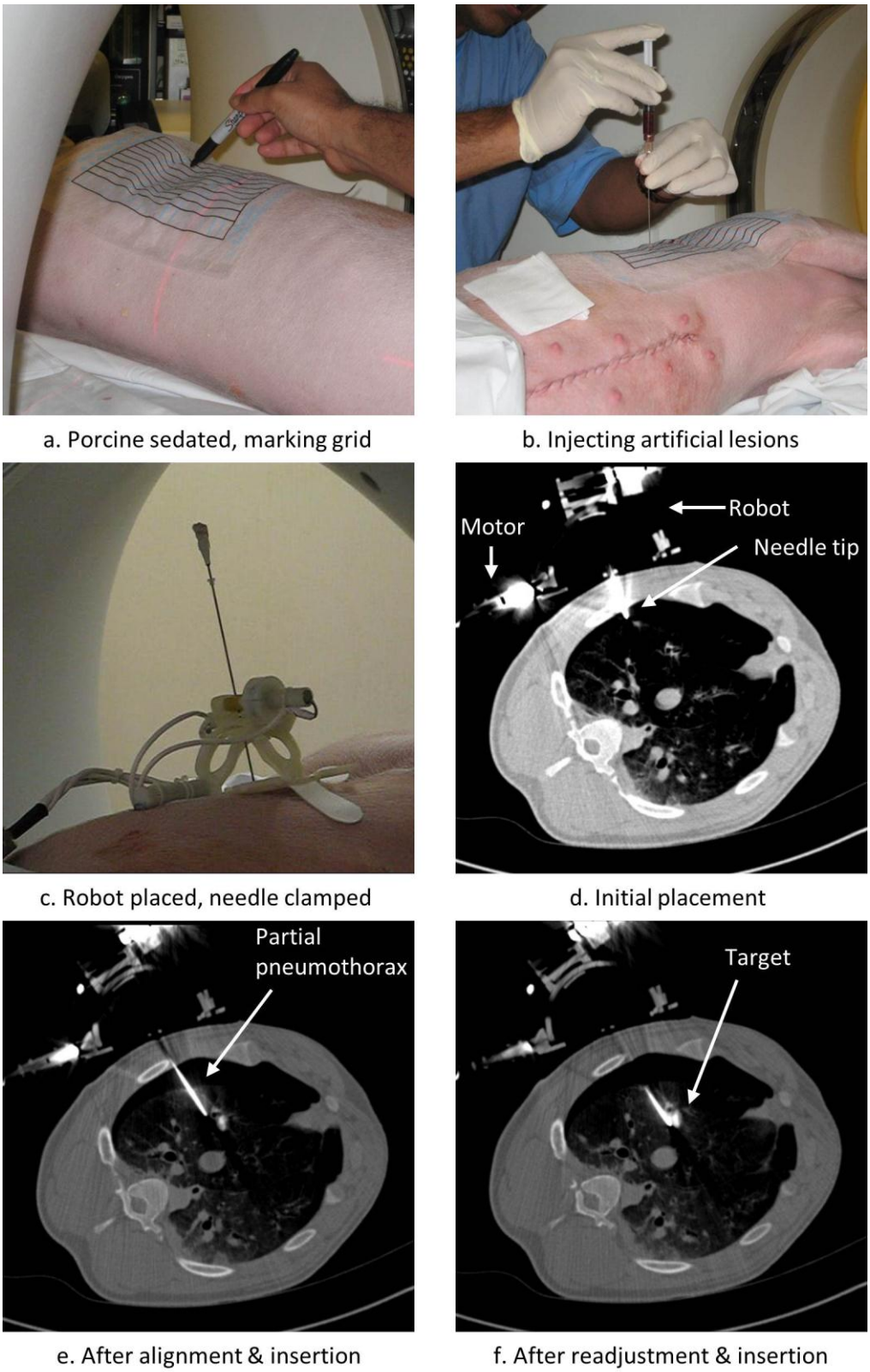

Figure 49 – Porcine testing with Beta system.

While this porcine trial further validated the mechanism, as the scans show, the procedure was not entirely successful: Firstly, the initial incision was of a depth such that when placed into the robot the needle already penetrated the thoracic cavity, as seen in panel (d). This prevented the needle from being accurately angulated pre-insertion. Secondly, backlash in the motors combined with the hardness of the artificial lesion resulted in a tangential, rather than central targeting of the ~15 mm diameter lesion. Thirdly, whereas a human is able to cross the pleura with a quick jabbing motion, as panel (e) shows, there is evidence that the robot's slower, steadier insertion can cause a pucker in pleura and a minor pneumothorax. This is also, in part, due to the ventilation of the porcine which was necessary due to the complete sedation. Measuring angles and depths on the CT display and transferring them to the interface proved undesirably complex, and this gave the impetus to implementing a direct point and click interface.

5.5.12. Patent

A U.S. provisional patent was filed on January 28, 2005 and followed with a utility patent application on January 27, 2006 [113], which is still pending. The assignee is the General Hospital Corporation d/b/a Massachusetts General Hospital, and is managed through their Corporate Sponsored Research Licensing (CSRL) office. Robopsy' twenty-four claims describe a structure and function that appears unique. They describe the mechanism and its intended function of aligning and inserting a generic tool into tissue. Claimed is a base which facilitates fixturing to a patient and supports the pair of opposed rotating hoops which drive a carriage. The carriage is equipped with a viewing window through which a tool passes and is selectively secured with a sliding clamp. The tool is driven into tissue via one or more rollers. A partially polymeric structure is claimed. Remote image guidance is covered, whereby the trajectory is adjusted via an image of the device and target surgical site, without specifying whether the doctor makes the adjustments while viewing the CT image, as with the current prototype, or the adjustments are made automatically by linking to the CT data.

Table 11 – Key Robopsy IP Claims

" Guidance and Insertion System"

- Base for patient mounting
- Rotating hoops describing two angles
- Needle clamping / unclamping
- Friction drive for insertion
- Polymer structure
- Image-based guidance

5.6. Gamma Prototype

5.6.1. Motors, Structure & Controller

In both the Alpha and Beta prototypes, motors represented the most costly element of the robot, with each small-quantity priced at ~$50-100, too expensive to be disposable. This led to investigating whether the motors and wiring harness could be made detachable from the disposable plastic structure and reused. This raised sterility concerns and protective sheathing was evaluated. Unfortunately, placement of the four motors, with two stationary and two moving with the carriage, as well as the needle's passage through the center of the device, would have made for an unduly complex and challenging to use challenging to use design. Alternately, sealed motors and gearboxes with heat resistant lubrication that could be autoclaved, e.g. Klübersynth UH1 64-62, Klüber Lubrication, Londonderry, NH, but were identified but found to be prohibitively expensive and only able to withstand limited sterilization cycles. In either case, reusing the motors and harness would require an intuitive

attachment/detachment method, with each motor keyed to the appropriate axis, as well as an extensive self-test procedure. Moreover, this would run counter to current practice in the CT suite. Whereas operating theatres are equipped to handle reusable devices, such as the hand pieces of surgical drills, all the equipment necessary for biopsies is disposable and delivered sterile and sealed in a plastic tray. (This includes gloves, drapes, needles, syringes etc.) Therefore, it was decided that following a fully disposable model with the Robopsy system, and indeed similar medical robotics, would best facilitate integration into current procedures. The challenge was to source a motor costing few dollars that could nevertheless provide position control.

Addressing this challenge, the Gamma prototype, shown in Figure 51 and Figure 52, was developed in partnership with Johnson Electric; the goal was a pre-production prototype of a fully disposable solution. Johnson Electric is a supplier of low cost motors and electrical systems to a wide range of industries and the Saia-Burgess division specializes in stepper motors and low volume prototypes. For the Robopsy project, they custom designed a low cost, high torque prototype stepper motor, with an all-plastic gearbox that snap fit onto the structure. The decision to return to steppers was made after further studying the operational procedure, described in Table 10 and which consists of measurements followed by and discrete movements with the loop closed through the clinician, and recognizing that the servos were underutilized when used solely as slaves.

The work of Saia-Burgess' Pre-Development team resulted in the custom design of a low cost, disposable stepper motor, estimated to cost under $10 per unit at volume. This was an adaptation of an existing base design UAG3 Saia bipolar stepper motor, to which a 3 stage, all polymer planetary gearbox was attached. Working from the stepper's specifications, the gearbox was designed based on desired output power. The approximate output requirement for each axis was determined based on the estimated speed and required torque; closing the slide and gripping the needle was determined to be the most demanding axis. Power at the output shaft (delivered to the slide) was conservatively calculated from the closing of the slide 25° at a radius of 50 mm in 1 s along with the gripping force, F_{grip} from Equation (2).

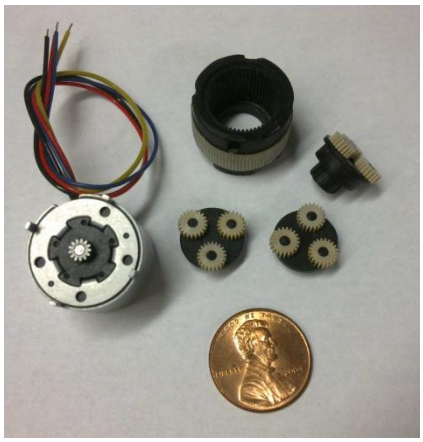

Figure 50 – Detail of Saia motor and gearbox.

$$P_{pinion} = V_{pinion} F_{grip} f_s = \frac{\pi \cdot 0.05m \cdot 25°}{180 \cdot 1s} \frac{10N}{0.25} 1.4 = 1.2W \quad (5)$$

From this estimate of 1.2 W at the output shaft, Johnson used proprietary tools to design the motor and gearbox. The combined package is sized 20 mm diameter by 37.5 mm long. In later testing, performance was found to be more than sufficient; however, broken pins (axels) on planetary carriers occurred. Correction of this would be expected in a production model. As can be seen in the picture, the final carrier terminates in a splined connector which mates with the device's structure, while the gearbox casing has two notches that mate with cantilevered snap fits projecting out of the structure.

Working from the Beta prototype CAD model, custom actuators were integrated and the design refined. Full covers were added to the motors, the slide was moved to the top of the carriage, notches were added to better indicate where the device should be aligned with the CT's laser beams and the four motor wires were brought together inside a handle which enables more convenient placement. In the alpha prototype up to 3° of undesirable backlash was observed and in a meeting in Dresden with Saia-Burgess a solution was developed. Two curved plastic springs that anchored to the base and connected to the axes of the hoops that these served to preload the gearboxes of the motors and greatly reduce backlash. The structure was made by first 3D printing a positive, then urethane casting a replica. The rubber tubing covering the drive roller was replaced with durable O-rings, between two of which the needle seated.

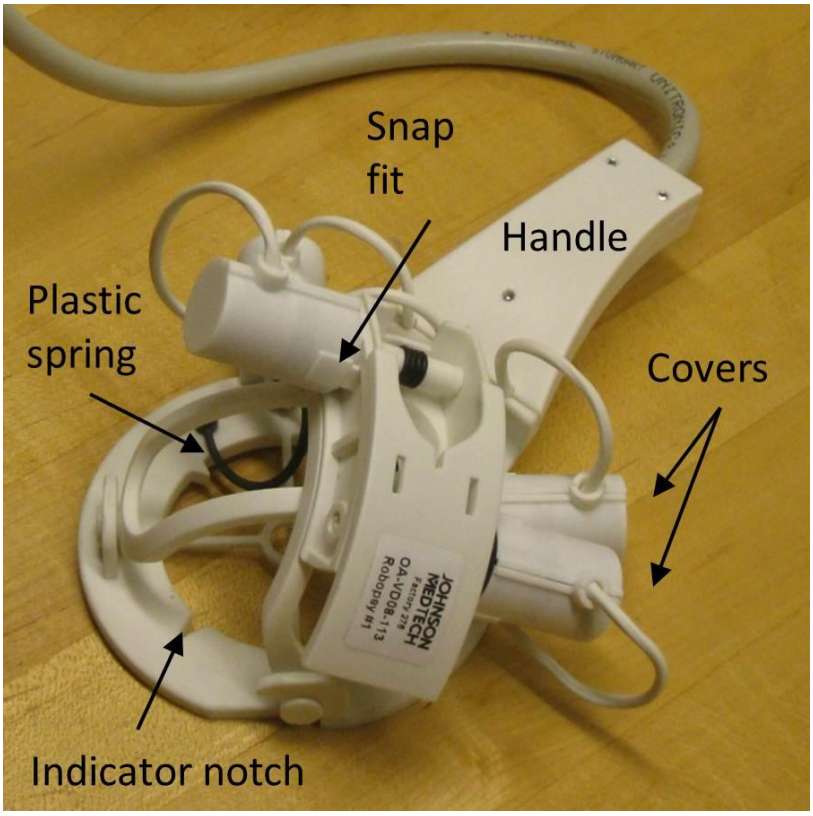

Figure 51 – Detail of Gamma prototype.

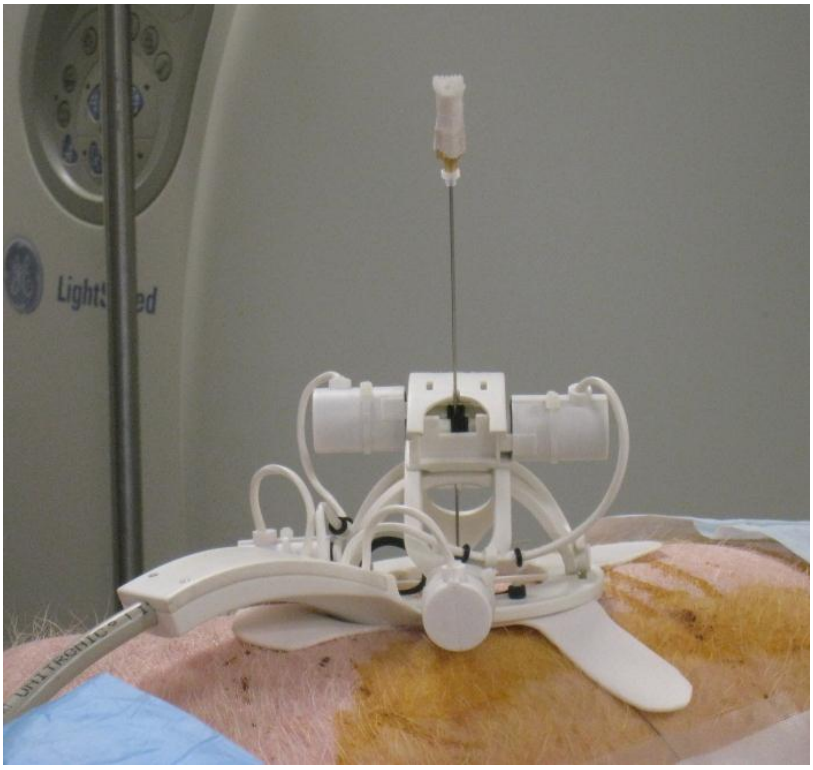

Figure 52 – Gamma prototype, shown during porcine testing with needle clamped.

For the third prototype a Galil DCM-2143 control board was used with an ICM-20100 breakout board that facilitated connection to four of Johnson's Samtronic 102 stepper control boards. In a production device, the control board and drives would be integrated. In this iteration the RS232 communication was used between the Galil board and the laptop; this left the laptop's Ethernet port free to receive images "pushed" to the third generation interface from the CT scanner via the hospital's PACS network. The control box was sourced from OKW Enclosures, Inc., Bridgeville, PA. Their Meditech line is highly customizable, equipped with handles and available in "medical white." The case assembly is shown in Figure 53. Connections to the robot and the laptop were placed on the case front along with red, yellow and green status indicator LED's. As can be seen by adding up the components and estimating for the donated parts, cabling etc. the entire reusable controller has an approximate and affordable cost of $2000. For completeness,

Table 13 provides a summary of all controllers and drivers tested in all three Robopsy prototypes. Rough production cost estimates for both the control hardware and robot are given in Table 12.

Table 12 – Estimated Volume Production Costs for Robopsy System

Control Module		**Disposable Actuator Module**	
Interface/software	$960	Motors	$65
Amplifiers	$600	Cables / Connectors	$15
Controller	$400	Plastic Body	$10
Cables / Connectors	$25	Assembly	$10
Other	$15	**Total**	**$100**
Total	**$2000**		

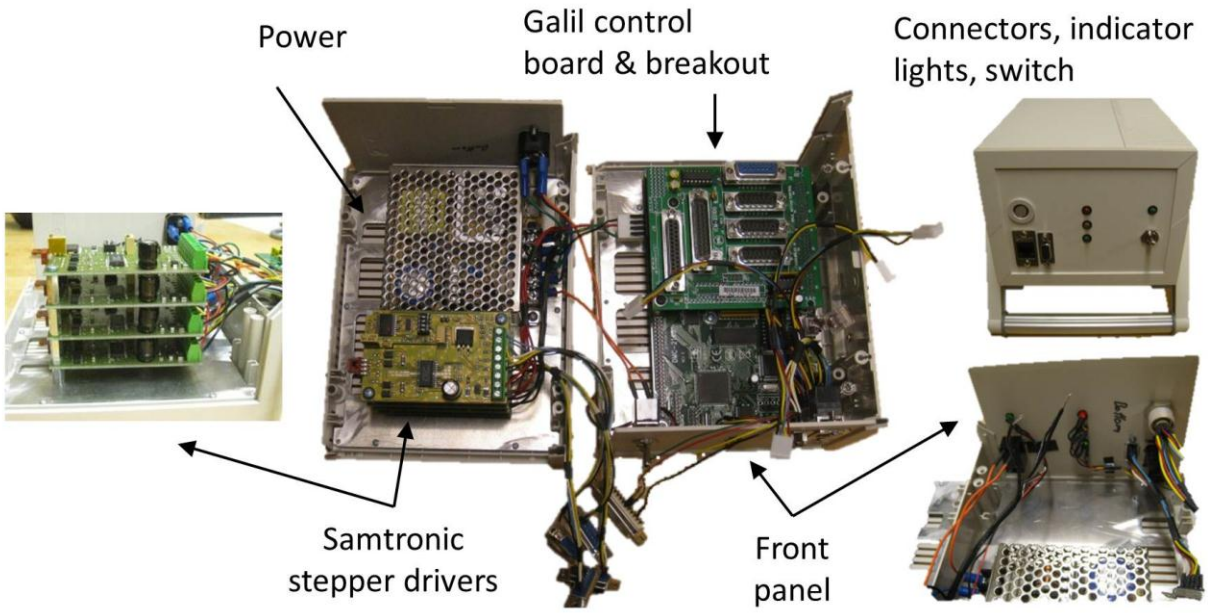

Figure 53 – Gamma prototype assembly

Table 13 – Three generations of Robopsy Motor & Controller Specifications

Prototype	*Alpha*	*Beta*	*Gamma*
Motor	Arsape AM 1020 Bipolar stepper 18° step, 4 wire	Faulhaber 101-1024 Brushed Servo with relative magnetic encoder	Johnson Electric Prototype* 0A-VD10-105 (Approx. $10 each)
Gearbox	Series 10/1 256:1 100 N- mm continuous 200 N-mm intermittent 10 x 34.8 mm with motor	Series 10/1 256:1 (same as Alpha)	Integrated custom all polymer 3 stage planetary
Controller	Proteus-XES 4 Axis	Galil DCM-2143	Galil DMC-2143-DC24 ($1295) Galil ICM-20100 ($95)
Driver	Data unavailable	Galil AMP-20341	Johnson Samotronic 102 ($50)
Power	Data unavailable	CUI Inc. VMPT-65B	Meanwell RS-50-12 ($75)
Case	Custom cut from acrylic	Project box	OKW Meditech ($50)
Cable	Telephone to motors USB to computer	Cooner Superflex Wire Ethernet to computer	Custom harness RS 232 to computer Ethernet to hospital PACS

* Denotes that item was donated

5.6.2. Gamma Interface

The final interface was designed in partnership with Alexander Seitel, a visiting PhD candidate from the DKFZ. Working from the desired workflow presented in Section 5.5.4 and using the DKFZ's Medical Imaging Interaction Toolkit (MITK), a prototype "point-and-click" interface was built where the stylized patient images were replaced with the CT images. The laptop running the third generation interface was issued with a static hospital IP address and provisioned with an open source DICOM client. Robopsy was then added to the CT machine's list of clients, so that after each scan the images could be pushed to it over the PACS network, while the system remained CT machine independent. The workflow was structured and the interface customized so as to completely replace the CT machine's display, however only those features appropriate for probe insertion procedures were incorporated. Safe operating procedure was enforced – after each needle motion, the interface locked and forced a new image to be loaded.

Screenshots from an 11 November 2008 porcine trial are shown in Figure 54 through Figure 56. In the first the planning image can be seen loaded into the interface. The path is described by clicking the "Insertion Point" button and using the crosshairs to indicate the appropriate point on the display, followed by the "Target Point" button and then another click on the display. Points may be located in multiple slices; the slider will allow the user to "fly down" a selected path to check for obstructions. To eliminate tilting of the gantry, a significant source of additional scans, the interface is equipped two non-traditional viewing options: A recomputed plane along the selected path or along the needle's trajectory (grayed out in the figure). These digitally "tilt" all the scan planes and, although this causes some image degradation, modern scanners provide significant resolution that viable images are generated. Once the ideal path has been selected the: "Accept Path" button is clicked. At this point the user is prompted to connect the robot and place it at the insertion point. The interface then locks until a new scan is loaded.

With the robot zeroed and affixed to the patient and the needle loaded and gripped, the next scan is taken and loaded into the interface. Once this scan is received, the needle is registered by first indicating its tip followed by an additional point on its length, as seen in Figure 55. With the needle registered the slider is moved until the crosshairs indicate the needle's intersection with the skin surface. In the first scan, this is nominally collocated with the insertion point, but in subsequent scans as the needle is inserted it is not. In this figure the robot can be seen connected with a green indicator, which matches the green LED illuminated on the control box in Figure 35, and the recomputed view corresponding to the needle's current trajectory is selected. With the insertion point and the target point, again, selected the "Accept Path" button is clicked, triggering the third interface panel to display.

The third panel enables control over needle motion. Based on the needle's current trajectory and the planned insertion, the in-plane and off-plane angles are displayed for confirmation; to prevent errors no opportunity is provided for adjustment other than the "Back" button. After successful angulation, the interface again locks preventing further motion until a new image is acquired and the needle and path are registered anew. Though slightly tedious, this modality prevents registration and planning errors from propagating, as well as accounts for anatomical shifts that can occur over the duration of a procedure; though possible, a deliberate decision was made not to permit the path to transfer from one scan to the next. After angulation the clinician uses arrows or the slider to indicate how far along the path he wishes to place the needle. This facilitates stopping midpoint, i.e. at the

pleura, for final adjustment. Needle gripping is again automated. In case of fault the “Stop” button will end motion and trigger the needle to be released.

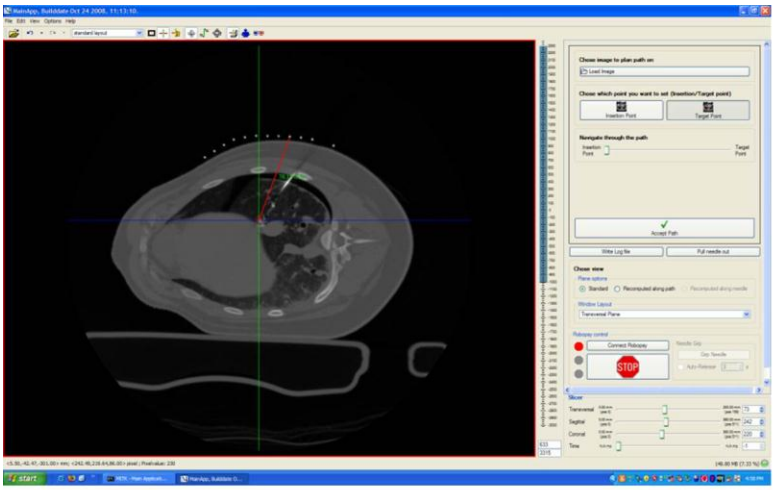

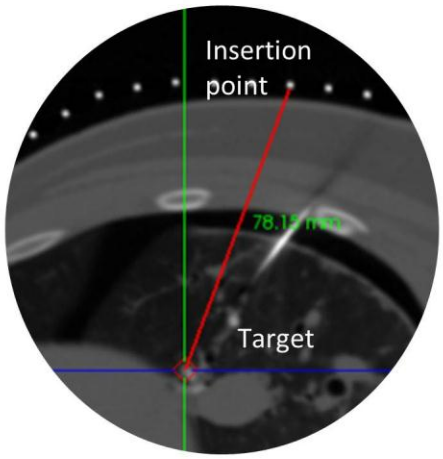

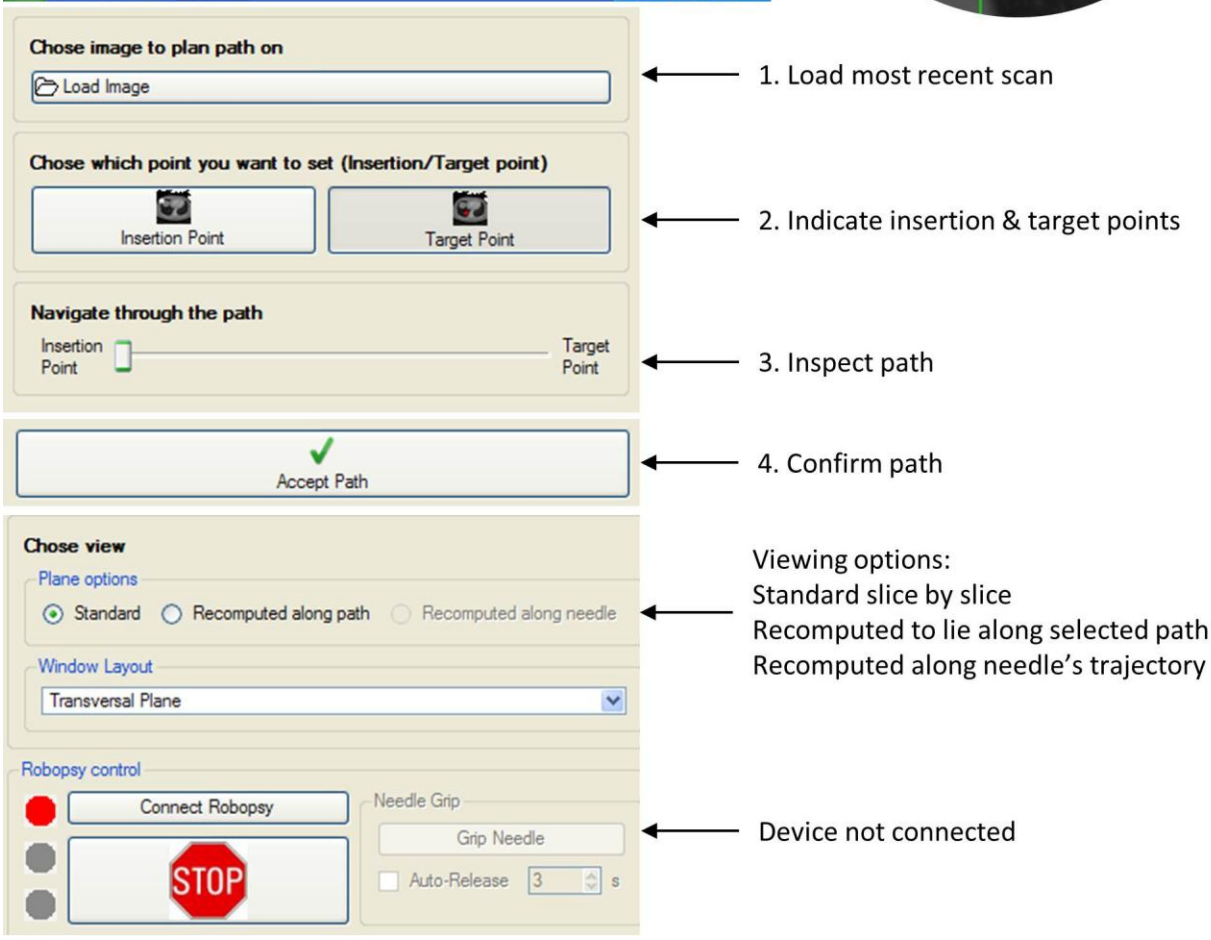

Figure 54 – Gamma Interface, planning stage showing the desired path from insertion point to target.

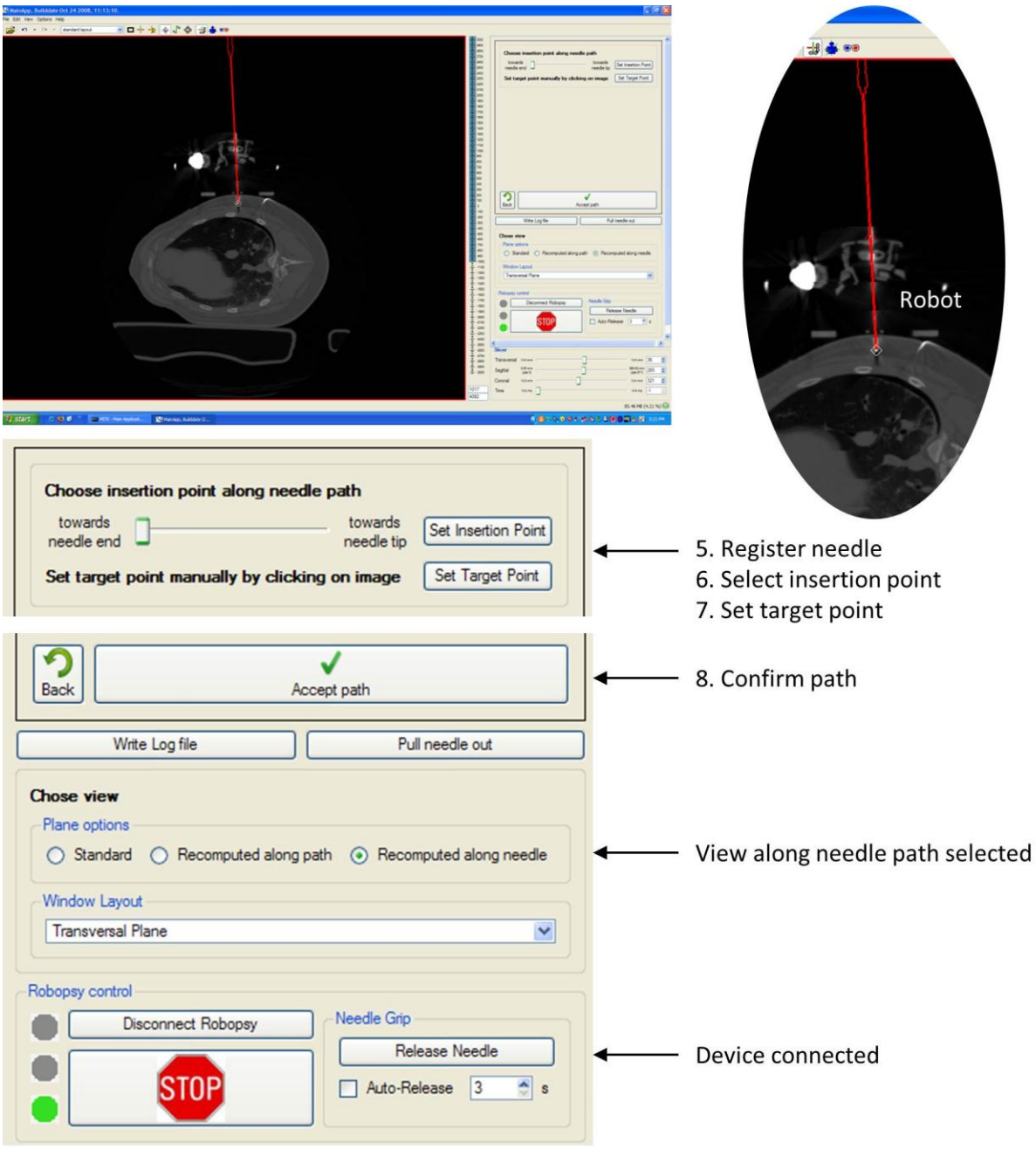

Figure 55 – Gamma Interface with needle registered and path from insertion point to target indicated.

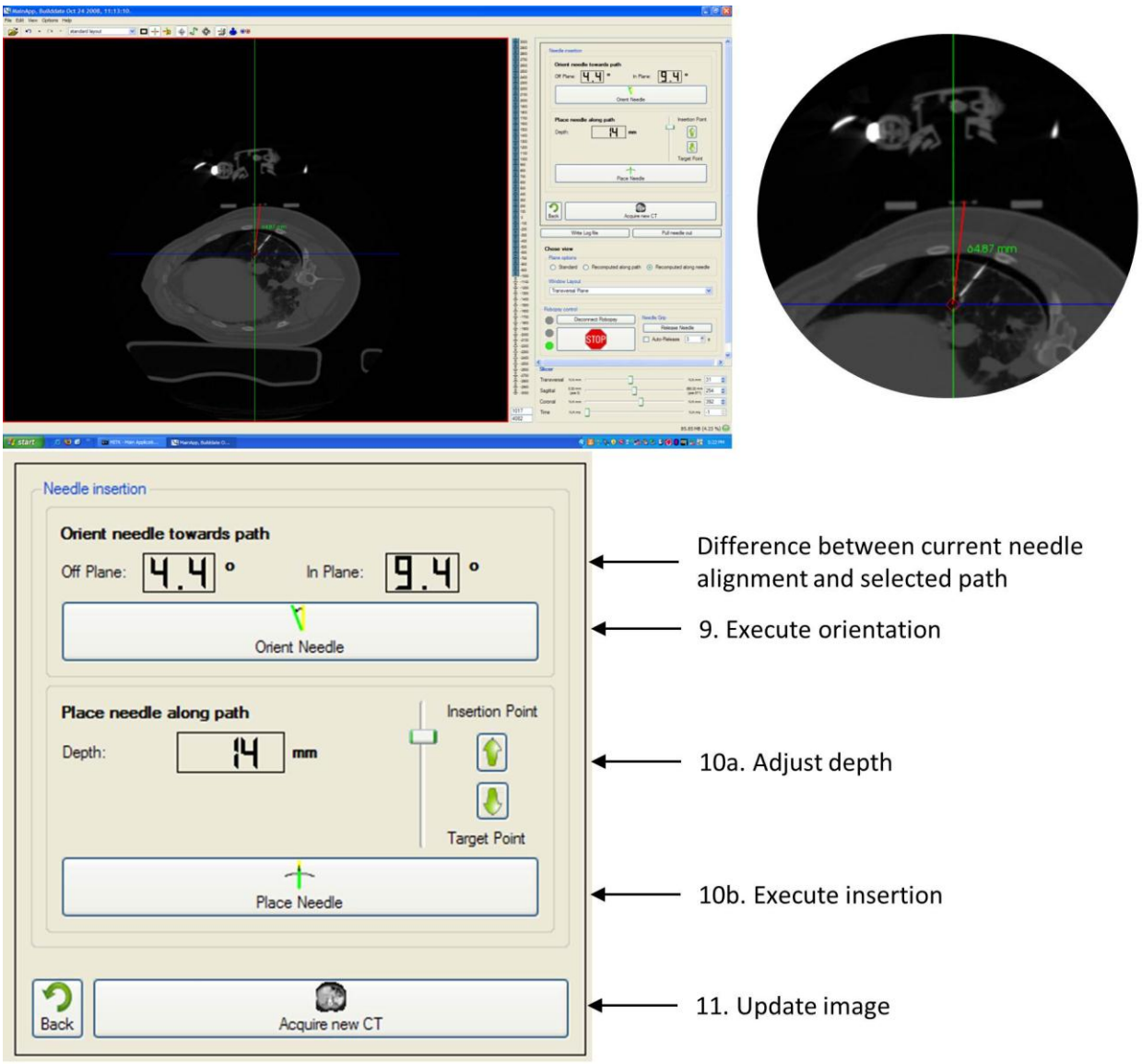

Figure 56 – Gamma Interface, needle actuation panel.

5.6.3. Phantom Trial with Gamma Interface

The Gamma prototype and MITK-based interface provided the first system, sufficiently functional and reliable, with which to conduct repeated tests. Both gelatin phantom and porcine trials were performed in November 2008 at MGH with a General Electric Lightspeed H16. In this phantom trial a selection of penetrable targets (fruit, clay) were cast into the gelatin, shown in Figure 57, and targeted using both the new and the previous interface. The results were presented in [114] by Alexander Seitel at the 2009 SPIE Medical Imaging conference and are reported here.

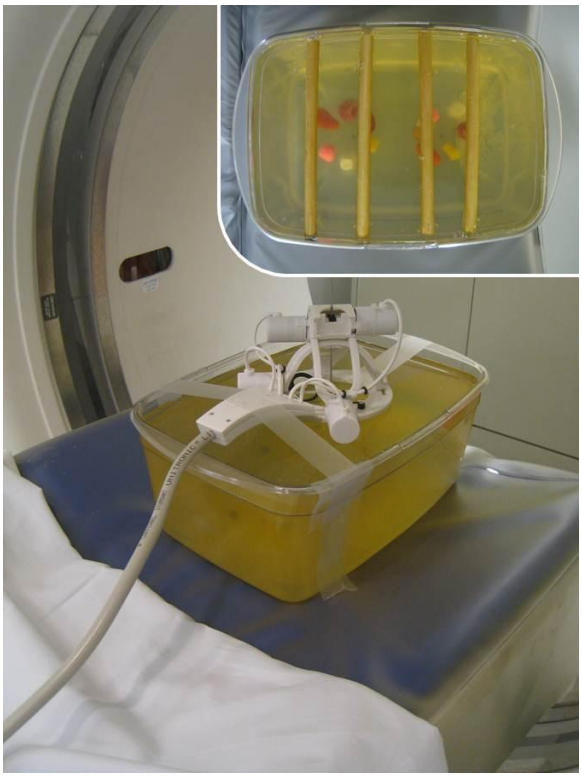

Figure 57 – Testing the gamma interface on gelatin phantom. Soft targets are under wooden dowels simulating ribs.

Two sets of 5 targets each were cast into the phantom with one set used for testing with the Beta interface and one set used for the (new) Gamma interface. To reduce the effects of needle bending, an 18 gauge (1.3mm diameter) coaxial needle was used. One target group was selected for use with the Beta interface and the other with the Gamma interface, with the preparation, planning and needle placement portions of the procedure timed and the results plotted in Figure 64. For each set of trials, the robot was placed once and then each target in the group was addressed individually with a "Path Planning" and "Needle Placement" stage. The path planning stage evidenced an approximate 3 min savings, 8:40 versus 12:04 minutes, with the use of the image guided interface. Additionally, slightly fewer scans were needed. The overall 11% decrease in procedure time was attributed to the elimination of gantry tilting. Contrarily, a 1 min increase in the needle placement time, 8:29 versus 7:39, was observed. This was attributed to the time spent transferring scan to the interface and repeatedly indicating the path and registering the needle.

This mini-study was severely limited in scope. Trained radiologists were not available, so the testing was conducted by a project team member who had significant biopsy observational experience. Comparison to first hand observation and the retrospective study indicated that the phantom provided a greatly simplified targeting challenge; it is predicted that under more realistic conditions with ribs and blood vessels to avoid and respiration, the benefits of direct image-based control would be more marked.

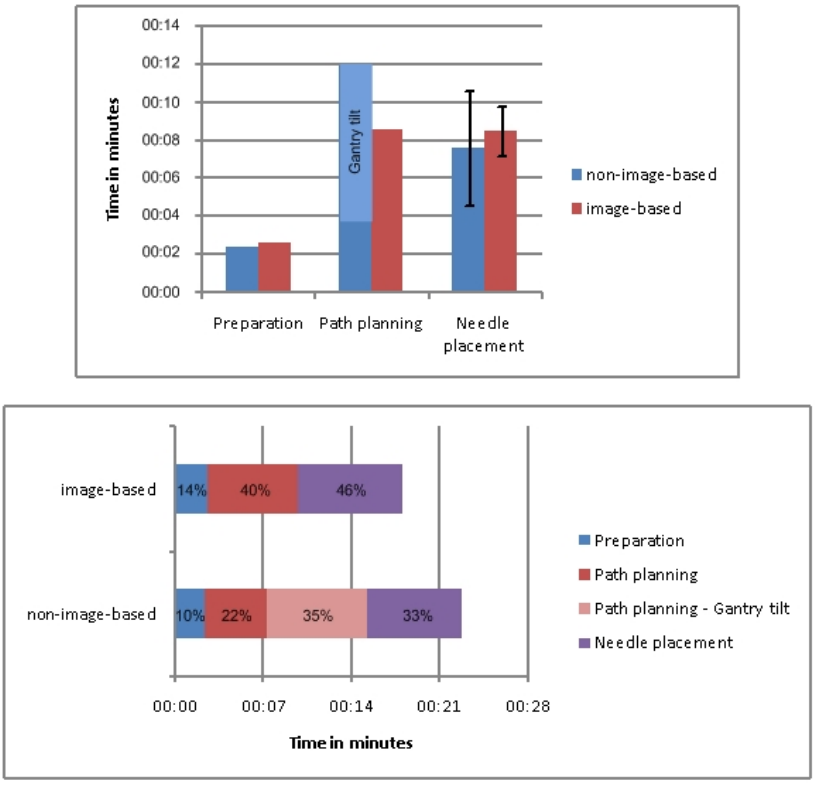

Figure 58 – Top: Averaged time needed for the different steps of the workflow. The standard deviation is only shown for the needle placement, because the other steps were not performed for all targets. Bottom: Total procedure time broken into percentages for the different steps. [114]

5.6.4. In-Vivo Porcine Trial with Gamma Interface

Directly after the phantom trial, a second porcine test of the Robopsy system was conducted at MGH with a GE LightSpeed. As with the previous porcine trial, this was conducted as an in-vivo validation of the system. Conducting a statistically significant comparative study of the conventional manual versus a Robopsy assisted procedure would have required the sacrifice of over a dozen porcines; unacceptable at this stage of the development. As before, the porcine was sedated, ventilated and placed in a head first, left decubitus position. Artificial lesions were injected into its lungs and the standard procedure was followed. Images from this trial are shown in Figure 54 through Figure 56, which as with the previous trial followed the protocol outlined in Table 10. Similar to the previous trial, an artificial lesion was targeted with 4 scans. However,

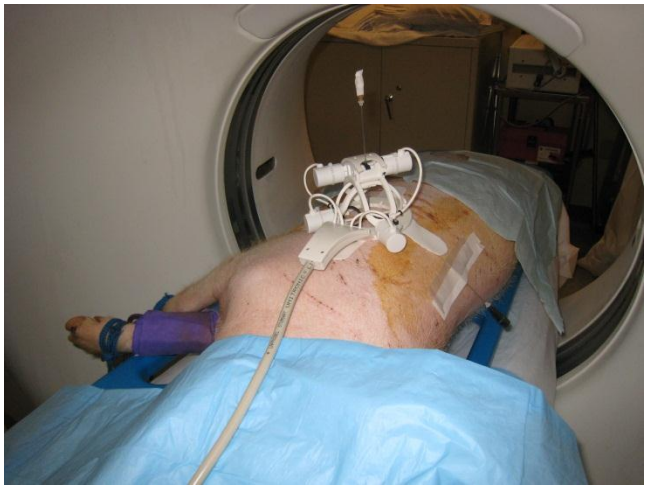

Figure 59 – Porcine test of Gamma system with porcine in scanner and robot mounted.

operational difficulties with the new interface which precluded timekeeping were encountered. The preload springs adequately reduced the backlash and the 0-rings provided a firm grip in the needle during insertion. Despite providing high torque, insertion motor speed proved too low, with a 6.5-cm insertion accomplished in 18 seconds. This tented the pleura and caused a significant pneumothorax. While the roller drive facilitates unclamping and free needle motion, the Light Puncture Robot is superior in more closely mimicking a clinician's swift jabbing motion.

5.7. Conclusions & Future Work

Development of the Robopsy system has demonstrated the potential for a small scale, disposable robot to increase the efficiency of a well-constrained procedure. In addition to lung biopsies, the system is applicable to a range of procedures where probes must be inserted into a patient under image guidance, such as lung, kidney, liver and pancreas biopsies, RF ablation, and prostate brachytherapy seed placement. In addition, a family of robots could be developed which would use similar image-guided interfaces and control hardware, but connect to different lightweight, low cost and disposable end pieces to facilitate a wide range of interventional procedures while limiting capital costs.

By mounting directly to a patient, the structural loop was minimized and patient motion accommodated. Through both phantom and porcine trials the device was shown to integrate satisfactorily into the current procedure and reduce the number of scans necessary for successful targeting. However, without a large porcine study comparing manual to Robopsy assisted interventions, it is not possible to definitively demonstrate time savings. Despite a cumbersome underlying architecture, the MITK-based interface provided an adequate replacement for the CT display. In the future images should be pushed to it automatically or with a single click. Indeed, the Robopsy software could be run on CT machines' own interfaces, however CT hardware is tightly locked down by manufacturers. Robotic interfaces, by walking a clinician through the procedure, have potential to serve as a training tool as well as enforce specific protocols. This suggests performing a phantom trial comparing the performance of experienced radiologists with neophytes using the interface. Regardless, intuitive operation and short learning curves are essential if more robots are to be integrated into clinical practice.

One major addition is needed to the interface: the ability to accept the robot in any orientation while sending the correct commands to the hoops' axes. Addressing this would, at a minimum, require the addition of 3 or more metallic sphere fiducials to the base. These would be identified in each scan and each clicked on by the clinician to define the device's orientation in space. Alternatively, in order to decrease the number of clicks, the clinician would register the robot and needle after each scan. It might also be possible to automatically detect the spheres and the needle and present a tentative registration to the clinician.

Respiratory gating is also a challenge, with the patient located remotely from the clinician while the needle is inserted. Adding a small, unidirectional accelerometer and displaying the trace on the interface would provide a representation of the patient's respiratory cycle with which the clinician would trigger the insertion. Another challenge is tenting of the pleura, observed during porcine testing. This suggests that, if powered needle insertion is maintained, there will need to be a mode that permits the rapid jabbing motion that a physician is able to execute manually. Ideally, this would be

accomplished with the existing friction drive and a software "button" that executes a rapid, limited travel motion, but it may be applicable to consider an alternate mechanism such as that of the Light Puncture Robot, discussed in Section 2.3.4.

Unfortunately, the Robopsy system, as conceived, is currently stalled. Extensive efforts were made to determine exactly what payments both hospitals and physicians received for biopsy and ablation procedures proved futile. Hospitals are unwilling to provide such data and, despite being public information, the fees schedule's numbers provided by the CMS's website appear to disagree with those of the local contractor responsible for the Boston area. The reason for this could not be determined. Nevertheless, it was estimated that biopsies of the chest, liver or lung reimburse in total at less than $1000. Therefore, at an estimated production cost of $100, even before applying a 2-3x markup, the device is too expensive to be disposed of after each biopsy procedure. Compounding this was a substantial reduction in reimbursement for radiological procedures in 2010, the exact details of which are mired in a political and legislative discussion. However, for procedures of higher value than biopsy, such as ablations, which were estimated to reimburse in the area of $4000, and brachytherapy seed implantation, adding cost to a procedure in exchange for increased precision would be more acceptable. Additionally, while a biopsy can relatively easily be repeated, should an insufficient or a diagnostically inconclusive sample be acquired, these procedures require precise probe placement on the first pass. Fluoroscopic interventions could also be conducted remotely with minimal radiation doses for the medical team.

Indeed, there is a dearth of developed, low cost actuation modalities that are compatible with imaging, particularly MRI. Johns Hopkins pneumatic stepper MRI actuator [43] represents a promising advance and thin hoses can be used to deliver short, high pressure blasts. In addition, the use of water (or saline) based hydraulics should be revisited. Pistons, vane actuators and even expanding bladders, could be made from cheap polymers, potentially resulting in lower-cost disposable actuators than the $10 motors prototyped for this project. Hose flexibility (without kinking) will still be a critical limiting factor. Piezoelectric actuators, whereby a vibrating beam is drives a surface in a linear or rotary motion, are also showing promise in MRI applications, however they are still cost prohibitive and require tight controls over assembly and preload in order to operate reliably and durably. There is certainly a potential space for a disruptive actuator technology.

Later, after the Robopy development, an additional product entered the market, which addressed the targeting challenge. The See Star, Figure 60, from AprioMed, Uppsala, Sweden, is a small, all-plastic device that with a patented design incorporates the same double hoop structure as the Robopsy system as well as projecting ears that are taped to the patient [115, 116]. The needle guide rides in the two hoops and is comprised of two parts that screw together; tightening them in place and locking the hoops. The center of the guide comprises a metal tube, through which the needle is inserted, that projects towards the rotation point. During scanning this is visible and creates a long, white artifact. Therefore, the device can be angulated so as to point at the target before the needle is inserted. The needle is then manually inserted, which allows the clinician to be in full control and feel the tissue as it is penetrated. The major shortcoming of this device is the lack of guidance in setting the angles; the clinician must still iterate to obtain the correct angle. Therefore, serving primarily as a needle support device, its popularity in clinical use is limited.

One way to address this, while leveraging the cost advantage of a non-powered device, would be by adding a smart interface and angular markings to the device. Considering that with the Robopsy planning interface, precise angulation interventions can be accomplished with just 4 -5 scans as opposed to over a dozen, it is pertinent to ask whether the device truly needs to be fly-by-wire. This gives rise to a manual Robopsy device concept. This is mocked up in Figure 61 and continues to fulfill the FRs described in Table 7. In this device, the hoops' motors are replaced with calibrated manual dials. Interventions would follow the same protocol as given in Table 10 and be planned using the same interface. Then, rather than commanding motors to actuate the hoops to the desired angles, the clinician would reenter CT room, reach into the bore and dial the hoops to the correct angle. After verifying this with another scan and making any adjustments, a slide on the needle would be set and the insertion conducted manually. This would enable both slow and steady and sharp piercing motions as the clinician desired. Rather than a bushing, the clamp is retained so the needle can be released. With this concept, all system intelligence and capital expense could be transferred to a single tablet PC, running the same interface as the Robopsy robot sans the motor driving commands, and disposable production cost would be minimal. Removal of all automated needle actuation would also address the significant safety and liability concerns, inherent in all robotic surgical systems, while still providing the clinician with an appropriate scale smart tool. Prototype development of this concept is recommended as the next project step.

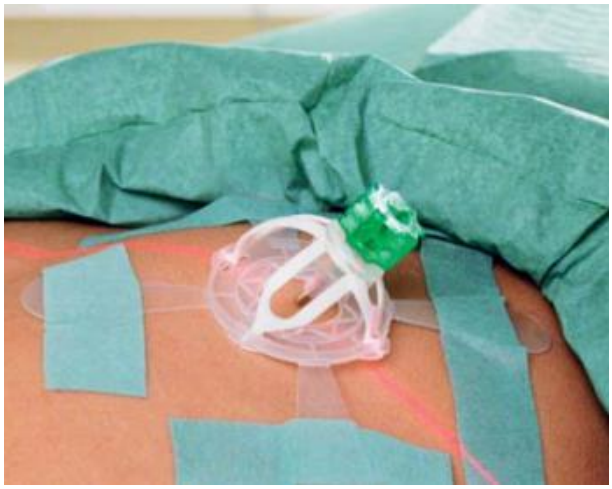

Figure 60 – AprioMed SeeStar taped to patient [117].

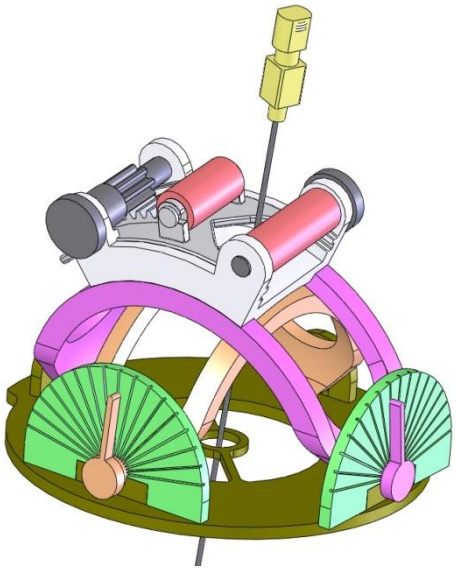

Figure 61 – Manual Robopsy concept with protractor-dials to indicate hoops' angles.

6. MITE – Minimally Invasive Tissue Extractor

6.1. Introduction

The design method and theme of appropriate scale medical robotics extends to procedural tasks which are necessary, but non-complex and often tedious. Consulting Table 1, it is seen that robots excel at tasks that are monotonous, without suffering fatigue or inattention. A means of identifying potential opportunities to improve efficiency is thus to divide a procedure into tasks that are *value adding* and *non-value adding*. Using an example from manufacturing, work on the piece that creates the desired geometry (that the customer will pay for) in a machining process is value adding, while cleaning up the chips and conducting regular machine maintenance represent costs that are non-value adding. Pinpointing similar tasks within a medical procedure can reveal neglected opportunities for innovation, where an increase in automation has the potential to improve procedural efficiency.

The Minimally Invasive Tissue Extractor (MITE) project prototyped a concept for a new morcellator, a tool that is used to remove masses of excised tissue during minimally invasive surgery which are too large to pass bodily through a trocar or its small incision. Design and prototyping of an improved morcellator was conducted in the summer of 2009, led by Ewout Arkenbout, a visiting student to the research group from TU Delft, Netherlands, and in collaboration with Dr. Jon Einarsson, Division Chief of Minimally Invasive Gynecology at Brigham and Women's Hospital.

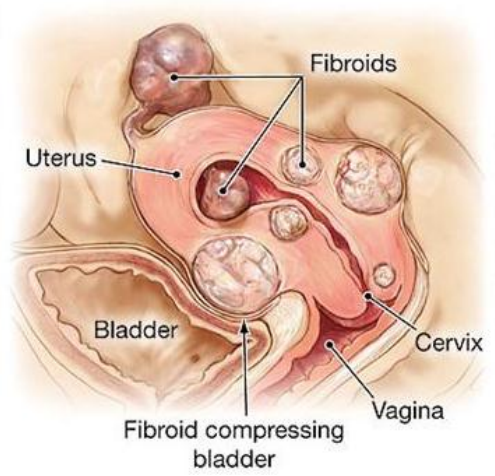

Figure 62 – Fibroids and uterus [118].

Two exemplary gynecological procedures where tissue removal is a challenge include myomectomy, where fibroids, benign uterine growths shown in Figure 64, are removed, and hysterectomy, where the entire uterus, including or excluding the cervix, is excised. Fibroids can reach the size of a grapefruit and have the consistency of rubber balls. Dr. Einnerson estimates that the mass of an excised uterus ranges from 40 (small postmenopausal) to 2000 g, with an average of 300 g. When growths are benign it is not necessary to preserve tissue margins and histology, therefore, widening (or tearing) of the trocar incision is not acceptable and tissue is removed piecemeal via morcellation. This method is slow and painstaking, with a typical achievable removal rate of 45 g/min. During actuation the tip of the morcellator must be carefully guided within the insufflated abdomen to avoid damage to surrounding organs. In an article on supercervical hysterectomy (cervix preserving) [119] a 10 mm morcellator was used to remove 41 uteri ranging from 60 to 569 g and averaging 146 g. Mean operating time was 94 minutes and, from 19 cases videotaped, morcellation times of 4 – 23 min were observed, with an average of 11.8 min, 12% of overall time.

Morcellation is applicable to a range of procedures and can even, at clinician discretion, be used to remove cancerous tissue provided that it is first contained within an endoscopic bag. With some techniques morcellation can also be used to directly remove masses from the underlying tissue. In the book, *Advanced Gynecologic Endoscopy* morcellation receives less than a single sentence and a picture

in the chapter *Total Laparoscopic Hysterectomy* [120].This lack of attention is commiserate with a task that is necessary, but requires minimal surgeon skill.

6.2. Current Devices & Operation Review

Most current morcellators share the following operating principles: The device consists of a hand piece from which a long, annular blade inside a sheath projects. A motor in the hand piece rotates the blade when a trigger or foot pedal is pressed. There is also a duckbill (or similar) seal inside the hand piece which maintains pressure inside the patient. In order to remove tissue, the barrel is placed into an insufflated patient through a large trocar or in place of the trocar. The tip is positioned in free space and then, in an iterative process, a grasper is inserted through seal and down inside the blade, a tissue mass is acquired, the blade is activated and the gripper is withdrawn, severing a strip of tissue against the blade. This is deposited outside the patient and the process repeated until the desired amount of mass is removed. In a total hysterectomy, the mass may be shaved down until it can be removed vaginally, but in a supercervical hysterectomy the entire mass must be removed via morcellation. Some morcellator tips feature shields which slide down around the blade, providing partial protection. These types of tip can also incorporate a lip, as seen in Figure 64, which encourages a peeling motion so that long strips of tissue can be removed from a mass, as opposed to short cores.

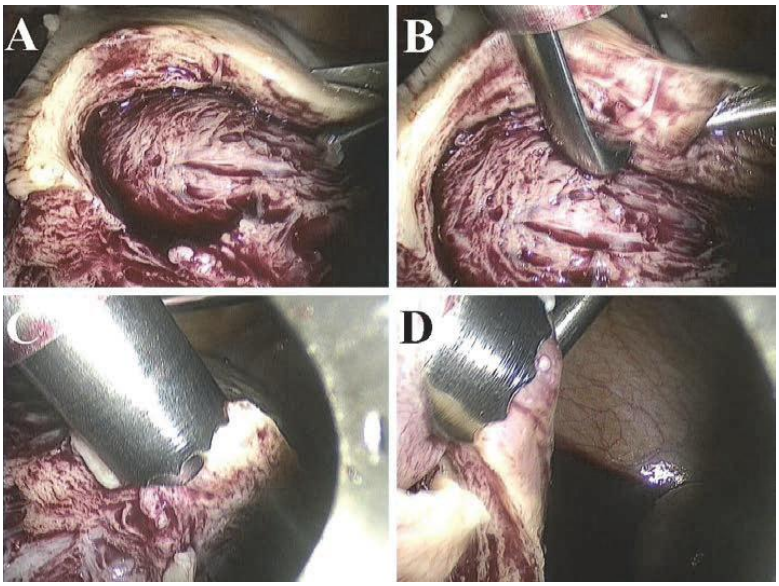

Figure 63 – Morcellation showing tissue drawn into the annular blade and cut [120].

A product search was conducted and the most common morcellators in use were identified:

- GyneCare Morcellex – Ethicon, Cincinnati, Ohio
- Wisap Morcellator – Wisap Endoscopy, Munich, Germany
- ROTOCUT G1 – Karl Stortz, Tuttlingen, Germany
- SAWALHE II Supercut Morcellator – Karl Stortz, Tuttlingen, Germany

Figure 64 –Left Ethicon GyneCare Morcellex - The single-use hand piece connects to the base via a flexible cable drive [121]. Right: Karl Stortz Sawalhe II Supercut, available in 12 and 15 mm diameters, shown with obturator (plug) inserted and matching forceps for grasping tissue [122].

An alternative morcellator design, shown in Figure 65, for removing intrauterine fibroids and polyps hysteroscopically incorporates a side-cutting blade which rotates and reciprocates to take small nibbles of tissue, which are then aspirated with a continuous flow of saline. According to the website of Interlace Medical, Framingham, MA (now part of Hologic Inc.) [123], a 3 cm diameter fibroid can be removed in 10 min. It is not clear that this tool design, relying on aspiration, with the assistance of fluid, as the transport mechanism, would be appropriate for large mass removal in a gas environment. Some morcellation techniques entail maneuvering the excised mass into an endoscopic bag, such as Covidien's Endobag™ or Cooks' LapSac™, and then morcellating it within the enclosure, so as to prevent tissue dispersion and possibly better control the mass. This and general morcellator technique is described in [124]. Bag perforation is a risk, though distending the bag with fluid or gas reduces it. In addition, no combined bag and trocar exist. Energy methods also exist for nibbling away small morsels of tissue, though they do not facilitate bulk removal and are not examined here.

Figure 65 – Interlace Medical Myosure Tissue Removal System incorporating a rotating, translating side cutting blade, irrigation and aspiration.

The project began with a first-hand observation of a laparoscopic hysterectomy at Brigham and Woman's Hospital and a review of the most common circular cutting, peeling morcellation method. From this the following weaknesses give in Table 14 were identified. The final point is most surprising: When conducting robot-assisted da Vinci surgery, no integrated tissue removal solution is available. At the end of a procedure, during which all the treatment has been conducted remotely, the robot must be undocked and displaced from the patient, then a standard morcellator is inserted and the tissue removed via traditional laparoscopic methods.

Table 14 – Primary Morcellator Challenges

- The discretized extraction procedure is manual, iterative and inefficient, motivated by the instrument's operating modality and capability, rather than a clinical need.
- The exposed rotating blade often scatters bits of tissue within the abdominal cavity, leading to a painstaking search for scattered morsels. All tissue must be removed since remaining tissue can cause inflammation, regrowth or necrosis; all serious complications. [125]
- The exposed rotating blade (even when partially shielded) can accidentally damage other organs. This necessitates that the clinician actively manage the tool's distal tip position throughout the procedure, leaving only one hand free to acquire and manipulate the tissue.
- Most current morcellators do not typically use trocar ports, thus the removal of a port is necessary. Tissue removal speed generally scales with morcellator diameter; however, a more efficient process could compensate for a smaller morcellator.
- There are no known solutions for integrating morcellation with robotic surgical equipment.

6.2.1. Predicate Concept

A first attempt at improving morcellator design was explored in 2006-2007 with Dr. Zev Williams, of Brigham and Women's Hospital, Boston, MA. The resulting concept was nicknamed the "Endoblender." This tool compromises a folding, spinning blade on the distal end of a slender stem sized to fit through a 15 mm trocar, a hand piece and integrated irrigation and suction. Using it involves inserting an endobag into the patient, maneuvering the excised organ into it, inserting and activating the Endoblender, then suctioning out the bag's contents. This tool was initially prototyped in the Precision Machine Design course and as a senior thesis of Daniel Hernandez-Stewart [126]. Subsequently Dr. Williams received a small grant which funded the creation of a more robust prototype by an outside design firm.

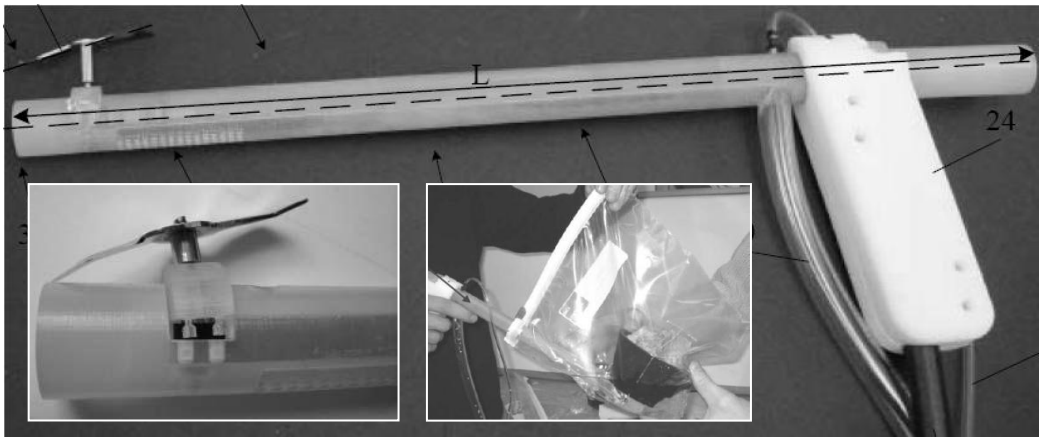

Figure 66 – Prototype "Endoblend" with details of the tip and the deployable guard in a bag.

Protecting the bag from the rotating blade remained a problem and a separate senior thesis [127] by Darragh Buckley focused on creating a deployable guard around the blade. The resulting guard employed three nitinol rings and polyethylene fibers, and was reasonably successful at protecting the bag and directing tissue into the blades. This method is most applicable for fluid filled, hollow organs and other situations where absolute containment is necessary. While development of the combined prototype proposed a creative solution to improving tissue removal efficiency, it represented a

significant change from current practice and an unnecessarily drastic method of debulking. Therefore, an alternate design was pursued.

6.3. Procedural Analysis & Functional Requirements

Morcellation is a common step in many procedures and, as such, may be treated as a mini-procedure, which be further broken down into discrete steps. This was done based on both a literature review and first hand procedural observation, and the current procedure's steps are shown in the left hand side of Table 15. From this list it was apparent that efficiency would be improved if steps 3 – 12 were automated. Taking the morcellator insertion and removal tasks away from the clinician's sphere of responsibility would not add any value. Therefore, working from the weaknesses summarized in Table 14 and the shortcomings of the first concept, the project mission was defined as:

To create a morcellator that automatically debulks, transports and disposes of excised tissue in a safe and continuous fashion.

Table 15 – Potential reduction of morcellation steps with automated morcellator

Traditional Morcellator	*Automated Morcellator*
1. Remove trocar	1. Remove trocar
2. Insert morcellator	2. Insert morcellator
3. Insert grasper through morcellator port	3. Activate morcellator
4. Find and grab tissue with grasper	
5. Manually draw tissue through morcellator's cutting blade	4. Use laparoscopic tools, already in patient, to continuously feed tissue into the morcellator's distal end
6. Deposit strip of tissue outside body	
7. Reinsert pincer	
Repeat 4 -7 as needed	
8. Look with endoscope to locate remaining, scattered pieces	5. *Tissue is debulked, transported and bagged*
9. Pick up piece with grasper	6. Look with endoscope to verify that all tissue has been removed
10. Draw piece out through morcellator (without morcellating action)	7. Feed any remaining masses into morcellator
11. Deposit tissue piece	
12. Reinsert pincer	
Repeat 8 - 12 as needed	
13. Remove morcellator	8. Remove morcellator
14. Conclude procedure	9. Conclude procedure

Table 16 – Improved Morcellator Functional Requirements

1. Cut tissue morsels from larger mass.
2. Transport tissue to exterior of patient and contain it.
3. Protect the patient from unintended laceration
4. Fit within a standard trocar or trocar incision.
5. Free one or both of the clinician's hands to manipulate tissue into the morcellator.
6. Work with multiple tissue types.

6.4. Strategy Development

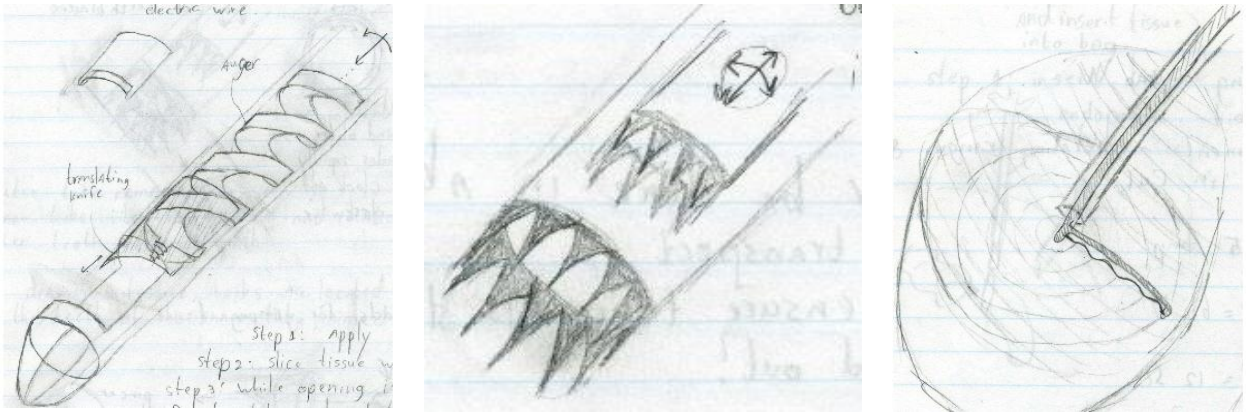

Figure 67 – Morcellator strategies, from left: Slicing blade and auger, dual serrated tubes, spiral electrocautery wire cutting, sketches by Ewout Arkenbout.

The automation challenge was broken down into cutting and transportation, with tissue disposal determined to be relatively trivial. Two broad operating modalities were considered: a continuation of the Endoblend where the tissue is placed in a bag and disintegrated or a more traditional operation with a tube incorporating automated cutting an integrated transport mechanism. The latter was selected and three new strategies, reproduced from Arkenbout's notebook, are shown in Figure 67. The first comprises a side opening below which a blade oscillates axially. Tissue is placed in this opening and morsels are sliced off. Simultaneously, a rotating auger transports the tissue away. The second features a pair of nested tubes, both with serrated ends, and the inner tube having rear-facing barbs. The outer tube is fixed and the inner tube vibrates in 2 DOF: the first about its axis, to slice off chunks with a scissors motion, and the second along its axis so that the barbs urge the tissue backwards. Tissue is still grasped and pulled through the device, but without a spinning blade, the risk of prematurely severing the tissue strip and scattering morsels is reduced. The third concept proposes placing the tissue in a bag and uses energy methods to slice it into a long, spiral strip that can be removed singly.

Figure 68 – Exemplary meat grinder by The Sausage Maker, Inc., Buffalo, NY [128].

Inspiration for the first strategy was taken from a meat grinder, which accepts cubed meat into a funnel and uses a rotating auger to force it through a cutting head into a sausage casing. It was hypothesized that if the auger was longer it would transport it out of the patient. The side port presented no sharp edges to the patient and contained the tissue, although use of a bag was not precluded. The second strategy addressed only the cutting challenge, but retained an exposed sharp edge and did not improve upon transport. The third strategy required initial

bagging of the tissue, inflation of the bag and then deployment of the cutting wire and its actuation in a helical manner. Overall this mechanism represented significant complexity.

Considering that the form factor and basic operating principle of exiting devices satisfied clinicians, but not the repetitive nature of the tissue removal or the chance of causing internal lacerations, the first strategy was selected as most versatile and the least disruptive to current practice. Additionally, this design is not likely to scatter tissue, thus further reducing procedure time. This strategy was then developed into a proof-of-concept prototype.

6.5. Concept Prototype

The linked functions of cutting and transport were identified as the most critical; therefore, all prototyping effort was focused on developing and validating this module. Tissue containment post extraction and the drive mechanism were not emphasized. The prototype device is composed of two nested tubes and an auger. The outer tube is fixed in position and has a bluntly capped distal end and openings in the side at the proximal and distal ends. Translating back and forth inside this tube is a second tube tipped with a circular blade, similar to those found in current morcellators. Two options for the slicing direction were considered: Sideways in a rotary direction, and up and down. Both were prototyped and the former was found more adept at pushing tissue aside than into the auger, while the latter took sharp bites as it passed over the inlet opening in the outer tube. Any tissue that enters the opening is nipped off and fed into the auger which rotates inside and oscillates along with the inner tube. This transports the tissue to the proximal end where an opening in the inner tube coincides with an opening in the outer tube. The tissue is forced out of this outlet and into a catch bag which can be removed, sealed and disposed of, or sent for pathological evaluation.

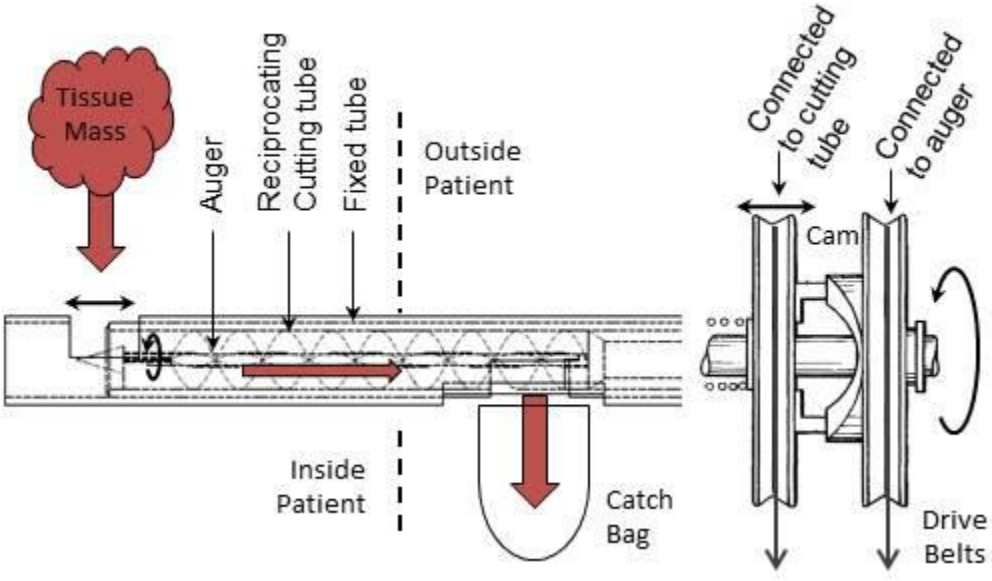

Figure 69 – Schematic side view of Minimally Invasive Tissue Extractor mechanism. The auger rotates and translates back and forth; the inner tube translates back and forth synchronous with the auger; the outer tube is passive. At the tip the slicing action is performed. Cam-action provides combined rotation and translational oscillation; image from [129].

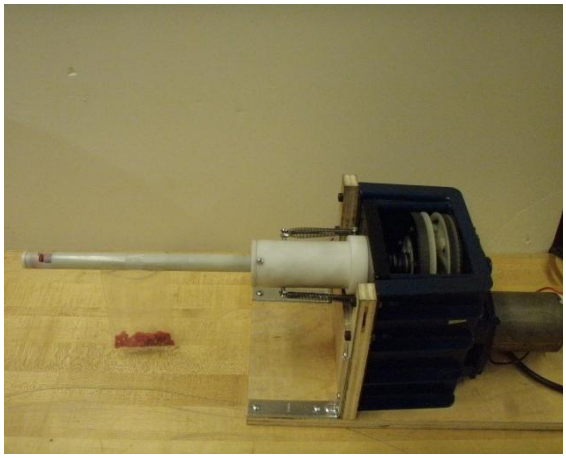

Figure 70 – MITE assembled.

Figure 71 – MITE disassembled.

The prototype's drive mechanism is built from the base of a repurposed oscillating spindle sander, the remnants of which may still be identifiable in the photo. (Note that the final device is unlikely to require a ¼ horsepower motor!) This sander's patented [129] design, shown in Figure 69, consists of two pulleys, separated by a cam and driven by a single motor. The pulleys have slightly different diameters and, consequently, different rotation speeds. The rear pulley is fixed axially and has a sinusoidal cam feature on its face. This engages a matching cam feature on the font pulley which moves axially, with return force provided by a spring. The front pulley is directly connected to the auger, which both rotates and translates. The front pulley also pushes, via a thrust bearing, against the inner tube which also oscillates synchronously with the auger, but is constrained to the stationary outer tube so that it cannot rotate. The prototype was tested with butcher-supplied meat and found to perform satisfactorily. A summary of the prototype is provided in Table 17.

Table 17 – Specifications and Features of MITE Prototype

Motor power	¼ HP	Approximate tissue volume per slice based on half-filled inlet assumption $V = \frac{1}{2}\left(\pi\left(\frac{OD}{2}\right)^2 l\right)$	~ 800 mm^3
Auger speed	1750 RPM		
Stroke frequency (f)	50 slices/min		
Stroke length	12.7 mm (½")		
Outer tube OD	19.05 mm (¾")		
Inner tube ID	12.7 mm (½")		
Semicircular inlet length (l)	12.7 mm long	Tissue removal rate (density of 0.001042 g/mm^3)	~ 42 g/min
Active length*	~ 101 mm (4")		

*The device was sized based on that of available components; hence this length was limited by that of the ½" auger bit.

- The rotating auger is not directly exposed and the translational, oscillation cutting blade is entirely contained within the stationary outer tube. The device's distal tip is completely blunt.
- There is no need to manually remove anything from the patient, once positioned the auger automatically transports and disposes morcellated tissue outside the abdominal area.
- The morcellation speed of the MITE, in the case of the proof-of-concept prototype, is only on par with that of the currently used device; during initial testing with fresh butchered meat a removal rate of 42 g/m minute was achieved. There is significant room for optimization of the design to greatly increase this speed.
- Two operational modes are proposed: 1) automatic and 2) semi-automatic. The former would continuously debulk and remove tissue fed into the mouth while the latter would be triggered in a "nibbling" fashion to remove tissue in situ.
- The design MITE can be scaled; no elements impose fundamental size limitations.

6.6. Future Work

The concept prototype appears promising and the few clinicians who have seen it expressed interest in testing a more polished prototype. Creating this will require a significant engineering design effort, beginning with optimization of the cutting method and evaluation with hard tissue. Thus far, testing has only been conducted with soft tissue and there is concern that the side cutting mechanism may not be able to acquire large diameter tissue or tough, spherical fibroids. A larger opening is needed and there may be aspects of the collapsible guard, designed for the Endoblender, that can be incorporated. Additionally, while tissue must currently be pushed directly into the inlet, it may be possible to design the cutting mechanism so that tissue is actively pulled inwards. Similarly, the transport mechanism will also require study and optimization with respect to thread profile and cutting speed to increase removal rate, and exploration of the effects of system scaling.

If the most critical module can be shown to work reliably, the next step will be to focus on the drive module. Ideally, the disposal module will be detachable and single use so that it can be discarded along with the excised, bagged tissue. Unlike the current morcellator that has one rotating blade, the MITE design has two independently moving parts to interface. The drive requires compaction and fitting inside a comfortable, sealed, sterilizable hand piece. Gears should probably replace belts, with care taken to eliminate vibrations. Offsetting the motor, which is currently axially aligned, will enable tissue to exit more directly from the end of the disposal module, rather than a slit in the side.

There is no need for the surgeon himself to manipulate the device: It can be mounted to an adjustable arm and "parked" within the patient or held by an assistant, leaving the surgeon two graspers free to manipulate the tissue mass in the abdomen. Finally, there exists the possibly of integrating the device with the da Vinci. In particular, the da Vinci arms are already designed to provide power and actuation to Intuitive's tools. It should be possible to configure a morcellator to mount onto and utilize the existing hardware for actuation, thus allowing an entire procedure culminating in tissue removal to be conducted minimally invasively.

Subsequent to this project, Arkenbout's Master's research focused on the design of morcellators. A detailed comparative literature study of morcellators is presented in [130] which identifies every morcellator design, since the first in 1993, and characterizes their procedural application, functional

modalities and removal rates. While he reports an increase in removal rate and with the current "peeling" modality as yielding the fastest removal rate, the paper concludes with a suggestion that morcellation safety and speed can be improved with the implementation of both a bag and a method that allows for continual rather than discretized tissue removal. A sister paper [131] proposes a method for better data gathering during a morcellation procedure and its subsequent analysis, so as to quantify morcellator performance and compare different morcellator models and designs.

Bringing this work together is an article [132], currently under revision, which uses in-vitro porcine tissue testing and data from actual hysterectomies to conduct a detailed time-action analysis of the function of a traditional rotary morcellator with peeling action. Data showed an overall morcellation rate of 20 g/min, which rose to 66 g/min if the time spent manipulating the tissue before and after cutting with the morcellator was included in the analysis. Removal rate was found to increase with organs; this is attributed to the steady peeling of long strips, which is not possible with small or irregular masses. An additional, final "cleanup" step was also identified, whereby the abdomen is irrigated to dislodge and aspirate very small debris hiding between organs and in folds of intestines. The larger the mass and more strips of tissue removed, the longer this takes. Together this research highlights an opportunity to create a more complete and automated solution to issue removal.

7. Development of a Medical Device Design Course

7.1. Introduction

The design methodology proposed in this thesis was developed over the past 9 years that the Precision Machine Design course has focused on the design of medical devices in partnership with CIMIT. Each of the 52 prototype-development projects has essentially been a mini-experiment and in the last 4 years, during which the author served as teaching assistant/instructor, significant work has been accomplished in optimizing the course including the project selection and team formation, design process and curriculum. Throughout, the working hypothesis has been that merging applied research and education can be educationally effective, while providing the means to rapidly and economically evaluate a wide range of ideas and designs and, thus, efficiently contribute to the launch of new technologies that have the potential to improve care. Therefore, in this section a review of the course is presented including the process' best practices, three case studies, the latter two for which the author served as a mentor, a review of student outcomes and an examination of past projects.

Figure 72 – Flyer advertising 2012 course and showing collaboration with the electrical engineering department.

Although the time frame and funding does not typically enable the development of full-scale robot systems, student teams are able to develop novel devices following efficient design principles. The course goal is demonstration of base function, not a beautiful, ergonomic device; form and finish can be improved in the follow-on development course, *Design of Mechanical Products* (2.753). Students' lack of clinical background, rather than being a hindrance, leaves them open to ingenious solutions which often represent translation from outside engineering experience. Projects initiated in the course have generated IP and peer-reviewed publications, stimulated additional research, furthered student and clinician careers and, recently, resulted in a technology license and a successful start-up venture. The model has been able to support traditional mechanical engineering devices, such as surgical tooling, as well as mechatronics projects that come closer to the robots or smart tools which are the subject of this thesis. In 2010, as a test, and the course partnered with the Electrical Engineering Department to increase student diversity and better incorporate sensors, custom circuitry and embedded control. The results were positive, in part resulting in the formation of the startup company described in Section 7.3.3, and this will be continuing in 2012.

7.1.1. Comparable Courses

Literature and books [133] consistently prove the effectiveness of project-based learning at all levels. One of the pioneer programs since 1963 is Harvey Mudd College's *Engineering Clinic*, which engages teams and resources on industry sponsored projects [134, 135]. Focusing exclusively on medical, Stanford University's *Biodesign Innovation Class* leads multi-disciplinary teams of students (medical, engineering and business) through a two semester program. Appropriate projects are

identified by experienced program fellows who spend three months in a hospital environment studying clinical needs. Stanford's Zenios, Makower and Yock have written the definitive book "Biodesign: The Process of Innovating Medical Technologies" [133]. Other analogous courses include the University of Minnesota's *New Product Design and Business Development Course* and the Johns Hopkins University's *Biomedical Device Innovation and Design Course* [136, 137]. The growing number of courses and dedicated programs in this field is encouraging.

7.2. Project Process

7.2.1. Project Selection & Team Formation

The first key to successful outcomes is the recruitment of enthusiastic clinicians and appropriate project selection. The same desired clinician and project characteristics apply whether selecting for the course or a for long-term research collaboration. Each spring a call for proposals is distributed to the Boston-area clinical community. Only two pages are requested covering the clinical challenge and its significance, current practice and background (pictures, videos and references), functional requirements of the desired solution and a disclosure of any previous work. The ideal proposal will define the challenge, but be sufficiently open, without a hardened, pre-conceived solution, so that students start with a clean slate. The project must require the development of new mechanical and mechatronic hardware and reasonably fit within the constraints of one semester, a workbench and $4,000 budget. Finally, project diversity is important commensurate with students' broad interests and skills. Experience has shown that projects having significant prior work or requiring only modification to an existing device do not furnish engaging challenges.

Finalist clinicians pitch their proposals to the 50-student class and the ultimate selection is made by the students, who self-form into teams of 3-5 people. This size facilitates efficient interaction and work distribution and correlates with research into team sizing and satisfaction [138][6]. Clinicians are expected to be active collaborators, rather than clients, with responsibilities, including biweekly team meetings, participating in brainstorming, sessions providing access to hospitals to view procedures and laboratory access for testing. Projects where a senior clinician delegates responsibility to a junior clinician have evidenced difficulties. Junior clinicians often lack free access to hospital facilities for equipment and testing and must give priority to fellowships and residencies. Often older clinicians have considerable medical mentorship experience and enjoy the change of working with engineering students.

7.2.2. Design Process

The second key is the structured, managed design process. By following the methods detailed din Section 4 and the steps shown in Figure 21, creativity is encouraged but focus maintained on the goal of producing a working prototype. The emphasis on narrowing the scope to only those functions where the clinician's performance or efficiency is limited as well as the constrained budget serves to encourage lean solutions; in choosing both concepts and strategies students are guided to the most reasonable

[6] As a result of this research 4.6 members is widely cited, particularly by pop psychology, as being the "ideal" group size, however this neglects the authors caveats that satisfaction does not necessarily map directly to performance. Additionally, testing was conducted at both Yale University and The University of Illinois with groups at the former indicating evidencing more severe interpersonal difficulties.

functionality/complexity ratio. The emphasis on analysis, bench level experiments and prototypes rapidly eliminates untenable designs, before significant resources are expended on detailing and hardware. Students are granted purchasing authority; however the instructors have oversight to detect instances where ordering a multitude of components to "see which works" is substituted for proper sizing and part selection. Three in-class presentations, occurring at the crucial check points before strategy selection, concept selection and final fabrication, serve to involve the entire class in the peer-review process, as well teach students professional communication of technical material.

Throughout the process course instructors serve as project managers and mentors, meeting with each team weekly to review progress, brainstorm solutions to current challenges, suggest resources and, if needed, assign action to individual team members. Instructors maintain a list of vendors (machine shops, 3D printers, blow molders, etc.) who are prepared to work with students, occasionally sample parts and invite them to visit their facilities. Instructors benefit from professional advancement; not only do they further hone their design skills through an active role, but they frequently contribute essential elements to the design and are, therefore, authors on papers as well as inventors on patents. The same is true for clinicians, especially those who continue with their projects, as seen with the ACL Repair Gun and 7.3.3. Sleep Sensing Shirt, Sections 7.3.1 and 7.3.3.

Good documentation is emphasized and all important drawings, calculations and findings are recorded in bound lab notebooks, which preserve IP. A secure wiki serves as a design history file and facilitates communication, without being a burden. Teams upload scanned sketches, working papers, testing notes, presentations, videos and CAD models.

The final prototypes are presented to an invitation-only academic, clinical and industry audience who are asked to sign confidentiality agreements and invited to provide feedback to the teams using the form shown in Figure 73. This does not factor into grading, but is immediately provided to the teams so that it can be incorporated into their documentation. The presentation begins with a 1 minute "pitch" that briefly summarizes the challenge and then proceeds to provide clinical background, present

Final Presentation Review Form

All guests, regardless of background, are kindly requested to help us provide feedback to the teams regarding their projects and presentations.

Team Name:
Reviewer Name (Optional):

	Please rate the following where: 1 =poor; 3 = neutral; 5 = excellent!	**Scale 1 - 5**	**Comments**
1	Did the elevator pitch pique your interest?		
2	Was the need clearly explained & justified?		
3	Were the functional requirements & specifications well defined?		
4	Were the design decisions supported by analysis?		
5	Was the prototype well executed?		
6	Was appropriate testing conducted?		
7	Are the results (positive or negative) credible?		
8	Does the design meet the specifications?		
9	Did the team elucidate the next development steps?		
10	Do you believe that this prototype could be refined into a product?		
	Total/50		

Additional Comments:

Figure 73 – Feedback form filled out by final presentation audience members

the design decisions and culminates in a demonstration of the final prototype. Outside assessment is valuable, with clinicians often identifying additional applications for a technology and medical device industry professionals demanding better testing data and evaluation. A consistent challenge has been to encourage students to present an accurate assessment and explanation of failures to meet functional requirements and specifications; more traditional final presentations often encourage a more positive tone. However, in this merging of research and education, the results of testing the final prototype can indicate that a design is ultimately impractical, as is often the case, without negatively affecting grades or the learning value.

Written deliverables include: a crisp, American Society of Mechanical Engineers journal-quality paper and a one-page prospectus, rather than a lengthy, more traditional "project report." This encourages conciseness and ensures that both students' time writing and instructors' reviewing are productive, since many papers are submitted to the ASME Design of Medical Devices (DMD) conference, held in April at the University of Minnesota, as well as form the basis of later journal papers. Increasingly, students are producing short, edited demonstration videos. In sum, the availability of professional documentation has proven essential to project continuation, review by MIT and hospitals' technology licensing offices and contacting potential corporate licensees and sponsors.

7.2.3. Curriculum

The third key is a supportive curriculum with clear educational goals. Formal lectures, held for only the first 2/3 of the semester, teach fundamental mechanical and electrical engineering design principles. Supporting guest presentations cover literature and IP searching, real product case studies and clinical topics. Supplementary tours to medical device industry facilities, such as Ximedica in Providence, RI, are also organized. The specific learning objectives are listed in Table 18. In a study conducted by and with Harvey Mudd undergraduates "the three most important skills that students require help on are: practical project planning and scheduling techniques; dealing with personality conflicts within the team; running efficient meetings" [135]. The MIT experience correlates and specific leadership and teamwork elements have been added to the curriculum. Particularly in order to fulfill undergraduate requirements, communication is a formal course element encompassing the presentations and written material and supported by a dedicated communication instructor, who also coordinates intra-team dynamics.

In the first weeks of class students are also assigned a short, hands-on mini-project. The goal of this assignment is to foster creativity and introduce students to campus fabrication resources, sourcing materials, building and testing. Each student is tasked with designing, modeling and testing something that demonstrates exact constraint (kinematic) design principles. Students start with a blank slate and no particular resources other than directions to MIT machining and hobby shop facilities whose staffs ensure that the students receive safety training and hands-on assistance with fabrication in wood, aluminum, steel and plastic. Students evaluate their devices' performance with respect to stiffness and mechanical repeatability. Many use dial indicators to measure both stiffness when loaded and positional repeatability. Others affix laser pointers to their devices and track the beam on graph paper on the other side of the room; working with limited equipment is a hallmark of the bench level experimentation. Brief reports are submitted and projects demonstrated to the class. Designs have included three ball and groove "kinematic coupling paperweights", wine bottle holders and a unicycle

stand. As stated from one student's course evaluation: "The lab assignment was useful to gain access to the shop, and a great way to get us started with a rapid design project."

The grading metric encompasses mastery of the lecture material, following the process to a functional prototype and individuals' performance, as observed during weekly meetings and validated by formal, confidential peer ratings of team members. These are administered using the online CATME – Comprehensive Assessment of Team Member Effectiveness, developed at Purdue University, primarily for academic use and based on research into team dynamics [139]. This assessment asks students to rate both their own and teammates effectiveness in five areas along a seven point scale; however, rather than asking for a number, a behavioral description of each rating is provided to which students match themselves and their teammates. Instructors receive detailed information that flags specific individual and group conditions, such as "low" where a student performs badly or "clique" where a team has fractured. Grade correction factors are also computed. Optionally, students can receive a summary of their self-ratings in comparison to teammates and the average. The CATME is loaded with the class list and administered twice during the semester; first at the midpoint to assess and, potentially, rectify problems, and then at the end to adjust grades by up to a letter.

Table 18 – Course Objectives

Students in the 2.75 course will learn:
• A structured, deterministic design process • Translating a challenge into requirements & specifications • Prior art & IP research • Advanced mechanical & electrical design • Multidisciplinary teamwork • Hands-on prototyping & testing • Hardware procurement & fabrication • "On-time" & "on-budget" project management • Effective, professional oral & written communication of technical material

Table 19 – Approximate Grading Metric

Distribution:	
Team project	50%
Execution of process	
Design & execution	
Demonstration of prototype	
Communications	20%
4 Presentations	
Written final documentation	
Individual, weekly progress	10%
Mini-project	10%
Peer ratings	10%
Total:	100%

7.3. Case Studies

7.3.1. ACL Repair Gun

In an audit of past projects, the earliest successful one identified was a gun to help repair torn anterior cruciate ligaments (ACL), a condition that affects over 450,000 Americans per year. The ACL's location in the center of the knee joint and bathed in synovial fluid prevents normal clotting and healing, thus grafts have not proven long term stability. In 2004, Dr. Martha Murray of Children's Hospital Boston, having developed a gel containing platelets and collagen which could serve as a scaffold to enable healing, described her need for a tool to warm, mix and deliver the gel during arthroscopic ACL repair surgery. By the end of the fall semester she and her graduate student team had developed a "gel gun," employing a heater and a collapsible augur, which served double duty as mixer and plunger, and a nozzle to deliver a drying CO_2 blast followed by a precisely metered amount of gel, all through a 1 cm incision. Dr. Murray stated: "The engineers helped us a great deal. They are working on a crucial

component of the project, and they are enthusiastic, dedicated and smart. We've really benefited from CIMIT helping us access some terrific engineering talent."

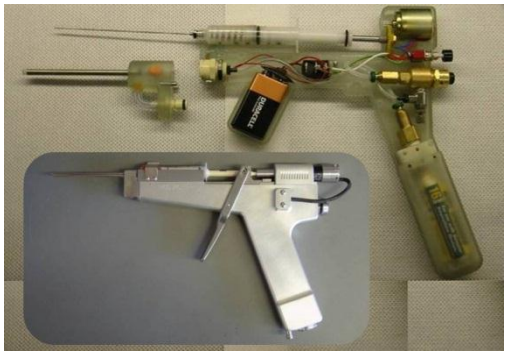

Figure 74 - Student prototype with inset showing second generation prototype.

Post course, while none of the students were able continue with the project, Dr. Murray obtained a $100K CIMIT Proof of Principle Grant and engaged a professional design firm to refine the prototype. Both are shown in Figure 74, where all the original design elements are retained in the "professional" prototype. The gel, along with a third generation device is currently undergoing testing with support from an NIH RO1. Preliminary results indicate significantly stronger ACL repairs [140, 141]. Dr. Murray is now scientific co-founder of Connective Orthopaedics, a venture funded startup.

7.3.2. Thoracoscopic Screwdriver

Development of the thoracoscopic screwdriver, a now licensed-out technology began in 2009 when Dr. Suresh Agarwal of Boston University Medical Center presented the challenge of stabilizing compound rib fractures. Such fractures cause flail chest and compromise breathing. The typical treatment is positive ventilation until healing occurs naturally; however this leads to long recovery times and complications. The alternative is an open thoracotomy, which cuts musculature, to place titanium osteosynthetic plates on the outsides of ribs. This team's mission was "to design a tool or method for minimally invasive video assisted thoracoscopic rib fracture stabilization," so that ribs could be fixed minimally invasively from the inside.

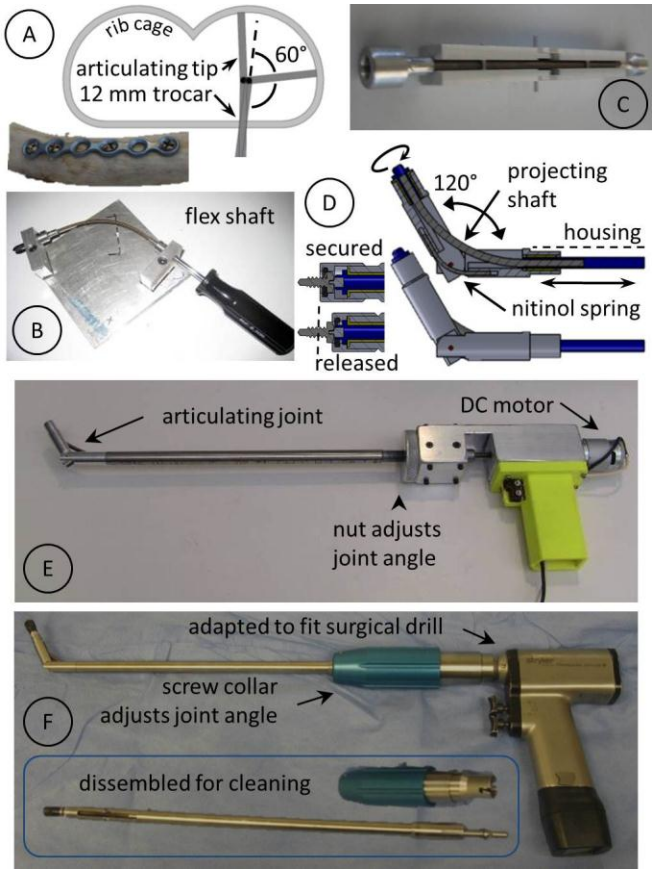

Figure 75 – Thoracoscopic screwdriver design from need (A) to final prototype (F).

Three main repair strategies were considered: custom, absorbable implants adhered to the rib, modular implants fitting around the rib and a minimally invasive method of installing the same plates used in open surgery, seen in Figure 75 (A). The first two strategies required significant technology development, while the third significantly narrowed the project scope to the design of a single surgical tool – a laparoscopic screwdriver. Key functional requirements included: fitting through a 12 mm trocar and

articulating by 60° to access fracture sites, as shown in (A). Additionally the tool needed to positively engage the 2 mm, self-drilling bone screws until placed, deliver sufficient torque and be operable with one hand.

The process accelerated as the team bench-level prototyped and tested mechanical concepts for the critical rotation and angulation functions. A universal joint failed to provide smooth rotation, adequate compactness or a sufficient angular range of motion and the flexible shaft (B) proved more promising, but did require a relatively large bend radius. The team struggled to find a simple angulation method, considering cable drives, push rods and linkages. With the realization that a flexible shaft could support both torque and axial load, a novel solution emerged!

As seen in (C) and (D), the flexible shaft passes through the joint, which is hinged off center. Pulling on the shaft causes the joint to bend, while a nitinol beam spring provides the return force. By slotting the joint, the flexible shaft is able to project outwards and maintain its necessary minimum bend radius. This mechanism was first bench level prototyped (C), validated and then the diameter was reduced, bushings and a pocket for the nitinol spring added and tolerances specified. By week ten this most critical module was complete, with housing and screwdriver tip. Following this module came a retaining collar which pops back only once the screw is seated in bone against the plate. Finally, the handle/drive module was constructed, containing a gear motor, a forward and reverse trigger and a nut, which pulls on the housing to actuate the joint.

The entire prototype was completed by week twelve and tested in a surgical simulator. The final paper won a presentation award at the 2010 Design of Med. Dev. Conference (DMD) [142]. Development continued into the spring semester course, culminating in the polished prototype, shown in (E). This was published in the ASME J. Med. Dev. Design [143], underwent porcine testing and was presented at the 2010 New England Surgical Society Annual Meeting [144]. Subsequently, the team formed a startup company, acquired the technology and in late 2012 signed a licensing agreement, details of which are not yet public.

7.3.3. Sleep Sensing Shirt

This case study presents the Sleep Sensing Shirt, a potentially disruptive technology that in just one year launched an angel funded startup and in two began clinical trials. In September 2010 Dr. Matt Bianchi, a Massachusetts General Hospital (MGH) neurologist, explained that 1 in 3 Americans reported sleeping problems, yet diagnosing them relies on in-hospital sleep labs that are inconvenient, uncomfortable, with sensors stuck all over a patient, and, too expensive, at $2,000 each; would it be possible to create an at-home sleep monitor that would produce clinically significant data?

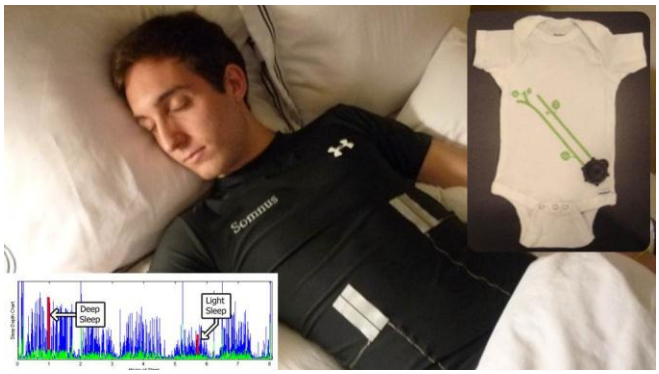

Figure 76 – Rest Devices Inc. co-founder Pablo demonstrating the sleep sending shirt, insets showing raw data and the latest infant monitoring model.

Three undergraduate roommates, who had vowed to select the “best” project and launch a company, signed on to the project. Studying current practice they realized that most primary care physicians receiving sleep study data relied on an aggregate “sleep score” to diagnose and refer; maybe a only a single sensor could provide data that would serve the vast majority of cases. After exploring a myriad of modalities, they hit upon the idea of a shirt with non-contact, co-planer, capacitive plates that would measure the fabric’s stretch as the patient breathed. Machine-sewing wire and bonding metal foil failed; the end design comprised silk screened metallic pads and traces, protected by iron-on vinyl appliqués. Circuits were first bread boarded and then ordered from a vendor. The final device features a tiny, snap on, micro-USB equipped data logger. As important as the patented hardware design, a custom algorithm capable of processing a night’s worth of data into a sleep stages and an equivalent score, in under 30 seconds. These results also won a presentation award at the 2011 DMD [145]. By August 2011 funding was secured and the sewing machine, silk-screening frame and heat press transferred from MIT to Rest Devices’ office, Boston, MA.

Quoting Dr. Bianchi, now promoted to director of the MGH Sleep Lab: "The course was an ideal setting to match clinical need with engineering solutions, and the resulting product has not only fueled my research productivity and career advancement, but also holds great potential for advancing patient care." Currently, the product is being sold for research purposes to sleep labs and a consumer baby monitor is under development. The work was presented in 2012 at the Associated Professional Sleep Societies Conference and the Military Health System Research Symposium.

7.4. Outcomes & Assessment

7.4.1. Overview

As seen in Figure 77, since 2004 enrollment has more than doubled from 20 students to a high of 49, with a total of 264 students having worked on the 52 projects. Team size has remained constant in the 3 - 5 student range and project selection has steadily become more competitive from all proposals selected to only 1 of 3. This allows a more precise tailoring of the projects presented to the students in terms of diversity and predicted feasibility. Overall of a total of 172 eligible proposals 30% have been addressed. By the most recent count there are a dozen provisional or utility patents currently pending on course-based technology. Course evaluations place it significantly above the department median, in the 1st quartile. Over two dozen papers have been published and aided students’, clinicians’ and instructors’ careers. Alumni data also show students consistently landing jobs in the medical device design industry. The model has also been extended to industry sponsored projects as well as energy related projects, which account for the “non-medical” bars on the graph.

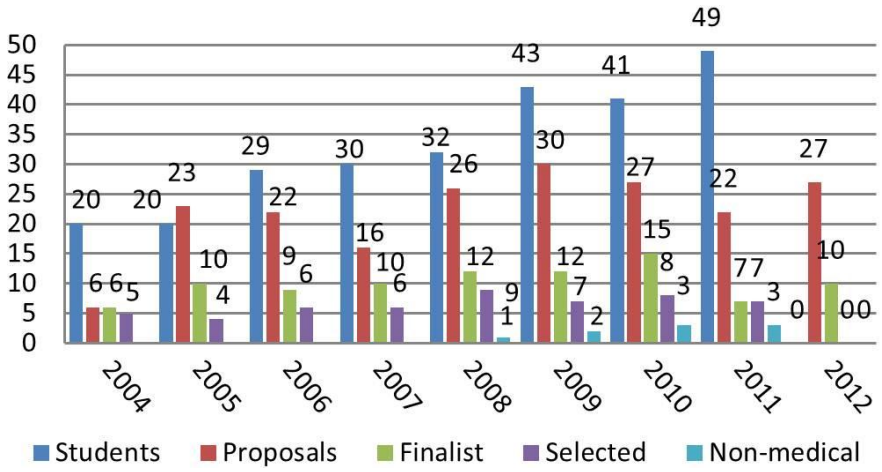

Figure 77 - Student enrollment and project statistics 2004 – 2012. (2012 data not complete) The course model has also been applied to select non-medical projects.

Clinicians, many of whom have strong creative instincts but lack in time and engineering resources, are now champions for the course among their colleagues. A prominent surgeon states: "It was fun to work with the student team. They grasped the clinical problem and developed a creative concept to address the challenge of negative pressure wound therapy in a low resource setting. I had been working in my basement workshop on a concept device, and the students opened my mind to other potential approaches which have led to the current prototype."

Assessing student learning is a special challenge in a course which presents an open ended design problem and expects deliverables in the form of a physical prototype, a presentation and a paper, rather than tests and other evaluation metrics that produce numerical data. Peggy Maki in "Assessing for Learning" states: "At the graduate level we educate people to become experts who explore new territories in their fields or professions and question findings, challenge claims, or rethink tradition-bound perspectives on or approaches to issues that lead to new directions in research and lines of enquiry" and, moreover, "standardized testing" fails to "represent our diverse learner's achievements or our institutions' education effectiveness" [146]. While an investigation of project-based learning is beyond the scope of this paper, three metrics are relevant to assessing student outcomes: 1) Student Evaluation of Teaching (SET) reviews, 2) Course alumni's careers and 3) Project Outcomes.

7.4.2. Student Evaluations of Teaching (SET)

SETs are administered independently by the Mechanical Engineering Department and ask students to numerically review and comment upon both the course in general and the performance of individual instructors. Course evaluations for the years 2004 – 2010, including survey questions and comments, were obtained. MIT students take the SETs seriously and often provide detailed feedback; one evaluation from 2010 speaks specifically to the process, as well as offers some criticism:

"It is such a fantastic opportunity to have the clients come to us and present such well researched project ideas. I am used to having to do all that myself. As I saw it we were handed a quarter of the design process on a plate and are then able to make significant progress in a semester. The involvement of an external client motivates students to really deliver and work hard on their design. I like the awareness of intellectual property introduced from the start, and thought about reciprocity a great deal.

This was a new approach to me so that was great. The prospect of publishing a paper, applying for a patent, and presenting at a conference are all personal goals of mine so this class was ideal. I think there is huge value in forgoing problem sets/exams in terms of allowing students to really work on something worthwhile so I think this is a great aspect of the course. It meant I could focus entirely on the project and get out of it what I thought was important. Whilst brief, it was useful for the quick fire lectures on the fundamentals notes to know that it was there and available although I will admit I did not use them. The lab assignment was useful to gain access to the shop, and a great way to get us started with a rapid design project. I zoned out during the electronics stuff and I do not think it added to my learning."

Numeric SET data was available from 2006 – 2011 and analysis focused on applicable questions in the sections: "Factors in Learning," "Assessment of Learning" and "Subject." Questions pertaining to particular instructors' performance were excluded. The mean rating data was examined for trends, hypothesizing that as the course process was honed over the last 7 years this should be reflected in student experience and feedback. Moreover, while it would be improper to compare the course to other design courses in the department, the course could be compared to a baseline rating of 5, corresponding to a rating of "Average." For each rating (M) and the number of students responding (N), standard errors were calculated and presented in Table 20. Then pooled t-tests were used to determine whether the means were higher (or lower) than the baseline (5) and to compare one year to the next looking for improvement, both at a 0.05 level of significance [147].

The primary statistic is the mean "Overall rating of the subject," plotted in Figure 78. In 2006, when the medical-focus was only 3 years old, the rating was not differentiable from Average and the course placed in the 3rd quartile of the department. (Departmental comparative data is not publically available, but was reviewed.) In subsequent years 2007, 2009 – 2011 the course rated higher than average and placed in the 1st quartile. On many other assessment questions, starred in the table, the rating is also significantly higher than baseline. It should be noted, that graduate elective courses generally score higher than mandatory courses. The responses' large standard deviations obscured yearly improvements so, despite the visible upward trend, only from 2009 and 2010 was the improvement significant.

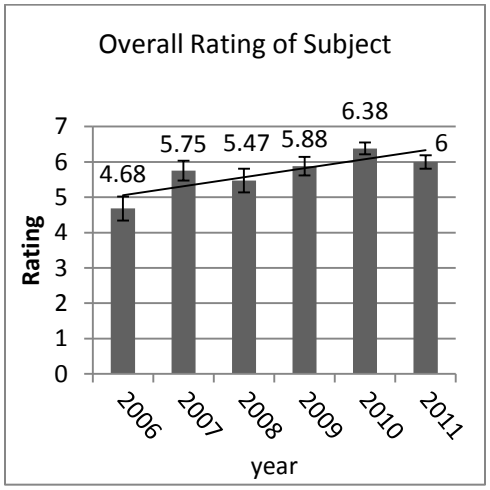

Figure 78 – Plot of mean course evaluation by year. Error bars show standard errors.

Table 20 – Student Evaluations of Teaching (SET) results showing means and standard errors (SEm).

	2006		2007		2008		2009		2010		2011[3]	
Total # of responses:	25		14		19		32		35		35	
Response rate of students registered for credit (%):	86		87		74		72		85		70	
	Mean	SEm[1]			**Mean**	SEm	**Mean**	SEm	**Mean**	SEm	**Mean**	SEm
Assessment Questions / Rating Scale	Rating Scale: 1=Very Poor, 4=Average, 7=Excellent											
1. Overall rating of the subject	**4.68**	0.34	**5.75***	0.28	**5.47**	0.33	**5.88***	0.26	**6.38***	0.16	**6.0***	0.19
2. Lectures contributed to my learning	**4.67**	0.33	**5.54***	0.27	**5.00**	0.41	**4.48**	0.40	**5.55***	0.26	**4.8**	0.32
3. Electronic material contributed to my learning	**4.12**	0.32	**5.73***	0.38	**5.35**	0.25	**5.38**	0.32	**5.66***	0.25	**5.9***	0.18
4. Feedback on assignments was helpful	**3.43**	0.29	**4.73**	0.54	**5.81***	0.25	**5.25**	0.37	**5.00**	0.36	**6.0***	0.33
5. I have a good understanding of the subject concepts	**4.12**	0.33	**5.92***	0.24	**5.65**	0.39	**5.88***	0.25	**5.91***	0.20	**5.8***	0.20
6. I can apply the subject concepts	**4.21**	0.34	**6.15***	0.25	**5.71***	0.40	**6.04***	0.23	**5.91***	0.22	**6.0***	0.18
7. I learned a great deal in this subject	**4.08**	0.40	**5.92***	0.26	**5.47**	0.42	**5.73***	0.30	**6.06***	0.21	**6.1***	0.22
8. Subject Pace (4 is best)	**4.62**	0.22	**4.25**	0.18	**3.53**	0.26	**4.14**	0.12	**4.14**	0.11	**4.6**	0.16
	Rating Scale: 1=Very Poor, 4=Average, 7=Excellent											
9. Graded fairly	**4.33**	0.24	**5.5***	0.26	**4.81**	0.36	**5.23**	0.24	**4.63**	0.21	**4.9**	0.20
	Rating Scale: 1=Too Light, 4=Good, 7=Too Heavy											
10. Subject workload	**4.36**	0.27	**4.75**	0.25	**4.35**	0.20	**4.65**	0.15	**4.50**	0.13	**4.9**	0.17
11. Average hours you spent on the subject per week[2]	**12.93**		**18.10**		**15.85**		**16.56**		**14.83**		**18.9**	

Starred (*) values are statistically higher than a baseline of 5, found by applying pooled t-tests at a 0.05 level of significance.

The 2007 data may not be representative since Prof. Slocum was on sabbatical and Prof. Culpepper taught the course with marked success; however students had the option of an alternate, traditional “precision machine design” track.

[1] Student response rates (N) differed by question and, although not shown, these numbers were used to calculate standard errors (SEm).

[2] Hours per week was originally broken into categories "class," "lab" and "homework," the averages of these were summed to obtain total hours.

[3] Question wording changed slightly in 2011 and the data was provided in a new online format with one less significant digit reported.

7.4.3. Alumni Careers

Anecdotal evidence suggests that students are entering the course with a specific interest in medical, rather than generic design, therefore a pertinent question is: Are course alumni employed by medical device companies? Using student rosters provided by the Registrar, the Alumni Association queried their records to obtain employment data for course alumni from 2004 - 2010. Currently graduates are employed at Adicept Technologies (the student's startup), Johnson & Johnson, Claros Diagnostics, GE Healthcare, Ethicon-Endosurgery, Hologic, The DNA Medicine Institute and Nyx Devices (a 2010 startup from the class). Two former graduate instructors are pursuing professorships at University of British Colombia and Harvard University with foci on medical devices. Another joined a tissue engineering research group at Massachusetts General Hospital as its first engineer and, after moving to new job, was replaced with a 2010 course graduate. Alumni data was limited with approximately a third still in school at MIT. As more course alumni graduate and enter the workplace, it may be possible to conduct longitudinal surveying. For comparison purposes, data was also obtained for 2003, the year before the course focused on medical projects. Seeing alumni employed at Smith & Nephew, Medtronic, MGH, Genomic Solutions and Rubicor suggests that the course may be serving an existing interest rather than driving it, a conclusion supported by the popularity and growth of medical device programs at institutions across the nation.

7.4.4. Project Outcomes

Project tracking remains a challenge and Table 21 presents a best effort to track the statues of all projects which have remained active. At least two dozen peer-reviewed papers are directly linked to projects originating in the course, in publications including the ASME Journal of Medical Devices, IEEE International Conference on Robotics and Automation, IEEE Engineering in Medicine and Biology Conference, the Design of Medical Devices (DMD) Conference, which often provides students with their first professional publication and networking experience, as well as clinical specialty-specific conferences and journals. From the 2009 class, 4 out of 8 projects were presented at the 2010 DMD with one winning a pitch prize. From the 2010 class, 7 of 8 medical projects were presented at the 2011 DMD and three competed in a pitch contest, winning 2 prizes. From the 2011 class, 5 of 7 projects were entered into the conference's student design showcase. Further funding has been secured from diverse sources. Projects have been tested in both simulation labs and in-vivo studies. The renal cooling device (2010) was tested in collaboration with Intuitive Surgical, a course sponsor. Over 12, provisional patents have been filed with at least 6, converted to utility patent filings, but none have issued yet. Six startup companies have been launched, four of which are active, and so far one license agreement has been signed.

Table 21 – Promising Course Projects 2004 – 2011

Project (Year), Publications & Clinician	Status
Endoscopic ultrasound needle biopsy (2004), [148] Bill Brugge, MD – Massachusetts General Hospital	Master's Thesis
ACL repair gun (2004), [140, 141] Martha Murray, MD – Children's Hospital	CIMIT grant, NIH RO1 grant Startup company (Connective Orthopaedics)
Robopsy – Robotic biopsy (2004), [102, 103, 112-114, 149] Rajiv Gupta, MD, PhD – Massachusetts General Hospital	CIMIT grant 1st Place 2007 MIT $100K Business Plan Comp. NCIIA BMEIdeas Comp. 2 Porcine trials completed Utility patent filing Startup company (ended)
Simplified negative pressure wound therapy (2005), [150-152] Rob Sheridan, MD – Massachusetts General Hospital Robert Riviello, MD – Brigham & Women's Hospital	Master's Thesis 3 IRBs received (Massachusetts General Hospital, Brigham & Women's, Rwandan Ministry of Health), Clinical testing in Rwanda Startup company (WiCare)
Port for minimally invasive cardiac surgery (2005), [153, 154] Pedro Del Nido, MD – Children's Hospital Nikolay V. Vasilyev's, MD – Children's Hospital	CIMIT Grant
Endoblender , now MITE (2006), [126, 127] Zev Williams, MD – Brigham & Women's Hospital	Ongoing development project at TU Delft Provisional patent filing
Pressure monitoring syringe for endotracheal tubes (2008), [155] Joan Spiegel, MD – Brigham & Women's Hospital	Utility patent filing Low volume manufacturing Startup company (Beaver Medical) Preparing for clinical trial
Endoscopic Vertebral Fusion Balloon (2008) Kevin McGuire, MD – Beth Israel Deaconess Medical Center	Provisional patent filing
Thoracoscopic screwdriver (2009), [142-144] Suresh Agarwal, MD – Boston University Medical Center	Winner pitch competition at 2010 DMD Utility patent filing Startup (Charles River Engineering) Licensed technology
Low–cost portable mechanical ventilator (2009), [156] Jussi Saukkonen, MD – Boston University Medical Center	Gates Foundation grant, CIMIT Grant
Improved nasal gastric tube tip and flushing device (2010), [157] Ali Tavakkolizadeh, MD – Brigham & Women's Hospital	Winner pitch competition at 2011 DMD Utility patent filing
Renal cooling for minimally invasive surgery (2010), [158-160] Nadeem Dhanani, MD – Mt. Auburn Hospital	Porcine Trial Completed Utility patent filing
Somnus Shirt – Home sleep monitoring (2010), [145] Matt Bianchi, MD, PhD – Massachusetts General Hospital	Winner pitch competition at 2011 DMD Winner CIMIT Primary Care Prize Utility patent filing Startup Company (Rest Devices)
Flexural laparoscopic grasper (2010), [161] Jennifer Rosen, MD – Boston Medical Center	Surgical simulation lab testing Provisional patent filing
Minimally invasive specimen remover (2011), DMD poster Ian Makey, MD – Beth Israel Deaconess Medical Center	Porcine Trial Completed Provisional patent filing
Rapid skin closure for long surgical incisions (2011), DMD poster Kyle R. Eberlin, MD – Massachusetts General Hospital	Provisional patent filing
Fine needle aspiration gun (2011), DMD poster Sareh Parangi, MD – Massachusetts General Hospital	Provisional patent filing

7.5. Future Work

Notwithstanding the current record, even for those projects which have particular technological promise and are supported by an enthusiastic clinician, project continuity remains a challenge. Once the educational goals are served, students may become "product champions" but when they are unable or uninterested in continuing, the projects stall. Successful projects and excellent students have continued on as senior theses or graduate research projects in the Precision Engineering Research Group. Graduate students, with their longer educational time constants, have supported project continuation. The addition of the follow-on course has served to postpone the "valley of death" by a semester and, while initially conceived as a next-step design course, the syllabus now states: "The primary focus of the class is to evolve a proof-of-concept prototype into a beta prototype suitable for presentation to potential licensees or investors." A crucial next step is to increase the participation of existing medical device companies to sponsor projects, hire more alumni and license technologies that have already been first-pass prototyped and de-risked. In addition, more financial support is needed for device design, which is often ignored by traditional academic funding sources.

8. Conclusions

Ever since robots were first conceptualized in the 1920's there has been an exploration of their relationship with humans. In the early days, automation was viewed as displacing workers and dehumanizing them, but today robots are widely accepted and used extensively in industrial settings, where they reduce workers' burden and increase manufacturing precision and productivity. These robots often operate at high speeds and forces and, therefore, both passive protection, such as guards and cages, and active protection, such as safety light curtains and dead man's switches, are necessary to ensure worker safety. Profoundly different are robots in healthcare that act directly upon a person and under a clinician's guidance. Despite patients' expectation that technology should enable more precise procedures and improve outcomes, and clinicians' general openness to devices that can help deliver better care, their application is still in its infancy. However, this relatively new opportunity to explore the relations between robots, clinician-operators and patients is exciting!

For the most part, the current state-of-the-art still evidences an industrial heritage in both size scale and cost. Orthopedic robots show promise when conducting relatively traditional milling procedures, integrating 3D data and shaping bones to receive implants. Probe placement robots are also being developed for the guidance of drills, screws and needles. For minimally invasive, soft tissue interventions, the multi-function da Vinci delivers superhuman dexterity inside a patient under direct visual guidance. For all these systems price and operating costs place them in the million dollar capital equipment range and proving efficacy is still challenging. In questioning the sustainability of the current trends and pondering the question, "What could be the most appropriate form for robots that interact closely with and in the human body?" the philosophy of appropriate scale medical robots emerged. From this a methodology has been evolved and is presented in this thesis that takes the first steps in enabling a wide range of inexpensive, procedure-specific robots to be developed. The fundamental elements of this method are herein summarized:

- Tight clinical involvement in design process – The design process should be driven by clinical need, not technological capability. Select clinicians should be involved, not as clients, but rather as active participants in iterative prototyping and testing. Furthermore, it may be possible to capture expert knowledge and structure robot operation and interface so as to enable a wide range of clinicians to conduct the procedure in a similar manner.
- Task partitioning & partnership with clinician –Designers must thoroughly evaluate the target procedure step by step. Only those steps where robotic assistance offers clear improvement over the clinician's capabilities should be targeted. Providing the clinician with assistance is the goal, rather than maximizing automation. Closing the control loop through the clinician reduces complexity and risk and enables for human judgment calls.
- Procedural integration – The device and its interface should enable close adherence to current procedure protocols. The goal is to reduce the number of overall steps, rather than developing an entirely new operating modality. The size of the robot should minimize the structural loop and not hinder access to the patient.
- Structured process & iterative prototyping – The design should proceed from coarse to fine, initially considering a wide range of strategies and concepts and then focusing in to address the

core functionality. Throughout the process, partial, appropriate prototypes are essential to evaluating and validating design elements and preventing early lock-down of sub-optimal or expensive paths.

- Feature minimization – Each feature added, particularly those later in the process, should be subject to strict testing to verify their necessity and whether the task might be as efficiently conducted by the clinician.
- Academic-clinical partnership – Teams comprised of students and clinicians have demonstrated effectiveness in evaluating a wide range of electromechanical challenges and rapidly prototyping solutions in a cost effective manner.

Conclusively proving the effectiveness of a design method, which still requires a component of inspiration, is never possible. However, as more technologies emerge from this method, it may be possible to create a metric that puts dollar values on certain individual tasks and that compares the cost of automating them to the time value of human labor. This will require greater transparency in hospital costs and insurance reimbursement than is currently typical, but would represent substantial and meaningful further research. An improved means of estimating production costs and sales prices, while still in the prototype stage, must also be developed.

Given the long development trajectories of medical projects, thus far only anecdotal evidence of the method's function is available from the handful of projects that are currently active. Nevertheless, this design method is showing promise as a means to rapidly generate novel, new technologies that are potentially cost effective and thus able to be more widely implemented than current medical robots. A handful of promising projects have been prototyped and an important further goal is to develop a means, both in terms of funding and design technique, to continue the rapid progression through licenses or spin-offs and FDA filings to viable products. Part of this will require the participation of existing players in the medical device space who will benefit from access to a wide range of lean technologies which, while unpolished, have been prototyped and evaluated. Additionally, by adopting similar design methods, internal development cycles can be shortened. Potentially, the method offers a new disruptive model for implementing technology in medicine.

9. Acknowledgements

To my parents I am infinitely grateful for their unconditional love and support these past thirty years. I am deeply obliged to Prof. Alex Slocum for eight years of guidance and tolerance of my flights of fancy, despite failing to ever convince me that triathlons would be good for me. I acknowledge those Pergies, friends and staff @ MIT who have been a constant source of amusement and support and effectively increased the size of my family. Likewise, I thank my old friends from Rhode Island, The Prout School and the University of Rhode Island for regularly reminding me that the real world exists. To the MIT Global Startup Workshop community, may the adventures continue. And to everyone a big hug for keeping me sane!

9.1. Statement of Collaboration

The Robopsy project began in the MIT Precision Machine Design (2.75) course taught by Prof. Alexander Slocum and the author wishes to acknowledge team members Steven Barrett, for his contribution to the initial research, concept generation, analysis and testing, and Conor Walsh and Dr. Rajiv Gupta, for continued collaboration throughout this project. Furthermore, the work of Alex Seitel in developing the image-guided interface is gratefully recognized. Special thanks are due to Drs. Jo-Anne Shepard, Subba Digumarthy and Amita Sharma from MGH Radiology, along with numerous patient staff and technicians who assisted with and showed great patience during testing. Initial work on this project was made possible by CIMIT, the Center for Integration of Medicine and Innovative Technology under a U.S. Army Medical Acquisition Activity cooperative agreement. Further support was received from the MIT Ideas Competition, the National Collegiate Inventors and Innovators Alliance BMEidea Competition and the MIT $100K Business Plan Competition. CT facilities were provided by MGH. Significant material and engineering support was provided by Johnson Electric and Dr. Thomas Roschke (now VP of Johnson Medtech) Dr. Joerg Gassmann and Patrick Anders from Saia-Burgess.

On the MITE lead credit is due to Ewout Arkenbout for making significant progress on an otherwise dormant project and, indeed, carrying it on into his Master's research. Additional thanks to Dr. Jon Einnerson for his clinical advice and TU Delft professor Just Herder for making Ewout's visit possible.

I would like to acknowledge my fellow 2.75 instructors including Alex (obviously), Dave Custer, Rajiv Gupta, Prof. Joel Dawson, Conor Walsh, Nikolai Begg and Folker Rojas. I especially thank those 2.75 students whose projects furnished case studies and recognize those 2.007 and 2.75 students who have made five year of TAing an enjoyable and formative experience.

I sincerely thank Alex Slocum and Leah Kelley for carefully reading and editing this work.

10. Works Cited

[1] C. M. Christensen, *The innovator's dilemma: when new technologies cause great firms to fail*, 1st Harper Business ed. New York: HarperBusiness, 2000.

[2] Oxford English Dictionary. (2012). *"efficient, adj. and n."*. Available: http://www.oed.com/view/Entry/59742

[3] C. Bolenz, A. Gupta, T. Hotze, R. Ho, J. A. Cadeddu, C. G. Roehrborn, and Y. Lotan, "Cost comparison of robotic, laparoscopic, and open radical prostatectomy for prostate cancer," *European Radiology,* vol. 57, pp. 453-8, Mar 2010.

[4] A. H. Slocum, *Precision machine design*. Englewood Cliffs, NJ: Prentice Hall, 1992.

[5] International Organization for Standardization, "Robots and robotic devices - Vocabulary," in *ISO 8373:1994* ed, 1994.

[6] G. Salvendy, *Handbook of industrial engineering: technology and operations management*, 3rd ed. New York: Wiley, 2001.

[7] R. H. Taylor and D. Stoianovici, "Medical robotics in computer-integrated surgery," *IEEE Transactions on Robotics and Automation,* vol. 19, pp. 765-781, Oct 2003.

[8] Centers for Medicare and Medicaid Service U.S. Department of Health and Human Services. (2012, Aug 30). *2009 National Health Expenditure Data Fact Sheet*. Available: https://www.cms.gov/NationalHealthExpendData/25_NHE_Fact_Sheet.asp

[9] Agency for Healthcare Research and Quality. (2012, Aug 30). *Medical Expenditure Panel Survey*. Available: http://meps.ahrq.gov/mepsweb/

[10] Social Security Advisory Board, "The Unsustainable Cost of Health Care," ed. Washington, DC, 2009.

[11] D. A. Squires, "Explaining High Health Care Spending in the United States: An international Comparison of Supply, Utilization, Prices, and Quality," The Commonwealth Fund, May 2012.

[12] J. Akhtar, "Robotic Surgery in Public Sector Hospitals: Irrational Use of Healthcare Resources," *Journal of Surgery Pakistan (International),* vol. 16, pp. 88-89, July - Sept 2011.

[13] Centers for Medicare and Medicaid Service. (2012, Aug 23). *Centers for Medicare and Medicaid Service*. Available: http://www.cms.gov/

[14] B. Preising, T. C. Hsia, and B. Mittelstadt, "A Literature-Review - Robots in Medicine," *IEEE Engineering in Medicine and Biology Magazine,* vol. 10, pp. 14-22, Jun 1991.

[15] T. Kande, B. Davies, and B. D. Riviere, "Scanning the issue - Special issue on medical robotics," *Proceedings of the IEEE,* vol. 94, pp. 1649-1651, Sep 2006.

[16] R. H. Taylor, "A perspective on medical robotics," *Proceedings of the IEEE,* vol. 94, pp. 1652-1664, Sep 2006.

[17] M. Kutz, *Standard handbook of biomedical engineering and design*. New York: McGraw-Hill, 2003.

[18] Y. S. Kwoh, J. Hou, E. A. Jonckheere, and S. Hayati, "A robot with improved absolute positioning accuracy for CT guided stereotactic brain surgery," *Biomedical Engineering, IEEE Transactions on,* vol. 35, pp. 153-160, 1988.

[19] B. L. Davies, R. D. Hibberd, W. S. Ng, A. G. Timoney, and J. E. A. Wickham, "The development of a surgeon robot for prostatectomies," *Proceedings of the Institution of Mechanical Engineers, Part H (Journal of Engineering in Medicine),* vol. 205, pp. 35-8, 1991.

[20] B. Davies. (2012, 5 Jan). *Research: Mechatronics in Medicine, The Probot*. Available: http://www3.imperial.ac.uk/mechatronicsinmedicine/research/theprobot

[21] Q. Mei, S. Harris, F. Arambula-Cosio, M. Nathan, R. Hibberd, J. Wickham, and B. Davies, "PROBOT — A computer integrated prostatectomy system," in *Visualization in Biomedical*

Computing. vol. 1131, K. Höhne and R. Kikinis, Eds., ed: Springer Berlin / Heidelberg, 1996, pp. 581-590.

[22] S. J. Harris, F. Arambula-Cosio, Q. Mei, R. D. Hibberd, B. L. Davies, J. E. A. Wickham, M. S. Nathan, and B. Kundu, "The Probot - an active robot for prostate resection," *Proceedings of the Institution of Mechanical Engineers Part H-Journal of Engineering in Medicine,* vol. 211, pp. 317-325, 1997.

[23] Curexo Technology Corp. (2012, Aug 28). *Robodoc*. Available: http://www.robodoc.com/

[24] P. Kazanzides, B. D. Mittelstadt, B. L. Musits, W. L. Bargar, J. F. Zuhars, B. Williamson, P. W. Cain, and E. J. Carbone, "An integrated system for cementless hip replacement," *IEEE Engineering in Medicine and Biology Magazine,* vol. 14, pp. 307-13, 1995.

[25] W. L. Bargar, A. Bauer, and M. Borner, "Primary and revision total hip replacement using the Robodoc system," *Clinical Orthopaedics and Related Research,* pp. 82-91, Sep 1998.

[26] A. P. Schulz, K. Seide, C. Queitsch, A. von Haugwitz, J. Meiners, B. Kienast, M. Tarabolsi, M. Kammal, and C. Jürgens, "Results of total hip replacement using the Robodoc surgical assistant system: clinical outcome and evaluation of complications for 97 procedures," *The International Journal of Medical Robotics and Computer Assisted Surgery,* vol. 3, pp. 301-306, 2007.

[27] J. Pransky, "ROBODOC - Surgical robot success story," *Industrial Robot,* vol. 24, pp. 231-233, 1997.

[28] T. Haidegger. (2011). *ROBODOC advances - the story of an FDA approval* Available: http://surgrob.blogspot.com/2011/08/robodoc-advances-story-of-fda-approval.html

[29] T. Haidegger. (2011). *ROBODOC advances - historical timeline* Available: http://surgrob.blogspot.com/2011/08/robodoc-returns-historical-timeline.html

[30] Curexo. (2012, Jan 10). *Inspiring the Human Care*. Available: http://www.curexo.com/

[31] U.S. Food and Drug Administration, "DigiMatch ROBODOC Surgical System, 501(k) Approval, K072629," Center for Devices and Radiological Health, Ed., ed, 1998.

[32] M. Jakopec, S. J. Harris, F. Rodriguez y Baena, P. Gomes, and B. L. Davies, "The Acrobot® system for total knee replacement," *Industrial Robot,* vol. 30, pp. 61-66, 2003.

[33] M. Jakopec, F. Rodriguez y Baena, S. J. Harris, P. Gomes, J. Cobb, and B. L. Davies, "The Hands-On Orthopaedic Robot "Acrobot": Early Clinical Trials of Total Knee Replacement Surgery," *IEEE Transactions on Robotics and Automation,* vol. 19, pp. 902-911, 2003.

[34] J. Cobb, J. Henckel, P. Gomes, S. Harris, M. Jakopec, F. Rodriguez, A. Barrett, and B. Davies, "Hands-on robotic unicompartmental knee replacement. A prospective, randomised controlled study of the Acrobot system," *Journal of Bone and Joint Surgery - Series B,* vol. 88, pp. 188-197, 2006.

[35] G. Ostrovsky. (2007, Jan 7). *The Acrobot Surgical System Gets Infusion of Capital*. Available: http://medgadget.com/2007/08/the_acrobot_surgical_system_gets_infusion_of_capital.html

[36] Stanmore Implants Worldwide Ltd. (2012, Aug 28). *Stanmore Sculptor RGA (Robotic Guidance Arm)*. Available: http://www.stanmoreimplants.com/stanmore-sculptor.php

[37] M. Lysaght. (2011, Dec 7). *Robotic Surgery*. Available: http://biomed.brown.edu/Courses/BI108/BI108_2005_Groups/04/index.html

[38] Frost & Sullivan. (2003, Dec 7). *Robot-Assisted Surgeries, What Next?* Available: http://www.frost.com/prod/servlet/market-insight-top.pag?docid=4453859

[39] J. P. Ruurda, T. J. van Vroonhoven, and I. A. Broeders, "Robot-assisted surgical systems: a new era in laparoscopic surgery," *Annals of The Royal College of Surgeons of England,* vol. 84, pp. 223-6, Jul 2002.

[40] R. Taylor, P. Jensen, L. Whitcomb, A. Barnes, R. Kumar, D. Stoianovici, P. Gupta, Z. Wang, E. DeJuan, and L. Kavoussi, "Steady-hand robotic system for microsurgical augmentation," *International Journal of Robotics Research,* vol. 18, pp. 1201-1210, 1999.

[41] R. Kumar, P. Jensen, and R. H. Taylor, "Experiments with a steady hand robot in constrained compliant motion and path following," *Ro-Man'99: 8th IEEE International Workshop on Robot and Human Interaction,* pp. 92-97, 1999.

[42] D. Stoianovici, L. L. Whitcomb, J. H. Anderson, R. H. Taylor, and L. R. Kavoussi, "A modular surgical robotic system for image guided percutaneous procedures," *Medical Image Computing and Computer-Assisted Intervention - MICCAI'98,* vol. 1496, pp. 404-410, 1998.

[43] D. Stoianovici, A. Patriciu, D. Petrisor, D. Mazilu, and L. Kavoussi, "A new type of motor: Pneumatic step motor," *IEEE-ASME Transactions on Mechatronics,* vol. 12, pp. 98-106, Feb 2007.

[44] L. M. Su, D. Stoianovici, T. W. Jarrett, A. Patriciu, W. W. Roberts, J. A. Cadeddu, S. Ramakumar, S. B. Solomon, and L. R. Kavoussi, "Robotic percutaneous access to the kidney: comparison with standard manual access," *Journal of Endourology,* vol. 16, pp. 471-5, Sep 2002.

[45] D. Stoianovici, K. Cleary, A. Patriciu, D. Mazilu, A. Stanimir, N. Craciunoiu, V. Watson, and L. Kavoussi, "AcuBot: A robot for radiological interventions," *IEEE Transactions on Robotics and Automation,* vol. 19, pp. 927-930, Oct 2003.

[46] Perfint Healthcare Pvt. Ltd. (2012, Jan 5). *New Directions in Intraventional Oncology*. Available: http://www.perfinthealthcare.com

[47] Perfint Healthcare Pvt. Ltd., "PIGA Robotic Assistance for Soft Tissue Interventions (Brochure)," 5 ed. Madras, India: Perfint Healthcare.

[48] Medical Physics Web. (2007, Sept 17, E-Pub: Sep 17, 2007). Piga-CT promises precise needle positioning. *Medical Physics Web*. Available: http://medicalphysicsweb.org/cws/product/P000002986

[49] B. Maurin, B. Bayle, O. Piccin, J. Gangloff, M. de Mathelin, C. Doignon, P. Zanne, and A. Gangi, "A patient-mounted robotic platform for CT-scan guided procedures," *IEEE Transactions on Biomedical Engineering,* vol. 55, pp. 2417-25, 2008.

[50] B. Maurin, C. Doignon, J. Gangloff, B. Bayle, M. de Mathelin, O. Piccin, and A. Gangi, "CTBot: A stereotactic-guided robotic assistant for percutaneous procedures of the abdomen," *Medical Imaging 2005: Visualization, Image-Guided Procedures, and Display, Pts 1 and 2,* vol. 5744, pp. 241-250, 2005.

[51] B. Maurin, J. Gangloff, B. Bayle, M. de Mathelin, O. Piccin, P. Zanne, C. Doignon, L. Soler, and A. Gangi, "A parallel robotic system with force sensors for percutaneous procedures under CT-guidance," *Medical Image Computing and Computer-Assisted Intervention - MICCAI 2004, Pt 2, Proceedings,* vol. 3217, pp. 176-183, 2004.

[52] N. Zemiti, I. Bricault, C. Fouard, B. Sanchez, and P. Cinquin, "LPR: A CT and MR-compatible puncture robot to enhance accuracy and safety of image-guided interventions," *IEEE-ASME Transactions on Mechatronics,* vol. 13, pp. 306-315, Jun 2008.

[53] A. Melzer, B. Gutmann, T. Remmele, R. Wolf, A. Lukoscheck, M. Bock, H. Bardenheuer, and H. Fischer, "INNOMOTION for percutaneous image-guided interventions," *IEEE Engineering in Medicine and Biology Magazine,* vol. 27, pp. 66-73, May-Jun 2008.

[54] Mazor Robotics Ltd. (2012, Mar 13). Available: http://www.mazorrobotics.com/

[55] M. Shoham, "Miniature bone-mounted surgical robot " US Patent 6837892, 4 Jan. 2005.

[56] M. Shoham, I. H. Lieberman, E. C. Benzel, D. Togawa, E. Zehavi, B. Zilberstein, M. Roffman, A. Bruskin, A. Fridlander, L. Joskowicz, S. Brink-Danan, and N. Knoller, "Robotic assisted spinal surgery - from concept to clinical practice," *Computer Aided Surgery,* vol. 12, pp. 105-115, Mar 2007.

[57] S. R. Kantelhardt, R. Martinez, S. Baerwinkel, R. Burger, A. Giese, and V. Rohde, "Perioperative course and accuracy of screw positioning in conventional, open robotic-guided and percutaneous robotic-guided, pedicle screw placement," *European Spine Journal,* vol. 20, pp. 860-8, Jun 2011.

[58] L. Uzdienskin. (2009, 20 Mar. 2012, E-Pub: 26 Oct. 2009). Mazor Surgical Technologies Raises $13M in Public Offering *Healthpoint Capital Exclusively Muskoskeletal Research*. Available: http://www.healthpointcapital.com/research/2009/10/26/mazor_surgical_technologies_raises_13m_in_public_offering/

[59] O. Hadomi, "Robotic Spine Surgery by Mazor Robotics, Company Presentation," Feb 2012.

[60] M. Shoham, M. Burman, L. Joskowicz, E. Batkilin, and Y. Kunicher, "Bone-mounted miniature robot for surgical procedures: Concept and clinical applications," *IEEE Transactions on Robotics and Automation,* vol. 19, pp. 893-901, Oct 2003.

[61] Hansen Medical. (2012, Fed 10). *Inspiring the Human Care*. Available: http://www.hansenmedical.com

[62] Cooley LLP. (2005, E-Pub: Sept 7, 2005). Hansen Medical and Intuitive Surgical Cross-License Robotic Technologies. Available: http://www.cooley.com/58110

[63] L. Di Biase, Y. A. N. Wang, R. Horton, G. J. Gallinghouse, P. Mohanty, J. Sanchez, D. Patel, M. Dare, R. Canby, L. D. Price, J. D. Zagrodzky, S. Bailey, J. D. Burkhardt, and A. Natale, "Ablation of Atrial Fibrillation Utilizing Robotic Catheter Navigation in Comparison to Manual Navigation and Ablation: Single-Center Experience," *Journal of Cardiovascular Electrophysiology,* vol. 20, pp. 1328-1335, 2009.

[64] P. Breedveld, J. S. Sheltes, E. M. Blom, and J. E. I. Verheij, "A new, easily miniaturized steerable endoscope," *IEEE Engineering in Medicine and Biology Magazine,* vol. 24, pp. 40-7, 2005.

[65] Intuitive Surgical Inc. (2012, Aug 30). Available: http://www.intuitivesurgical.com/

[66] S. Kichen. (2005, 8 Mar, E-Pub: Jul 27, 2005). Medical Renaissance. *Forbes.com*. Available: http://www.forbes.com/2005/07/26/surgery-science-medicine-cz_sk_0727surgery.html

[67] G. S. Guthart and K. J. Salisbury Jr, "Intuitive telesurgery system: overview and application," in *ICRA 2000: IEEE International Conference on Robotics and Automation, April 24, 2000 - April 28, 2000*, San Francisco, CA, USA, 2000, pp. 618-621.

[68] U.S. Food and Drug Administration. (2012, 12 Mar). *MAUDE - Manufacturer and User Facility Device Experience*. Available: http://www.accessdata.fda.gov/scripts/cdrh/cfdocs/cfMAUDE/search.CFM

[69] Intuitive Surgical Inc., "2008 Annual Report," Sunnyvale, CA 2009.

[70] K. Fogarty. (2010, 20 Mar. 2012, E-Pub: 10 Feb. 2010). Why Surgical Robotics Is Unstoppable. *Robotics Business Review*. Available: http://www.roboticsbusinessreview.com/article/why-surgical-robotics-is-unstoppable/

[71] L. Kowalczyk. (2012, 26 May, E-Pub: 14 Oct 2009). Caution sounded on robot-aided prostate surgery. *Boston.com*. Available: http://www.boston.com/news/local/massachusetts/articles/2009/10/14/study_scrutinizes_robot_assisted_prostate_surgery/

[72] S. V. Burgess, F. Atug, E. P. Castle, R. Davis, and R. Thomas, "Cost analysis of radical retropubic, perineal, and robotic prostatectomy," *Journal of Endourology,* vol. 20, pp. 827-830, Oct 2006.

[73] J. C. Hu, X. Gu, S. R. Lipsitz, M. J. Barry, A. V. D'Amico, A. C. Weinberg, and N. L. Keating, "Comparative effectiveness of minimally invasive vs open radical prostatectomy," *JAMA,* vol. 302, pp. 1557-64, Oct 14 2009.

[74] F. R. Schroeck, T. L. Krupski, L. Sun, D. M. Albala, M. M. Price, T. J. Polascik, C. N. Robertson, A. K. Tewari, and J. W. Moul, "Satisfaction and regret after open retropubic or robot-assisted laparoscopic radical prostatectomy," *Eur Urol,* vol. 54, pp. 785-93, Oct 2008.

[75] Center for Integration of Medicine and Innovative Technology. (2012, Aug 23). Available: http://www.cimit.org

[76] P. v. Dam, J. Hauspy, L. Verkinderen, B. Trinh, L. V. Looy, and L. Dirix, "Do Costs of Robotic Surgery Matter?," in *Advanced Gynecologic Endoscopy*, A. Darwish, Ed., ed. Rijeka, Croatia: http://www.intechopen.com, 2011.
[77] A. H. Slocum and M. M. Graham, "Product Development by Deterministic Design," in *1st Annual CDI Conference*, Queens University, Kingston, Ontario, Canada, 2005.
[78] M. M. Graham, "Teaching product development by deterministic design," PhD Dissertation, Mechanical Engineering, Massachusetts institute of Technology, Cambridge, MA, 2006.
[79] M. Graham, A. Slocum, and R. M. Sanehez, "Teaching high school students and college freshmen product development by deterministic design with PREP," *Journal of Mechanical Design,* vol. 129, pp. 677-681, Jul 2007.
[80] M. Rother and J. Shook, *Learning to See, Value Stream Mapping to Create Value and Eliminate Muda*. Cambridge, MA: Lean Enterprise Institute, 2003.
[81] F. W. Taylor, *The Principles of Scientific Management*: ReadaClassic.com, 2012.
[82] USPTO Patent Technology Monitoring Team, "Medical Devices, A Patent Technology Monitoring Team Report ", P. T. M. Team, Ed., ed, 2012.
[83] American Lung Association. (2012, May 31). *Lung Cancer Fact Sheet*. Available: http://www.lung.org/lung-disease/lung-cancer/resources/facts-figures/lung-cancer-fact-sheet.html
[84] Y. Ohno, H. Hatabu, D. Takenaka, T. Higashino, H. Watanabe, C. Ohbayashi, and K. Sugimura, "CT-guided transthoracic needle aspiration biopsy of small (< or = 20 mm) solitary pulmonary nodules," *AJR Am J Roentgenol,* vol. 180, pp. 1665-9, Jun 2003.
[85] D. R. Aberle, A. M. Adams, C. D. Berg, W. C. Black, J. D. Clapp, R. M. Fagerstrom, I. F. Gareen, C. Gatsonis, P. M. Marcus, and J. D. Sicks, "Reduced lung-cancer mortality with low-dose computed tomographic screening," *N Engl J Med,* vol. 365, pp. 395-409, Aug 4 2011.
[86] Associated Press, "Americans get most radiation from medical scans," in *USA Today*, ed, 2010.
[87] S. W. Kwan, M. Bhargavan, R. K. Kerlan, Jr., and J. H. Sunshine, "Effect of advanced imaging technology on how biopsies are done and who does them," *Radiology,* vol. 256, pp. 751-8, Sep 2010.
[88] NeoRad AS. (2012, Aug 30). Available: http://www.neorad.no/
[89] LAP GmbH Laser Applikationen. (2012, Aug 30). *Lap Laser Medical Systems*. Available: http://www.lap-laser.com/medical-systems/
[90] J. H. Yanof, K. J. West, C. Bauer, and D. M. Kwartowitz, "Tactile feedback and display in a CT image guided robotic system for interventional procedures," US Patent 6,785,572, Aug 31, 2004.
[91] C. D. Bidwell, "Biopsy needle guide for use with CT scanner," US Patent 5,053,042, Oct 1, 1991.
[92] R. Maciunas, J. M. Fitzpatrick, J. Calvin R. Maurer, J. J. McCrory, and R. Randall, "Biopsy guide," US Patent 5,984,930, Nov 16, 1999.
[93] V. L. Ferrara, "Biopsy guide," US Patent 4,809,694, Mar 7, 1989.
[94] C. Cermak, "Multiple angle disposable needle guide system," US Patent 5,941,889, Aug 24,1999.
[95] F. J. B. W. A. Friedman, "Computer controlled guidance of a biopsy needle," US Patent 6,546,279, April 8, 2003.
[96] T. W. Livingston, "Light beam locator and guide for a biopsy needle," US Patent 5,320,111, Jun 14, 1994.
[97] R. Filly, R. Gordon, and B. Severence, "Adjustable needle guide apparatus and method," US Patent 6,379,307, Apr 30, 2002.
[98] C. J. Walsh, B. H. Sapkota, M. K. Kalra, N. C. Hanumara, B. Liu, J. A. O. Shepard, and R. Gupta, "Smaller and Deeper Lesions Increase the Number of Acquired Scan Series in Computed Tomography-guided Lung Biopsy," *Journal of Thoracic Imaging,* vol. 26, pp. 196-203, Aug 2011.

[99] Imaging Performance Assessment of CT Scanners Group. (2007, 30 Aug). *impactscan.org*. Available: http://www.impactscan.org/
[100] R. Y. Dien and E. C. Luce, "Spherical robotic wrist joint," US Patent 4,628,765, Dec 16, 1986.
[101] M. E. Rosheim, *Robot wrist actuators*. New York: Wiley, 1989.
[102] S. R. H. Barrett, N. C. Hanumara, C. J. Walsh, A. H. Slocum, R. Gupta, and J. A. O. Shepard, "A remote needle guidance system for percutaneous biopsies," *Proceedings of the ASME International Design Engineering Technical Conferences and Computers and Information in Engineering Conference, Vol 7, Pts A and B,* pp. 481-489, 2005.
[103] C. J. Walsh, N. C. Hanumara, A. H. Slocum, J. A. Shepard, and R. Gupta, "A Patient-Mounted, Telerobotic Tool for CT-Guided Percutaneous Interventions," *Journal of Medical Devices-Transactions of the ASME,* vol. 2, Mar 2008.
[104] A. M. Okamura, C. Simone, and M. D. O'Leary, "Force modeling for needle insertion into soft tissue," *IEEE Transactions on Biomedical Engineering,* vol. 51, pp. 1707-1716, Oct 2004.
[105] J. F. Barrett and N. Keat, "Artifacts in CT: recognition and avoidance," *Radiographics,* vol. 24, pp. 1679-91, Nov-Dec 2004.
[106] N. C. Hanumara, "Characterization and analysis of an MRI compatible robot design for wrist psychophysics and rehabilitation " SM Thesis, Mechanical Engineering, Massachusetts Institute of Technology, Cambridge, MA, 2006.
[107] Johnson Electric. (2012, Aug 30). *Innovating Motion*. Available: http://www.johnsonelectric.com
[108] G. Boothroyd, P. Dewhurst, and W. A. Knight, *Product design for manufacture and assembly*, 2nd ed. New York: M. Dekker, 2002.
[109] H. Dreyfuss, *Designing for people*. New York: Allworth Press, 2003.
[110] D. A. Norman, *The design of everyday things*, 1st Basic paperback. ed. New York: Basic Books, 2002.
[111] M. S. Sanders and E. J. McCormick, *Human factors in engineering and design*, 7th ed. New York: McGraw-Hill, 1993.
[112] N. C. Hanumara, C. J. Walsh, A. H. Slocum, R. Gupta, and J. A. Shepard, "Human factors design for intuitive operation of a low-cost, image-guided, tele-robotic biopsy assistant," *2007 Annual International Conference of the IEEE Engineering in Medicine and Biology Society, Vols 1-16,* pp. 1257-1260, 2007.
[113] R. Gupta, S. R. H. Barrett, N. Hanumara, J.-A. O. Shepard, A. H. Slocum, and C. J. Walsh, "Guidance and Insertion System," US Patent 11/307231, Aug 3, 2006.
[114] A. Seitel, C. J. Walsh, N. C. Hanumara, J.-A. Shepard, A. H. Slocum, H.-P. Meinzer, R. Gupta, and L. Maier-Hein, "Development and evaluation of a new image-based user interface for robot-assisted needle placements with the Robopsy system," in *Proc. SPIE Medical Imaging: Visualization, Image-Guided Procedures, and Modeling*, Lake Buena Vista, FL, 2009, p. 72610X.
[115] A. Magnusson and P. Egnelöv, "Guide for a medical device," US Patent 7,824,417, Nov 2, 2010.
[116] AprioMed. (2012, Aug 27). *AprioMed - Interventional Radiology Devices*. Available: http://www.apriomed.com/
[117] Radi Medical Devices AB, "See Star Guiding Device," 29003 Rev. 02 2006-10 ed. Uppsala, Sweden, 2006.
[118] C. J. Hildreth, C. Lynm, and R. M. Glass, "JAMA patient page. Uterine fibroids," *JAMA,* vol. 301, p. 122, Jan 7 2009.
[119] J. F. Daniell, C. Channell, J. Lindsay, S. Staggs, and T. Henry. (2011, 30 Aug. 2012, E-Pub: Early Evaluation Of An Electromechanical Morcellator For Laparoscopic Supracervical Hysterectomy. *OBGYN.net*. Available: http://hcp.obgyn.net/laparoscopy/content/article/1760982/1893942#

[120] W. Kondo, M. T. Zomer, L. Charles, N. Bourdel, G. Mage, and M. Canis, "Total Laparoscopic Hysterectomy: Surgical Technique and Results," in *Advanced Gynecologic Endoscopy*, A. Darwish, Ed., ed. Rijeka, Croatia: http://www.intechopen.com, 2011.
[121] Ethicon Inc. (2012, Aug 30). *Gynecare Morcellex Tissue Morcellator*. Available: http://www.ethicon360.com/products/gynecare-morcellex-tissue-morcellator
[122] Karl Storz GmbH & Co. KG. (2012, Aug 30). *Karl Stortz - Endoskope*. Available: http://www.karlstorz.com
[123] Hologic Inc. (2012, Aug 23). *MyoSure Fibroid Removal Simplified*. Available: http://www.myosure.com/
[124] H. Oizumi, N. Kanauchi, H. Kato, M. Endoh, J. Suzuki, and M. Sadahiro, "Morcellation Technique to Remove Large Tumor in Thoracoscopic Surgery," *Annals of Thoracic Surgery,* vol. 92, pp. 1141–1143, Sept 2011.
[125] M. Lieng, O. Istre, B. Busund, and E. Qvigstad, "Severe complications caused by retained tissue in laparoscopic supracervical hysterectomy," *J. Minimally Invasive Gynecology,* vol. 13, pp. 231-3, May-Jun 2006.
[126] D. Hernandez-Stewart, "Enclosure Module Design Thesis for Endoblend: A Novel Surgical Device for Laparoscopic Hysterectomy," BS Senior Thesis, Mechanical Engineering, Massachusetts Institute of Technology, Cambridge, MA, USA, 2007.
[127] D. Buckley, "Development of a Collapsible Guard Component for a Novel Surgical Instrument," SB Senior Thesis, Mechanical Engineering, Massachusetts Institute of Technology, Cambridge, MA, 2007.
[128] The Sausage Maker Inc. (2012, Aug 30). Available: http://www.sausagemaker.com/
[129] T. Hashii and R. C. Everts, "Oscillating spindle sander," US Patent 5,860,852, Jan 19, 1999.
[130] E. A. Arkenbout and F. W. Jansen, "A Comparitive Overview of Existing and Experimental Morcellators in Gynecology and Urology," in *Proceedings of Design of Medical Devices Conference*, Minneapolis, MN, 2011.
[131] E. A. Arkenbout, J. L. Herder, and F. E. Jansen, "Proposed Protocol for Objective Morcellator Analysis," in *Proceedings of Design of Medical Devices Conference*, Minneapolis, MN, 2011.
[132] E. A. Arkenbout, A. Thurkow, and F. W. Jansen, "In-Vitro and Clinical Morcellator Functionality Assessment," Masters of Science Master's, BioMedical Engineering, TU Deflt, Delft, Netherlands, 2012.
[133] C. L. Dym and P. Little, *Engineering design : a project-based introduction*. New York: John Wiley, 2004.
[134] A. Bright, "Student, faculty and liaison roles in the Engineering Clinic Program at Harvey Mudd College," *Frontiers in Education 1996 - 26th Annual Conference, Proceedings, Vols 1-3,* pp. 1449-1452, 1996.
[135] A. Bright and J. R. Phillips, "The Harvey Mudd engineering clinic past, present, future," *Journal of Engineering Education,* vol. 88, pp. 189-194+243+246, 1999.
[136] W. Durfee. (2012, Aug 21). *New Product Design and Business Development*. Available: http://www.npdbd.umn.edu/
[137] Johns Hopkins University. (2012, 30 Aug). *Center for Bioengineering innovation and Design*. Available: http://cbid.bme.jhu.edu
[138] J. R. Hackman and N. Vidmar, "Effects of Size and Task Type on Group Performance and Member Reactions," *Sociometry,* vol. 33, pp. 37-54, 1970.
[139] M. Ohland. (2012, Aug 22). *Comprehensive Assessment of Team Member Effectiveness*. Available: www.catme.org

[140] M. P. Palmer, E. L. Abreu, A. Mastrangelo, and M. M. Murray, "Injection temperature significantly affects in vitro and in vivo performance of collagen-platelet scaffolds," *Journal Orthopedic Research,* vol. 27, pp. 964-71, Jul 2009.
[141] S. M. Joshi, A. N. Mastrangelo, E. M. Magarian, B. C. Fleming, and M. M. Murray, "Collagen-platelet composite enhances biomechanical and histologic healing of the porcine anterior cruciate ligament," *American Journal Sports Medicine,* vol. 37, pp. 2401-10, Dec 2009.
[142] J. E. Petrzelka, D. Chatzigeorgiou, M. C. Menon, M. Lustrino, C. J. Stefanov-Wagner, A. H. Slocum, and S. K. Agarwal, "An Articulating Tool for Endoscopic Screw Delivery," in *Proceedings of Design of Medical Devices Conference*, Minneapolis, MN, 2010.
[143] J. E. Petrzelka, M. C. Menon, C. J. Stefanov-Wagner, S. K. Agarwal, D. Chatzigeorgiou, M. Lustrino, and A. H. Slocum, "An Articulating Tool for Endoscopic Screw Delivery," *Journal of Medical Devices-Transactions of the ASME,* vol. 5, Mar 2011.
[144] S. K. Agarwal, J. E. Petrzelka, M. C. Menon, C. J. Stefanov-Wagner, D. Chatzigeorgiou, M. Lustrino, and A. H. Slocum, "Thoracoscopic Stabilization of the Chest Wall," in *2010 New England Surgical Society Annual Meeting*, Saratoga Springs, NY, 2010.
[145] T. Lipoma, P. Bello, C. Darling, and M. T. Bianchi, "Somnus: A Sleep-Measuring Shirt Based on Chest Expanison and Respiratory Patterns," in *Proceedings of Design of Medical Devices Conference*, Minneapolis, MN, 2011.
[146] P. Maki, *Assessing for learning : building a sustainable commitment across the institution*, 2nd ed. Sterling, VA: Stylus Pub., 2010.
[147] N. A. Weiss, *Introductory statistics*, 7th ed. Boston: Pearson Addison Wesley, 2005.
[148] S. L. Figueredo, "Design of an endoscopic biopsy needle with flexural members," SM Thesis, Mechanical Engineering, Massachusetts Institute of Technology, Cambridge, MA, 2006.
[149] C. J. Walsh, N. Hanumara, A. Slocum, R. Gupta, and J. A. Shepard, "Evaluation of a patient-mounted, remote needle guidance and insertion system for CT-guided, percutaneous lung biopsies," *Proceedings of the 2nd Frontiers in Biomedical Devices Conference,* pp. 39-40, 2007.
[150] D. R. Zurovcik, "Development of a simplified negative pressure wound device," SM Thesis, Mechanical Engineering, Massachusetts Institute of Technology, Cambridge, MA, 2007.
[151] D. Zurovcik, A. Slocum, G. Mody, R. Riviello, and R. Sheridan, "Development of Simplified Negative Pressure Wound Therapy Device for Low-Resource Settings," in *Global Humanitarian Technology Conference (GHTC), 2011 IEEE*, 2011, pp. 91-97.
[152] D. P. Orgill, D. R. Zurovcik, and G. N. Mody, "Reply: Alternative Materials in Vacuum-Assisted Closure," *Plastic and Reconstructive Surgery,* vol. 128, pp. 785e-786e, Dec 2011.
[153] C. M. DiBiasio, K. V. Durand, J. Hopkins, Z. Traina, A. H. Slocum, N. V. Vasilyev, and P. J. del Nido, "Design of a Surgical Port for Minimally Invasive Beating-Heart Intracardial Procedures," *Journal of Medical Devices-Transactions of the ASME,* vol. 5, Dec 2011.
[154] N. V. Vasilyev, M. Kawata, C. M. DiBiasio, K. V. Durand, J. Hopkins, Z. J. Traina, A. H. Slocum, and P. J. del Nido, "A novel cardioport for beating-heart, image-guided intracardiac surgery," *Journal of Thoracic and Cardiovascular Surgery,* vol. 142, pp. 1545-1551, Dec 2011.
[155] A. H. Slocum, A. H. Slocum, and J. E. Spiegel, "Design and In Vitro Testing of a Pressure-Sensing Syringe for Endotracheal Tube Cuffs," *Anesthesia and Analgesia,* vol. 114, pp. 967-971, May 2012.
[156] A. M. A. Husseini, H. J. Lee, J. Negrete, S. Powelson, A. Servi, A. Slocum, and J. Saukkonen, "Design and Prototyping of a Low-cost Portable Mechanical Ventilator," in *Proceedings of Design of Medical Devices Conference*, Minneapolis, MN, 2010.
[157] J. A. Ankrum, A. L. Olechowski, J. A. Canseco, E. E. Greenblatt, M. P. Roberts, N. C. Hanumara, A. H. Slocum, and A. Tavakkolizadeh, "Nasogastric Tube Design to Reduce Clogging and Simplify Flushing," in *Proceedings of Design of Medical Devices Conference*, Minneapolis, MN, 2011.

[158] E. Summers, T. Cervantes, R. Batzer, J. Stark, and R. Lewis, "Innovative Renal Cooling Device for Use in Minimally Invasive Surgery," in *Proceedings of Design of Medical Devices Conference*, Minneapolis, MN, 2011.

[159] E. Summers, T. Cervantes, R. Batzer, C. Simpson, R. Lewis, and J. Stark, "Renal Cooling Device for Use in Minimally Invasive Surgery," *Journal of Medical Devices-Transactions of the ASME,* vol. 6, Jun 2012.

[160] T. M. Cervantes, E. K. Summers, R. Batzer, C. Simpson, R. Lewis, N. N. Dhanani, and A. H. Slocum, "Evaluation of a minimally invasive renal cooling device using heat transfer analysis and an in vivo porcine model," *Medical Engineering & Physics,* 2012.

[161] H. O'Hanley, M. Rosario, Y. Chen, A. Maertens, J. Walton, and J. Rosen, "Design and Testing of a Three Fingered Flexural Laparoscopic Grasper," in *Proceedings of Design of Medical Devices Conference*, Minneapolis, MN, 2011.